1. Report No. FHWA-SA-91-044	2. PB92178524	ecipient's Catalog No.

4. Title and Subtitle THE FLAT DILATOMETER TEST	5. Report Date February 1992
	6. Performing Organization Code

7. Author(s) Jean-Louis Riaund and Jerome Miran	8. Performing Organization Report No.

9. Performing Organization Name and Address PSC Associates, Inc. 200 Blossom Lane Mountain View, CA 94041	10. Work Unit No. (TRAIS)
	11. Contract or Grant No.

12. Sponsoring Agency Name and Address Federal Highway Administration Office of Technology Applications 400 Seventh Street, SW Washington, D.C. 20590	13. Type of Report and Period Covered Final Report
	14. Sponsoring Agency Code

15. Supplementary Notes

FHWA Project Manager: Chien-Tan Chang, HTA-22   Contractor project manager: Peter Chan

FHWA Technical Consultants: Richard Cheney, Jerry DiMaggio, and Chris Dumas (HNG-31)

16. Abstract

A dilatometer test consists of pushing a flat blade located at the end of a series of rods. once at the testing depth, a circular steel membrane located on one side of the blade is expanded horizontally into the soil. The pressure is recorded at three specific moments during the test. The blade is then advanced to the next testing depth.

The design applications of the dilatometer test includes: deep foundations under horizontal and vertical load, shallow foundations under vertical load, compaction control, and any other geotechnical problems which can be make use of the soil parameters obtained from the dilatometer test.

17. Key Words Dilatometer, soil parameters, foundation design, in situ testing	18. Distribution Statement No restrictions. This document is available to the public from the National Technical Information Service, Springfield, Virginia 22161

19. Security Classif. (of this report) Unclassified	20. Security Classif. (of this page) Unclassified	21. No. of Pages 113	22. Price

Form DOT F 1700.7   (8-72)   Reproduction of completed page authorized   ii-a

GENERAL DISCLAIMER

UNIT CONVERSIONS

Acceleration $9.81\ m/s^2 = 386.22\ in./s^2 = 32.185\ ft/s^2$, Paris: $g = 9.80665\ m/s^2$ London: $g = 3.2174 \times 10^1\ ft/s^2$

Area $1\ m^2 = 1.5500 \times 10^3\ in.^2 = 1.0764 \times 10^1\ ft^2 = 1.196\ yd^2 = 10^6\ mm^2 = 10^4\ cm^2 = 2.471 \times 10^{-4}\ acres^2 = 3.861 \times 10^{-7}\ mi^2$

Coefficient of Consolidation
$1\ m^2/s = 10^4\ cm^2/s = 6 \times 10^5\ cm^2/min = 3.6 \times 10^7\ cm^2/h$
$= 8.64 \times 10^8\ cm^2/day = 2.628 \times 10^{10}\ cm^2/month$
$= 3.1536 \times 10^{11}\ cm^2/year$
$= 1.550 \times 10^3\ in.^2/s = 4.0734 \times 10^9\ in.^2/month$
$= 1.3392 \times 10^8\ in.^2/day = 4.8881 \times 10^{10}\ in.^2/year$
$= 9.4783 \times 10^5\ ft^2/day = 2.8830 \times 10^7\ ft^2/month$
$= 3.3945 \times 10^8\ ft^2/year$

Flow $1\ m^3/s = 10^6\ cm^3/s = 8.64 \times 10^4\ m^3/day = 8.64 \times 10^{10}\ cm^3/day$
$= 3.5314 \times 10^1\ ft^3/s = 3.0511 \times 10^6\ ft^3/day$

Force $10\ kN = 2.2482 \times 10^3\ lb = 2.2482\ kip = 1.1241\ t$ (short ton = 2000 lb)
$= 1.0194 \times 10^3\ kg = 1.0194 \times 10^6\ g = 1.0194\ T$ (metric ton = 1000 kg)
$= 10^9\ dynes = 3.5971 \times 10^4\ ounces = 1.022\ tl$ (long ton = 2200 lb)

Force per Unit Length $1\ kN/m = 6.8526 \times 10^1\ lb/ft = 6.8526 \times 10^{-2}\ kip/ft$
$= 3.4263 \times 10^{-2}\ t/ft$
$= 1.0194 \times 10^2\ kg/m = 1.0194 \times 10^{-1}\ T/m$

Length $1\ m = 3.9370 \times 10^1\ in. = 3.2808\ ft = 1.0936\ yd$
$= 10^{10}\ Amgstrom = 10^6\ microns = 10^3\ mm = 10^2\ cm$
$= 10^{-3}\ km = 6.2137 \times 10^{-4}\ mile = 5.3996 \times 10^{-4}\ nautical mile$

Moment or Energy $1\ kN.m = 7.3759 \times 10^2\ lb.ft = 7.3759 \times 10^{-1}\ kip.ft = 3.6879 \times 10^{-1}\ t.ft$
$= 1.0194 \times 10^3\ g.cm = 1.0194 \times 10^2\ kg.m = 1.0194 \times 10^{-1}\ T.m$
$= 10^3\ N.m = 10^3\ Joule$

Moment of Inertia $1\ m^4 = 2.4025 \times 10^6\ in.^4 = 1.1586 \times 10^2\ ft^4 = 6.9911 \times 10^{-1}\ yd^4$
$= 10^8\ cm^4 = 10^{12}\ mm^4$

Moment per Unit Length $1\ kN.m/m = 2.2482 \times 10^2\ lb.ft/ft = 2.2482 \times 10^{-1}\ kip.ft/ft$
$= 1.1241 \times 10^{-1}\ t.ft/ft$
$= 1.0194 \times 10^2\ kg.m/m = 1.0194 \times 10^{-1}\ T.m/m$

Pressure $100\ kPa = 10^2\ kN/m^2 = 1.4503 \times 10^1\ lb/in.^2 = 2.0885 \times 10^3\ lb/ft^2$
$= 1.4503 \times 10^{-2}\ kip/in.^2 = 2.0885\ kip/ft^2$
$= 1.0442\ t/ft^2 = 7.5003 \times 10^1\ cm$ of Hg (0 °C)
$= 1.0197\ kg/cm^2 = 1.0197 \times 10^1\ T/m^2$
$= 9.8689 \times 10^{-1}\ Atm = 3.3455 \times 10^1\ ft$ of H_2O (4 °C)
$= 1.0000\ bar = 10^6\ dynes/cm^2$

Temperature °C = 5/9 (°F - 32), °K = °C + 273.15

Time 1 yr. = 12 mo. = 365 day = 8760 hr = 5.256×10^5 min = 3.1536×10^7 s

Unit Weight, Coefficient of Subgrade Reaction $10\ kN/m^3 = 6.3654 \times 10^1\ lb/ft^3 = 3.6837 \times 10^{-2}\ lb/in.^3$
$= 1.0196\ g/cm^3 = 1.0196\ T/m^3 = 1.0196 \times 10^3\ kg/m^3$

Velocity or Permeability $1\ m/s = 3.6\ km/h = 2.2369\ mile/h = 6 \times 10^1\ m/min = 10^2\ cm/s$
$= 1.9685 \times 10^2\ ft/min = 3.2808\ ft/s$
$= 1.0346 \times 10^8\ ft/year = 2.8346 \times 10^5\ ft/day$

Volume $1\ m^3 = 6.1024 \times 10^4\ in.^3 = 3.5315 \times 10^1\ ft^3 = 7.6455\ 10^{-1}\ yd^3$
$= 10^9\ mm^3 = 10^6\ cm^3 = 10^3\ dm^3$
$= 10^3\ liter = 2.1998 \times 10^2\ gallon$ (U.K.) $= 2.6417 \times 10^2\ gallon$ (U.S.)

Volume Loss in a Tubing $1\ cm^3/m/kPa = 8.91 \times 10^{-4}\ in.^3/ft/psf$

Preceding Page Blank

iii

TABLE OF CONTENTS

LIST OF TABLES

LIST OF FIGURES

1. INTRODUCTION

1.1 Introduction

The purpose of this report is to provide guidelines for the proper use of the Flat Dilatometer (DMT). This includes the proper way to perform a dilatometer test (DMT test), to reduce and interpret the data, and to use the data in design. Anyone wishing to learn about the DMT in more details than provided in this manual can refer to the list of references and in particular to the reports written by Schmertmann (1988) for the Pennsylvania DOT.

A single dilatometer test consists of pushing into the soil and to a desired depth, a flat blade located at the end of a series of rods (figures 1.1, 1.2, 1.3, 1.4, 1.5). Once the test depth is reached, the operator uses gas pressure to expand horizontally into the soil a circular steel membrane located on one side of the blade. The operator records two pressures (A and B pressures). The pressure A is the pressure on the blade before expansion while the pressure B is the pressure required to produce an expansion of 1 mm of the membrane into the soil. The operator then deflates the membrane and records a third pressure (C pressure). This test sequence requires about 1-2 minutes. The blade is then advanced to the next test depth. A series of single dilatometer tests is referred to as a DMT sounding.

The design applications of the DMT includes: deep foundations under horizontal and vertical load, shallow foundations under vertical load, compaction control, and any other geotechnical problems which can make use of the soil properties obtained from the DMT (chapter 6).

The flat dilatometer was designed by an Italian professor, Silvano Marchetti, in the 1970's and was patented in 1977 in Italy. The dilatometer test was then introduced in the USA through Schmertmann & Crapps, Inc. The test is increasingly used in research and in practice.

In 1986, an ASTM suggested method for performing the flat dilatometer test was proposed by Schmertmann (1986a).

1.2 Definitions

The following definitions are from this ASTM suggested method.

DMT

DMT is an abbreviation for DilatoMeTer.

1
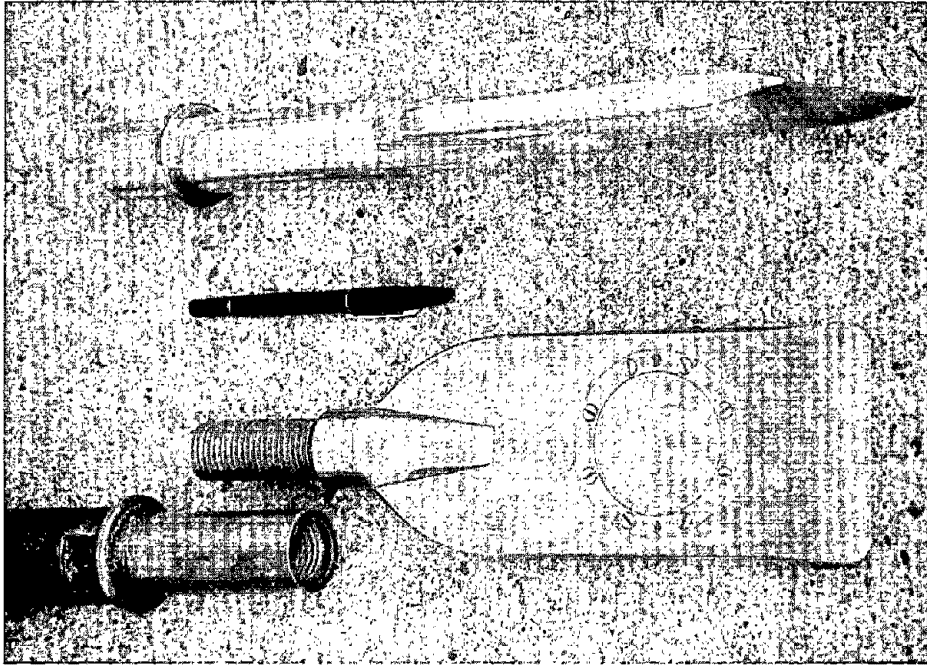
FIG. 1.1. Flat Dilatometer Blade
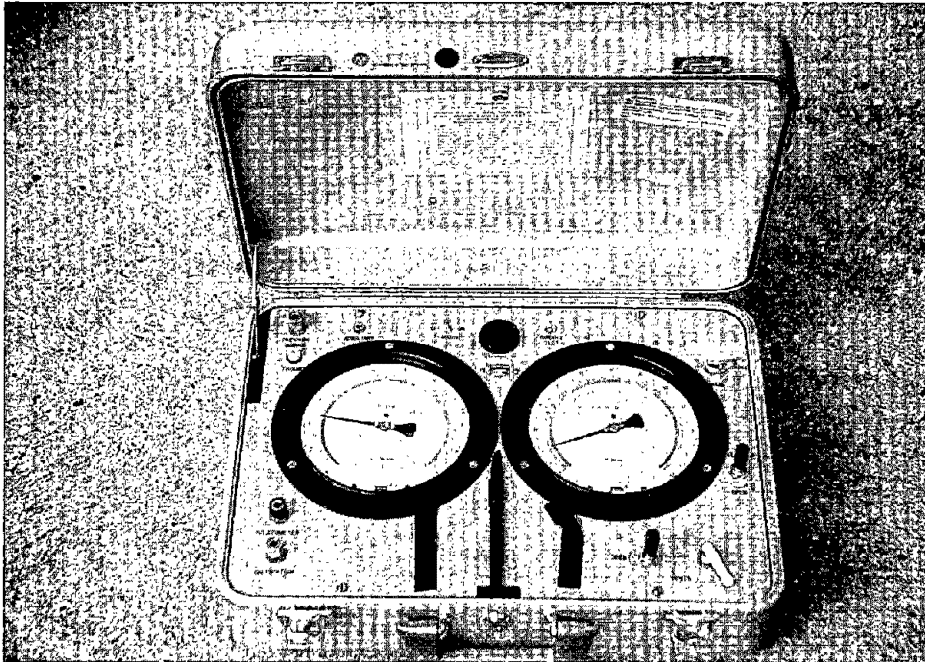
FIG. 1.2. Control Unit

FIG. 1.3. Insertion of the flat Dilatometer Blade
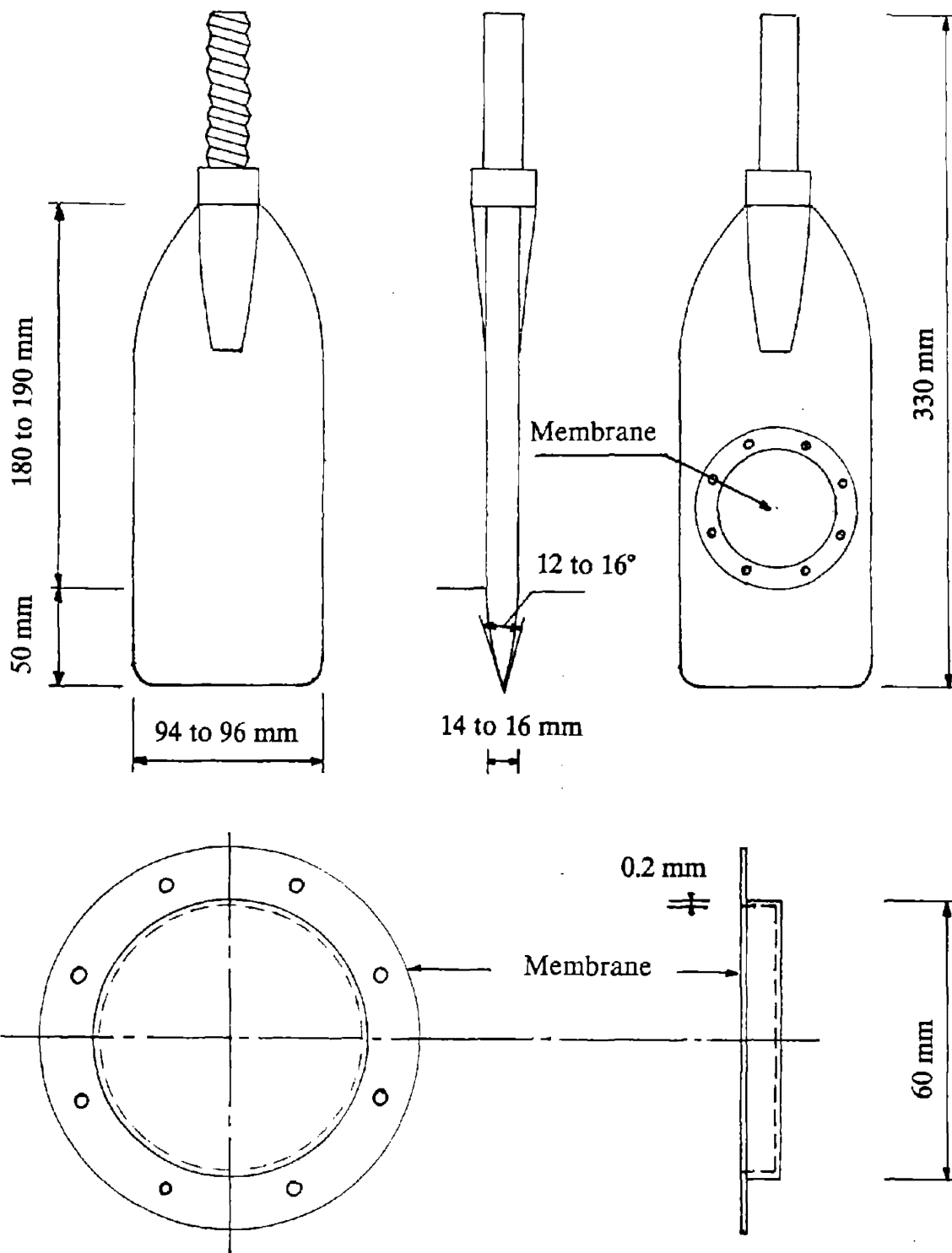
FIG. 1.4. Blade and Membrane Dimensions

180 to 190 mm

50 mm

94 to 96 mm

Membrane

12 to 16°

14 to 16 mm

330 mm

0.2 mm

Membrane

60 mm

Screws

Retaining Ring

Membrane
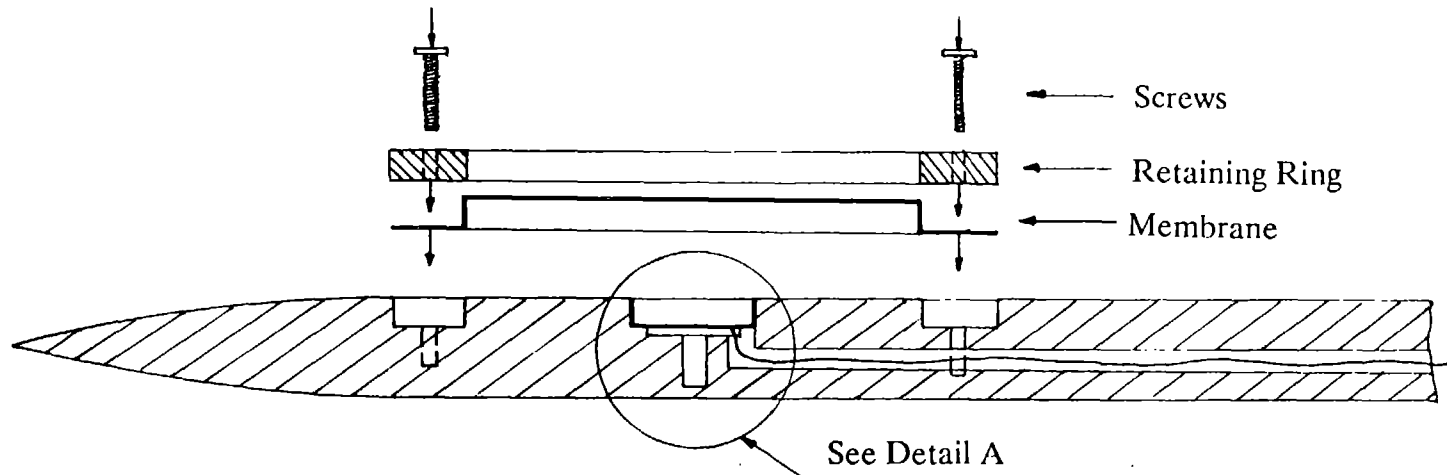
See Detail A

BLADE SECTION (FULL SCALE)

Membrane

Plexiglass Cylinder

Sensing Disk (metal)

Feeler

Plastic Insulating Seat

Stainless Steel
Spring

Stainless Steel
Cylinder

Electrical
Wire

Membrane Fully Expanded
(Buzzer On)

Membrane is Expanding
(Buzzer Off)

Membrane is Collapsed
(Buzzer On)
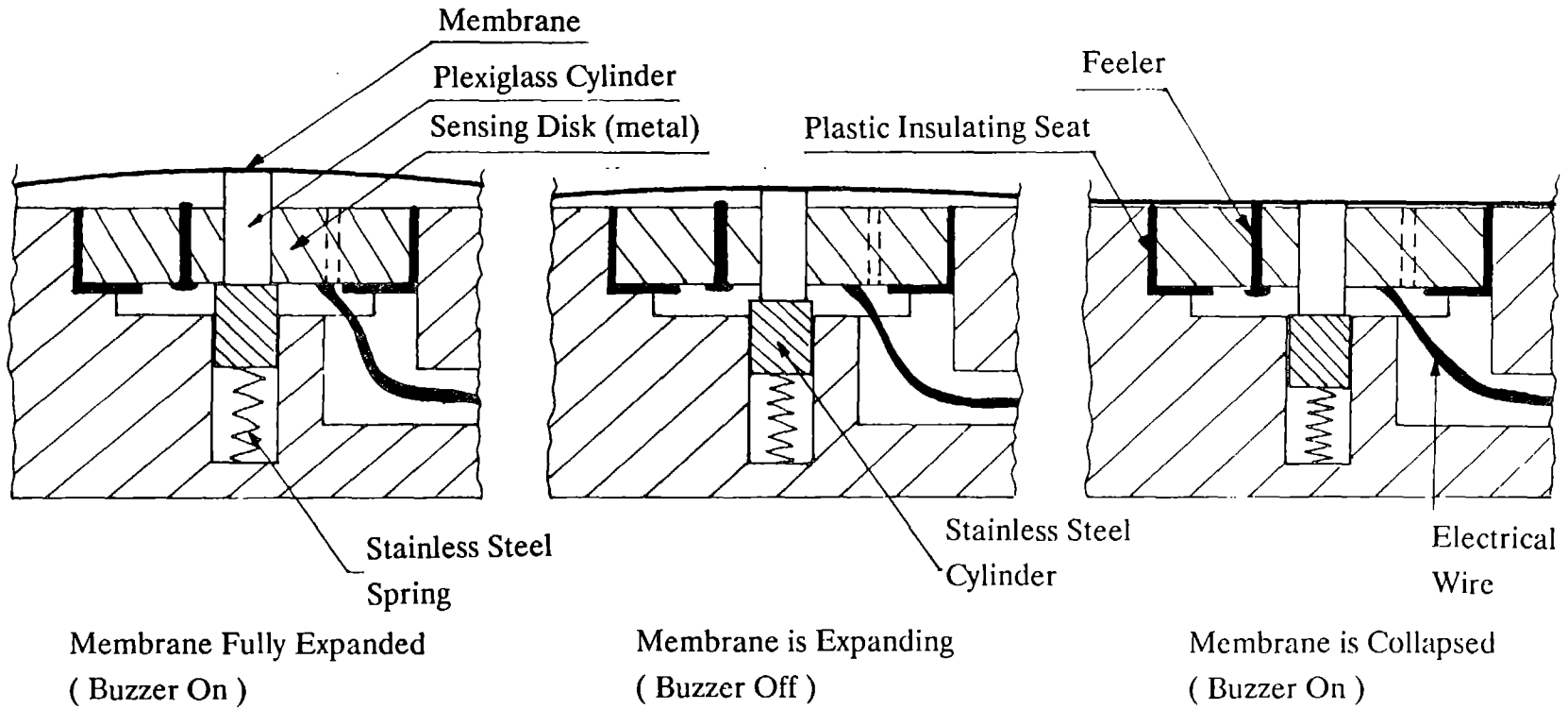
DETAIL A (ELECTRIC SWITCH)

FIG. 1.5. Components of the DMT Blade

<u>A-Pressure or p_0</u>

The A-pressure is the gas pressure against the inside of the membrane when the center of the membrane has lifted above its support and moved horizontally 0.05 (+0.02,-0.00) mm into the soil surrounding the vertical blade.

<u>B-Pressure or p_1</u>

The B-pressure is the gas pressure against the inside of the membrane when the center of the membrane has lifted above its support and moved horizontally 1.10 ± 0.03mm into the soil surrounding the vertical blade.

<u>C-Pressure or p_2</u>

The C-pressure is the gas pressure against the inside of the membrane obtained by slowly deflating the membrane (after the A and B pressure readings) until contact is reestablished (membrane is flushed with the side of the blade).

1.3 Soils Suited for a DMT

The DMT is best used in soils which are finer than gravelly sands. It is not recommended in soils which have penetration obstructions such as rock layers, concretions, cobbles, cemented zones, large shells (bouldery glacial sediments or gravelly deposits). The previous soils resist penetration and may damage the blade and the membrane.

Table 1.1 prepared by Schmertmann (1988) will help to appreciate the suitability of the DMT for a given soil.

TABLE 1.1. Suitability of DMT in Different Types of Soil (From Schmertmann 1988)

Suitability ranking: 0 = do not use DMT   2 = good

                      1 = sometimes suitable   3 = best application

                    Note: Hammer-driving alters the DMT results and decreases the accuracy of correlations.

Soil Type	Weak, Loose [*] $N_{SPT} < 5$[***] $q_c < 15$[****]		Medium $N_{SPT} = 25$[***] $q_c = 75$[****]		Stiff, Dense [**] $N_{SPT} > 40$[***] $q_c > 150$[****]	
	Fills Dumped, Pumped	Natural	Fills Light cmpxn	Natural	Fills Heavy cmpxn	Natural
Clays	3	3	2	2	2	2
Silts	2	2	2	2	1	1
Sands	3	3	2	2	1	1
Gravel, lg. shell and concretions	1	1	0	0	0	0
Cobbles	0	0	0	0	0	0
Rocks (weathered)	0	1	0	0	0	0
CL+SI+SD	3	3	3	2	2	2
CL+SI+SD+Shell	2	2	2	2	0	0
CL+SI+SD+Rock	1	1	1[**]	1[**]	0	0
Sand+Gravel	2	2	2[**]	1[**]	0	0
Organic CL+SD	3	3	2	2	1	1
Residual w/o rock	3	3	2	2	1	1
Residual w rock	1	1	0	1[**]	0	0
Cemented sand	-	1	-	1[**]	-	0
Tallus with rock	-	1	-	1[**]	-	0
Glacial till	0	1	0	0	0	0
Varved Clays	3	2	2	2	1	1
Loess	3	2	2	2	-	-
Peats	3*	2*	2	2	-	-
Slimes, tailings	3*	-	2	-	-	-

*   Sensitive testing in very weak soils.

**   High risk of damage; use high strength blade and membrane.

*** N_{SPT} = Standard Penetration Test blow count: Blows/ft.

**** q_c = Cone Penetrometer point resistance: bars.

2. COMPONENTS

2.1 Flat Dilatometer Blade

The **flat dilatometer blade** is a stainless steel blade with an expandable circular steel membrane mounted flush on one face. The blade is also fitted with a three position electric switch which indicates three phases in the membrane expansion (figure 1.5):

* "Collapsed" (expansion < 0.05 mm).
* "Expanding" (0.05 mm $\leq$ expansion < 1.10 mm).
* "Fully expanded" (expansion $\geq$ 1.10 mm).

(The A reading corresponds to 0.05 mm expansion, and the B pressure corresponds to 1.10 mm expansion.)

The shape and dimensions of the blade are presented in figure 1.4. According to the ASTM suggested method (Schmertmann 1986a) "the blade should have no discernible bend, defined as a clearance of 0.5mm or more under a 150 mm straight edge placed along the blade parallel to its axis. Its penetrating edge should not deviate more than 2 mm from the axis of the rods to which the blade attaches."

The **circular membrane** is made of stainless steel and is screwed to the blade. Its dimensions are presented in figure 1.4. There are two kinds of membrane:

* The S (standard) type is relatively soft and should only be used when the thrust necessary to advance the blade is less than 2 tons or when the hammer blowcount is less than 5 blows per inch of penetration, in order to avoid damage.
* The H (high strength) type is strong, can be used in any soil, and is much less susceptible to damage than the S type. The H type therefore provides the best overall service (Schmertmann 1988).

The **electric switch** is constituted of a sensing disc, a plastic insulating seat, a plexiglass cylinder, a stainless steel cylinder, a feeler, and a stainless steel spring. The way this switch works is described in figure 1.5.

2.2 Push Rods

Push rods are used to transfer the thrust from the pushing equipment to the blade. Cone Penetrometer Test (CPT) rods or drill rods can be used, providing the necessary adaptors are available. The recommended tolerances for the CPT rods are the following:

* The deflection at the mid-point of a 1 m push rod shall not exceed 0.5 mm for the five lowest push rods, and 1 mm for the remainder.

8

* For any pair of connected push-rods, the deflection at the joint shall also not exceed these limits.

2.3 Pneumatic-Electrical Cable

The pneumatic-electrical cable (p-e cable) is made of a spring-temper stainless steel wire enclosed within nylon tubing with special connectors at either end (figure 2.1). It transmits gas pressure and electric continuity from the control unit to the blade. There are three types of p-e cables (figure 2.1):

* The non-extendable type.
* The extendable type.
* The short Connector cable.

These cables are quite stiff and should not be twisted in order to prevent damage to the wire. The operator should always choose the shortest possible cable to minimize this problem.

2.4 Control Unit (and Calibration Unit)

The control unit is used to monitor the A, B, and C pressures at each test depth. There are several types of control units (two of them are described in detail by Schmertmann 1988) which typically include one (or two) manually read bourdon gage(s), a pressure source quick connect, a quick connect for the pneumatic-electric cable, an electrical ground cable connection, a galvanometer and an audio buzzer signal which indicates when to read the A, B and C pressures, and valves to control gas flow and vent the system. The buzzer and the galvanometer are activated by the electric switch built-in the blade as follows:

. Buzzer and galvanometer on: membrane expansion < 0.05 mm or
                                                      membrane expansion $\geq$ 1.10 mm.

. Buzzer and galvanometer off: $0.05 \leq$ membrane expansion < 1.10 mm.

A typical control unit is shown in figure 2.2. For measuring membrane calibrations (section 3.1) a calibration unit is required, which consists of a low range sensitive Bourdon gage and a large syringe to accurately pressurize (or depressurize) the membrane. The calibration unit can be built in the control unit or clipped in the control unit.

Male Stainless
Steel Terminal

Female Stainless
Steel Terminal

Single End Shut-Off
(Quick Connect)

1. Nylon Tubing
2. Stainless Steel Wire
3. Tube Connector Nut
4. PVC Insulator
5. PVC Retainer
6. Plastic Washer
7. Tube Connector Union
8. Single End Shut Off
9. Brass Nut

Short Connector Cable

Extendable Cable

Non-Extendable Cable

FIG. 2.1. Components of the Pneumatic-Electrical Cables

Pressure Source
Quick Connect

Auxiliary
Connector

Audio
Switch

Audio
Buzzer

Galvanometer

Circuit Test
Button

Ground Cable
Plug-in

Main On/Off
Flow Valve

Low-Range Gage
(Protected by
Reglator)

High-Range
Gage

Micrometer
Flow Valve

P-e Cable
Quick Connect
to Blade

Calibration Quick-Connect
For Syringe

Pressure
Circuit

Presure
Regulator

Micrometer
Vent Valve

Toggle Vent
Valve

R_1

Auxiliary
Connector

Audio Buzzer

Galvanometer

R_2

R_3

Circuit Test
Button

Battery (9 V)

Blade Electric
Switch

ELECTRIC CIRCUIT

FIG. 2.2. Control Unit

11

2.5 Insertion and Pushing versus Driving

In order to force the flat dilatometer blade into the soil, the use of a hydraulic jacking system, or a hammer is required. The preferred method is to push the DMT rather than to drive it. The procedures in this manual are based on pushed DMT results unless otherwise specified. Usually, the thrust capacity needed (or number of blows/inch) varies between 2 tons (5 blows/inch) for soft soils and 15 tons (45 blows/inch) for very hard soils. Because the value of the thrust force is a useful quantity (required for some soil parameters' determination, such as the friction angle) it is desirable to measure this force with a load cell. This load cell is usually located at the top of the rods, under the hydraulic jacking system. The penetration rate should be about 2 cm/s like the cone penetrometer.

The best available equipment is the CPT equipment mounted in a heavy duty truck (15 to 20 tons of thrust) with a dead weight of 20 tons to provide the necessary reaction. The CPT truck usually has a working cabin which is air-conditioned for the comfort of the operating crew. The limitation is that if refusal is reached, drilling is required before resuming to push the DMT; drilling is not possible with a cone truck.

Other hydraulic jacking systems can be mounted on lighter trucks or trailers which can be equipped with earth screw anchors to provide the necessary reaction (5 to 15 tons thrust). Drill rigs can also be used to push the blade and to bore through impenetrable soil or rock layers above the layer(s) to be tested. Drill rigs usually provide reactions varying between 2 to 5 tons but can be anchored to provide reaction up to 20 tons.

Driving the blade may be accomplished by using a hammer such as the one used in the standard penetration test SPT (ASTM D-1586). However, Schmertmann (1988) stated that the method of penetration affects the test results, and that quasi-static push (CPT equipment) best minimizes this effect. Therefore a hydraulic jacking system should be preferred.

The difference between pushing and driving was studied by Briaud (1991) who showed experimentally that the initial horizontal pressure σ_{hi} on a driven pressuremeter is very different from the initial horizontal pressure on a pushed pressuremeter. In a stiff clay σ_{hi} from driven insertion was 2.5 times smaller than σ_{hi} from pushed insertion (average of 2 tests). In a medium dense sand, the trend was reversed and σ_{hi} from driven insertion was 4.3 times larger than σ_{hi} from pushed insertion (average of 2 tests).

Basnett (1991) makes the following comments on driving versus pushing the DMT based on a detailed comparison of driven DMT versus pushed DMT performed by

Davidson et al. (1988). Driving the blade generally reduces the A and B pressures proportionally but the C pressure appears unaffected by driving in free draining soils. The driving effect is most prevalent in loose to very loose sand deposits. Different hammer drop heights (6 in. compared to 18 in.) did not conclusively demonstrate different reductions in A and B pressures. More research is still needed in this area.

If the driving technique is used, it is recommended that as a minimum 2 soundings be performed side by side: one by pushing and one by driving. This would give a site and soil specific correlation which would allow to get back to the parameters obtained from correlations based on the pushing insertion (with added imprecision, however). At this time, the pushing insertion should be preferred.

2.6 Pressure Source

In order to expand the DMT membrane, a gas pressure source is necessary. The membrane and the gas source must be air dry or moisture will condense in the blade. The best suited gas is Dry Nitrogen. This gas is contained in tanks which should be equipped with a pressure regulator to protect the DMT equipment. The regulator should regulate the pressure to supply no more than the control unit gage(s) range or 80 bars, whichever is less.

3. CALIBRATION, PREPARATION

3.1 Calibration

In air, under atmospheric pressure, the membrane is naturally lifted above its support between the A position at 0.05 mm expansion and the B position at 1.10 mm expansion, and the buzzer of the control unit is off as explained in section 2.4. The gas pressure necessary to overcome the membrane stiffness and move it in air to both the A position and B position are referred to as ΔA and ΔB respectively; they are not negligible. The calibration procedure consists in obtaining the ΔA and ΔB pressures in order to correct the A, B and C readings (section 1.2) to account for membrane stiffness.

To perform the calibration in air, the operator progressively applies a vacuum behind the membrane until the buzzer of the control unit activates (membrane expansion < 0.05 mm). Then he slowly releases the vacuum and reads the ΔA pressure when the buzzer stops (expansion = 0.05 mm). In order to obtain ΔB, the operator progressively applies a positive pressure behind the membrane and reads the ΔB pressure when the buzzer activates (expansion = 1.10 mm). This procedure should be repeated several times for consistency (the calibration values of an undamaged membrane remain relatively constant during a calibration and during a DMT sounding), and the average ΔA and ΔB should be recorded. The detailed calibration procedure is equipment specific and is not described here. The reader is referred to Schmertmann's (1988) report where a detailed calibration procedure can be found.

The ΔA_{avg} pressure is added to the A and C pressures as a positive correction (sections 5.1.2 and 5.1.3), and the ΔB_{avg} pressure is subtracted from the B-pressure as a negative correction (section 5.1.1).

The calibration values depend on the membrane type: they are higher for the H type than for the S type. The expected calibration values for both types are presented in table 3.1. Calibration values outside these ranges indicate that the membrane is damaged or requires exercise (section 3.2). In any case a DMT test should not be performed if the calibration values do not fall within expected ranges.

If a load cell is to be used to measure the thrust force, it should be calibrated properly and regularly.

3.2 Exercising the Membrane

New membranes usually have calibration values outside of the expected range (table 3.1). Also, the calibration values of a new unexercised membrane usually vary during a DMT sounding or during calibration. The solution to these problems is to exercise the membrane. To do so, the operator repeatedly pressurizes (do not pressurize beyond 6 bars for an S membrane and 20 bars for an H membrane) and depressurizes the membrane, increasing ΔA and decreasing ΔB until they fall within the recommended values of table 3.1.

At the end of this process, the final ΔA value of H membranes is usually too high. In this case, the operator may not be able to start a DMT test because the soil pressure acting against the membrane might be less than the ΔA pressure (buzzer stays off). To solve this problem the operator must use a plastic hammer to knock the edge of the membrane back down in order to reduce ΔA (do not hit the center of the membrane).

TABLE 3.1. Expected Calibration Values (from Schmertmann 1988)

Membrane Type	ΔA Calibration (bars)			ΔB Calibration (bars)		
	Minimum	Maximum	Average	Minimum	Maximum	Average
Standard "S"	0.10	0.20	0.13	0.10	0.70	0.35
Hard "H"	0.10	0.25	0.19	0.10*	1.50	0.90**

* $\Delta B < 0.30$ is unusual for "H" membranes and may indicate damage.

** considerable variation

15

4. RUNNING THE TEST

At this time ASTM is proceeding with the development of an ASTM standard for the DMT test (Lutenegger, chairman). A suggested method for performing the flat dilatometer test was published in 1986 and represent the work of committee D18.02 (Schmertmann, 1986a). The following procedure is a step by step abbreviated version of that method.

4.1 Test Procedure

1. If the equipment used to push the blade is a hydraulic jacking system which transfers the thrust by a clamping system (CPT equipment), it is recommended to pre-thread the p-e cable (Pneumatic-Electrical cable) through the push rods (do not twist the cable in the process) as shown in figure 4.1.
   If the equipment used to push the blade transfers the load to a thrust head on top of the push rods, or if a hammer is used to drive the blade, the p-e cable should be left outside of the push rods and taped to them every 1 meter during the test as shown in figure 4.2.

2. Connect the p-e cable to the blade, and connect the blade to the first push rod. If the cable is to be taped on the rods, insert the cable exit adaptor between the blade and the first push rod as shown in figure 4.2.

3. Prepare the control unit and the pressure source for the test (this step is equipment specific and is therefore not described here; see Schmertmann, 1988).

4. Connect the other end of the p-e cable to the control unit.

5. Connect the ground cable at the control unit "ground" and clip the other end to the push-rods or the truck chassis.

6. Check electrical continuity by pressing on the membrane (the buzzer signal of the control unit should activate).

7. Perform the membrane calibration in air (section 3.1) and record ΔA and ΔB.

8. Record the gage zeros, the rod type, the type of friction reducer and the blade serial number.

9. Advance the blade to the desired test depth (at a constant rate of 2 cm/s if using a CPT pushing equipment) and record the thrust required to advance the blade, or the hammer blowcount (recording the thrust is not necessary but is very desirable). If the thrust necessary to advance the blade exceeds 5 tons or if the hammer blowcount exceeds 15 blows per inch of penetration, the risk of

16
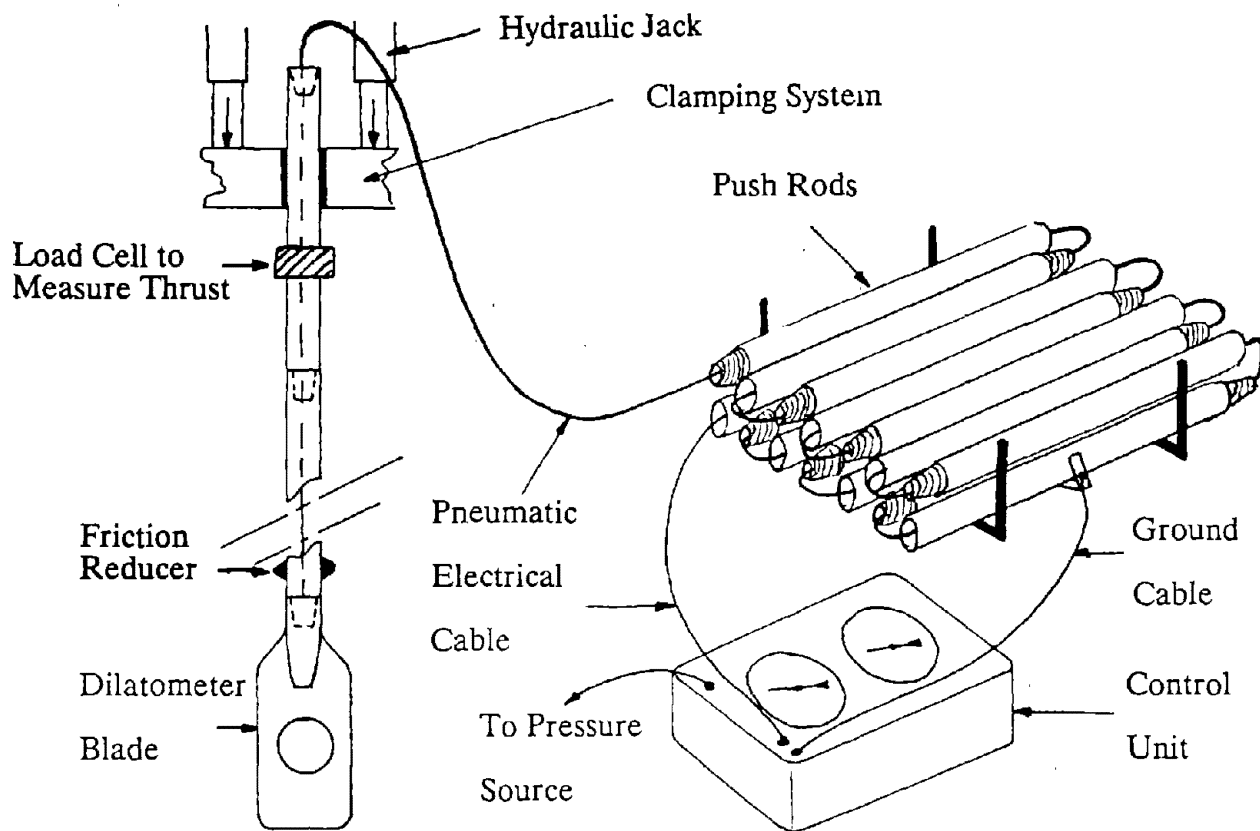
FIG. 4.1. DMT Equipment Preparation
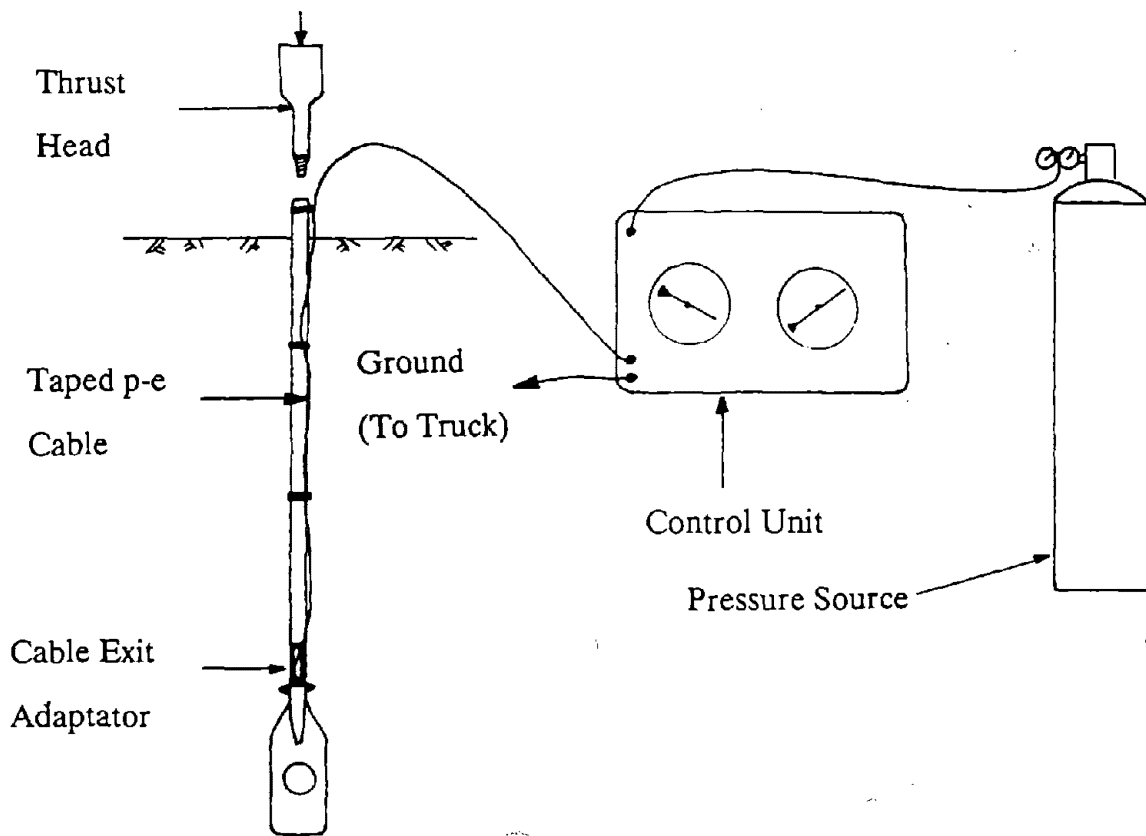
FIG. 4.2. DMT Equipment Preparation

equipment damage becomes significant. In this case it is recommended to predrill down to the test depth. Then the blade can be pushed at least 15 cm ahead of the bottom of the drilled hole.

10. Release the load on the rods (the buzzer should be on). Start the test within 15 seconds after reaching the test depth. Apply a positive pressure behind the membrane. As the pressure rises take the A-reading when the buzzer signal stops. Do not stop at this time, keep on increasing the pressure and take the B-reading when the buzzer reactivates. Then vent the pressure rapidly until the buzzer signal stops. Failure to vent the pressure immediately after the buzzer sounds will allow continued expansion of the membrane and possible damage. Then release slowly the remaining pressure and read the C-pressure when the buzzer reactivates (the meaning of the buzzer signal is explained in section 2.4). Record the A, B and C pressures on the field data sheet (table 4.1). Step 10 should be performed in less than 2 minutes. (This step is equipment specific and is not described in detail here; see Schmertmann 1988).

Note: the C reading is not necessarily taken every 20 cm. It is taken at least every 2 to 3 m. When possible it is performed in the most cohesionless lenses (high material index I_d, see section 5.1.4). In clay deposits the C reading is taken while deflating very slowly, perhaps 3 min to go from the B reading to the C reading. This is to allow water to fill the gap.

11. Advance the blade to the next test depth as in step 9, and repeat step 10.

12. Retrieve the blade without delay when the test is over.

13. Perform the membrane calibration in air, and record the values. Check them against the initial values from step 7, and record the average ΔA_{avg} and ΔB_{avg} on the field data sheet.

Note: As Basnett (1991) points out, one will not obtain the C pressure until the (hydrostatic) pore pressure overcomes the compressive membrane stiffness. This membrane stiffness corresponds to 1.3 to 1.9 m of water pressure depending on the membrane type. Until this water pressure occurs, one can apply vacuum in order to obtain the C pressure.

TABLE 4.1. DMT DATA SHEET

DILATOMETER SDG. NO.:   DATE: CLIENT:

Location: Blade No.:   DMT Operator:

Low Gage Zero (bars): ΔA_{avg} (bars):   Rig Operator:

High Gage Zero (bars): ΔB_{avg} (bars):   Rig Type:

GWT depth (m):   Casing Depth (m):   Rod Type:

Predrill Depth (m):   Membrane Type: Frict. Red. Diam. (cm):

Depth ( )	Thrust or blows/ 30 cm ( )	A (Bars)	Time (sec)	B (Bars)	Time (sec)	C (Bars)	Time (sec)	Depth ( )	Thrust or blows/ 30 cm ( )	A (Bars)	Time (sec)	B (Bars)	Time (sec)	C (Bars)	Time (sec)
		ΔA	ΔB												

Notes:

4.2 Problems That May Occur During The Test

4.2.1 Membrane Damage

Damage to the membrane mainly occurs when penetrating through gravel, large shells, miscellaneous fill, rocks, etc. Membrane damage can be diagnosed during the test when:

. it is impossible to obtain the A or B readings even at high pressure,
. the buzzer does not activate after advancing the blade,
. it is impossible to maintain pressure,
. the test readings are erratic, choppy, high or low,
. the pressure suddenly decreases.

In any case, the blade must be retrieved and cleaned because of the possibility of water and soil ingress. The damaged membrane can be replaced in the field, providing the blade does not need to be cleaned.

4.2.2 Cable Damage

When the cable is taped on the rods, it can be damaged. Cable damage can be diagnosed when:

. the buzzer stays on continuously (short below water table) or stays off continuously (cable is cut), and pressure drops,
. it is impossible to maintain pressure.

It is very difficult to repair a p-e cable in the field. Therefore it is recommended to bring a back up p-e cable to the field.

4.2.3 Blade Damage

The blade damages that may occur are:

. denting of the blade's leading edge (repairable in the field),
. bending of the blade (not repairable in the field),
. breaking of the rod-blade connection (loss of the blade)

Schmertmann (1988) proposed the following table which will help to avoid blade damages:

Thrust P (tons)	SPT 140 Lb Hammer Blowcount N (Blows/inch)	Risk of Damage
P < 2	N < 5	Very Little
P = 5	N = 15	Significant
P > 10	N > 30	High

4.2.4 Push Rod Buckling

In very loose or soft soils such as swamps or backwater organic deposits, silty hydraulic fill, or loose sand, rods can buckle when being pushed into the soil. One way to avoid this problem is to limit the thrust applied on the rods.

4.2.5 Reaction Force Exceeded

This problem may occur during a test and may be due to the presence of a hard layer. One way to prevent this from happening is to reduce the friction along the rods. A friction reducer should always be used; it is usually made of an enlarged ring around the rods near the blade. It is located approximately 350 mm above the tip edge of the blade (figure 1.3).

4.3 DMT Dissipation Test

The dilatometer test has the potential of providing estimates of the in situ horizontal coefficient of consolidation C_h from dissipation tests (section 6.11 and figure 6.24). The dissipation test which makes use of the C reading is called the DMTC dissipation test and can be performed at any depth as suggested in the following procedure by Robertson et al. (1988):

1. After penetration to the test depth, follow the normal sequence of A-B-C readings. Start a stopwatch at the instant of the thrust release. Note the time elapsed at the moment of the C-pressure reading and record the data.

2. Repeat the test sequence to obtain reasonably spaced data points for the curve obtained in step 3 below. A factor of 2 increase in time at each C-pressure reading test is satisfactory. (i.e. C-pressure readings at 1, 2, 4, 8, 15, 30 min after the instant of the thrust release).

3. Plot the C-pressure against a square root of time scale, making at least enough measurements to find C_{50}, the pressure at 50% of the dissipation to the equilibrium C pressure, C_{100} (see section 6.11 and figure 6.26).

21

This procedure is based on the assumption that the C pressure is the pore pressure. While data exists to prove that point (Lutenegger and Kabir, 1988, Robertson et al. 1988), others have not found a clear relationship (Powell and Uglow, 1988). Mrachetti and Tottani (1989) propose another approach to obtain C_L. This approach makes use of the A reading and is called the DMTA dissipation test. The procedure is identical to the DMTC procedure except that only the A reading is taken.

1. The stopwatch is started when the DMT reaches the desired depth. The A reading is taken after an elapsed time t_o of 0.5 minute. The pressure is released back to zero, omitting the expansion to get the B and C readings.

2. Step one is repeated for an elapsed time t_o equal to 1, 2, 4, 8, 15, 30 minutes.

3. Plot the A pressure versus $\log t$ (see section 6.11).

5. REDUCING THE DATA

5.1 Data Reduction

The data collected for each test consist of the A-pressure, the B-pressure and the C-pressure; these data are recorded every so often as a function of depth. These data must be corrected in order to obtain the corrected A-pressure p_o, the corrected B-pressure p_1, and the corrected C-pressure p_2.

5.1.1 Corrected B-pressure, p_1

The B-pressure measured during a DMT test is the gas pressure against the inside of the membrane required to push the center of the membrane 1.10 mm into the surrounding soil. This B-pressure needs to be corrected to account for the effect of membrane stiffness (section 3.1) and for the gage pressure deviation from zero when vented to atmospheric pressure. The net soil pressure p_1 at 1.10 mm expansion of the membrane is:

$$p_1 = B - Z_M - \Delta B \qquad (5.1)$$

where:

Z_M = the pressure gage reading when vented to atmospheric pressure.

ΔB = the gage pressure inside the membrane required to overcome the stiffness of the membrane and move it outward to a center-expansion of 1.10 mm into the air.

5.1.2 Corrected A-pressure p_o

The A-pressure measured during a DMT test is the gas pressure against the inside of the membrane required to move the center of the membrane horizontally 0.05 mm into the surrounding soil. The pressure p_o is the net soil pressure against the membrane immediately before its expansion into the soil (0.00 mm expansion). In order to obtain p_o, it is necessary to correct the A-pressure to account for the effect of membrane stiffness, the 0.05 mm expansion itself, and the gage pressure deviation from zero when vented to atmospheric pressure. If the relationship between the pressure at the soil-membrane interface and the membrane displacement is assumed to be linear (figure 5.1), p_o can be calculated as follows:

$$p_o = 1.05(A - Z_M + \Delta A) - 0.05(B - Z_M - \Delta B) \qquad (5.2)$$
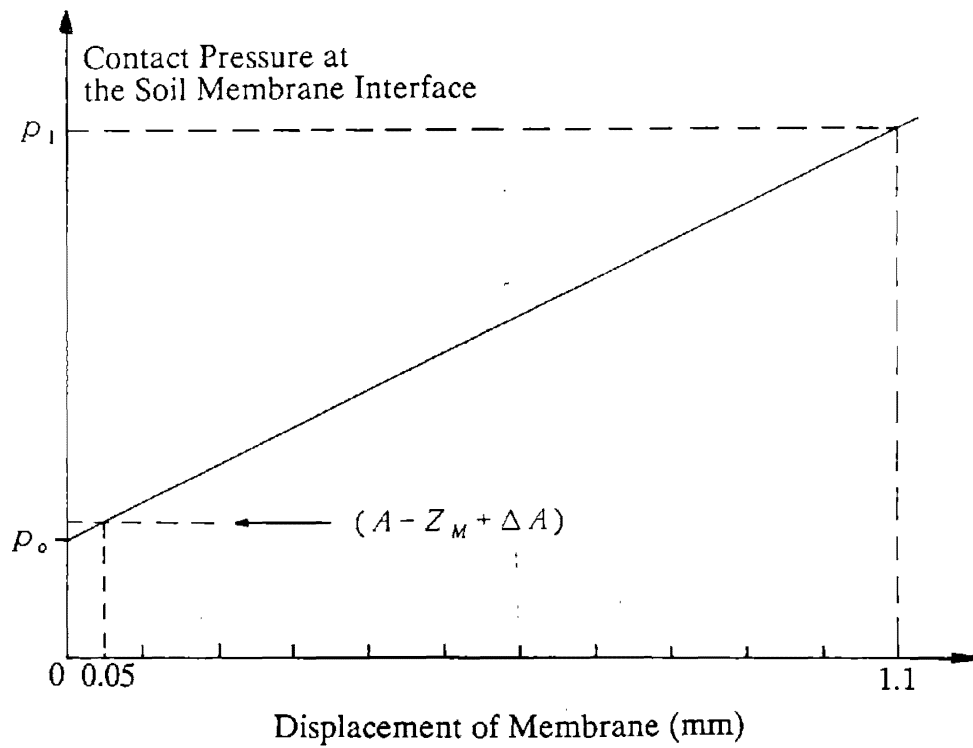
where:

23

FIG. 5.1. Linear Extrapolation to Estimate p_o at Zero Displacement (After Marchetti and Crapps 1981)

Z_M, ΔB = defined as before.

ΔA = the gage pressure inside the membrane required to overcome the stiffness of the membrane and move it outward to a center-expansion of 0.05 mm into the air.

5.1.3 Corrected C-pressure p_2

Following the normal pressure expansion sequence to obtain the conventional DMT A and B pressures, an additional pressure reading (C-pressure) may be taken to obtain the pressure at which the membrane comes back to 0.05 mm expansion during controlled deflation. This pressure reading, corrected for membrane stiffness and for the gage pressure deviation from zero when vented to the atmospheric pressure, gives a pressure referred to as p_2 such that:

$$p_2 = C - Z_M + \Delta A \tag{5.3}$$

where Z_M and ΔA are defined as before.

5.1.4 Dilatometer Modulus E_D, Material Index I_D, Horizontal Stress Index K_D, Pore Pressure Index U_D

If the membrane expansion into the surrounding soil is modelled as the flexible loading of a circular area at the surface of an elastic half space, having a Young's modulus E and a Poison's ratio μ, the outward movement S of the center of the membrane subjected to a normal pressure Δp is (Gravesen, 1960):

$$S = \frac{4 \cdot R \cdot \Delta p}{\pi} \frac{(1 - \mu^2)}{E} \tag{5.4}$$

where:

R = radius of the membrane = 30 mm.

Δp = applied pressure.

The ratio $E / (1 - \mu^2)$ is termed the dilatometer modulus E_D and is calculated by replacing S = 1.10 mm and $\Delta p = p_1 - p_o$ in equation 5.4:

$$E_D = 34.7 (p_1 - p_o) \tag{5.5}$$

The normalized lateral stress on the blade is called the horizontal stress index, K_D:

$$K_D = \frac{p_o - u_o}{\sigma'_{vo}} \tag{5.6}$$

25

where:

σ'_{vo} = vertical effective stress.

u_o = pre-insertion water pressure.

p_o = corrected A-pressure.

The material index I_D (mainly used to estimate soil stratigraphy and soil type) is:

$$I_D = \frac{p_1 - p_o}{p_o - u_o} \qquad (5.7)$$

where p_1, p_o, u_o are defined as before.

The pore pressure index U_D (mainly used to help classifying the soil type) has been defined by Lutenegger and Kabir (1988):

$$U_D = \frac{p_2 - u_o}{p_o - u_o} \qquad (5.8)$$

where p_2, p_o, u_o are defined as before.

5.2 Data Presentation, and Report

5.2.1 Data Presentation (table 5.1 and figures 5.2-5.3)

1. A-pressure versus depth.
2. B-pressure versus depth.
3. C-pressure versus depth.
4. Average calibration values: $\Delta A_{avg}, \Delta B_{avg}$.
5. Corrected A-pressure p_o versus depth.
6. Corrected B-pressure p_1 versus depth.
7. Corrected C-pressure p_2 versus depth.
8. Thrust
9. Dilatometer modulus E_D versus depth.
10. Material index I_D versus depth.
11. Horizontal stress index K_D versus depth.
12. Pore pressure index U_D versus depth.

TABLE 5.1. DATA REDUCTION SHEET

Test Location: Low Gage Zero: Blade Number:

Sounding Number: High Gage Zero: Rod Type:

Date: ΔA_{avg}:   Diam. Frict. Red.:

Client: ΔB_{avg}:   Rig Operator:

Depth ( )	Corrected Readings						Thrust or blows/30 cm	Dilatometer Index			
	p_o ( )	Time (sec.)	p_1 ( )	Time (sec.)	p_2 ( )	Time (sec.)	Q ( )	E_D	I_D	K_D	U_D

27

DATA REDUCTION SHEET

Test Location: TAMU, sand site   Low Gage Zero: 0.025 bars   Blade Number: TAMU 3

Sounding Number: SD2   High Gage Zero: 0.025 bars   Rod Type: NW

Date: July 5, 1990 ΔA_{avg} : 0.15 bars   Diam. Frict. Red.: 58.4 mm

Client: Texas A&M University ΔB_{avg} : 1.35 bars   Rig Operation: Mr. Dean

| Depth		Gage Readings			Corrected Readings			Dilatometer Index		
(m)	(ft)	A (bars)	B (bars)	C (bars)	p_o (bars)	p_1 (bars)	p_2 (bars)	E_D (bars)	I_D	K_D
	4	5.6	10.6	0	5.6	9	0.15	117.9	0.61	20.7
	9	5.6	13.0	0	5.4	11.4	0.15	208.2	1.11	9.8
	14	5.5	13.4	0	5.3	11.8	0.15	225.5	1.23	6.6
	19	5	18.2	0	4.5	16.6	0.15	419.9	2.68	4.3
	24	10.8	18.2	3.2	10.6	16.6	3.35	208.2	0.56	8.5
	29	12	29.5	0.05	11.3	27.9	0.20	576.1	1.47	8.2
	34	11.2	31.2	0.05	10.4	29.6	0.20	666.2	1.85	7.0
	39	13	35	0.1	12.1	33.4	0.25	739.1	1.84	7.6
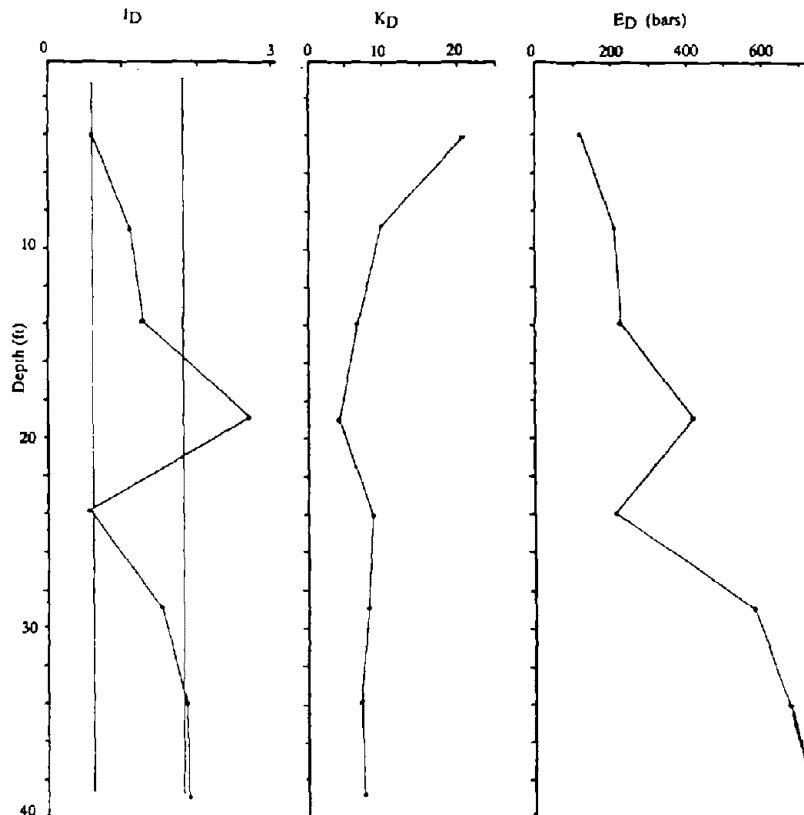
FIG. 5.2. Data Presentation (Texas A&M University; Sand Site)

28

DATA REDUCTION SHEET

Test Location: TAMU, clay site   Low Gage Zero: 0.025 bars   Blade Number: TAMU 3

Sounding Number: CD1   High Gage Zero: 0.025 bars   Rod Type: NW

Date: July 6, 1990 ΔA_{avg}: 0.10 bars   Diam. Frict. Red.: 58.4 mm

Client: Texas A&M University ΔB_{avg}: 1.35 bars   Rig Operation: Mr. Dean

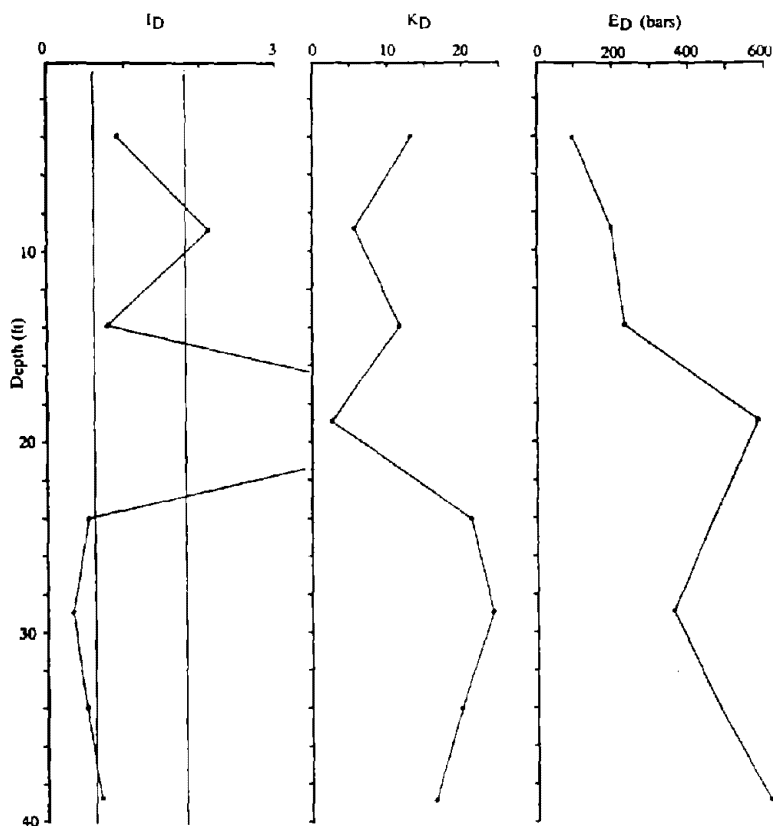| Depth		Gage Readings			Corrected Readings			Dilatometer Index		
(m)	(ft)	A (bars)	B (bars)	C (bars)	P_o (bars)	P_1 (bars)	P_2 (bars)	E_D (bars)	I_D	K_D
	4	3	7.2	0.03	2.9	5.6	0.13	93.7	0.93	13.2
	9	2.9	10	0	2.7	8.4	0.1	197.8	2.11	5.7
	14	9	17	2.1	8.7	15.4	2.2	232.5	0.77	11.6
	19	3.4	21	0	2.7	19.4	0.1	579.5	6.18	2.7
	24	26.5	41	9.2	25.9	39.4	9.3	468.5	0.52	21.3
	29	33	44.6	9.6	32.6	43.0	9.7	360.9	0.32	24.2
	34	29	43.8	9.0	28.4	42.2	9.1	478.9	0.49	19.3
	39	27.2	45.6	4.6	26.4	44.0	4.7	610.7	0.68	16.4

FIG. 5.3. Data Presentation (Texas A&M University; Clay Site)

13. The date and the time of the test, and the name of the firm.
14. The number of the test and its location.
15. Any abnormal interruption of the test procedure (section 4.1).
16. The identification number of the blade.

5.2.2 Report

The report should include all the information described in section 5.2.1. In addition the following information should be included:
1. The pushing equipment used.
2. The maximum test inclination.
3. The name of the operator who performed the test.

6. INTERPRETATION OF THE DATA

A wealth of parameters can be obtained from the DMT through various procedures and correlations. The validity of those techniques is only as good as the size of the data base used to develop them, the similarity of geology between the data base and the particular application at hand, and the period of time over which the techniques have been used. Because the DMT is a relatively recent device, some of these procedures are likely to evolve in the future. These procedures are presented in sequence. The order in which the parameters are presented is not tied to any particular order of reliability. Wherever possible appropriate notes of caution have been inserted.

6.1 Penetration Pore Water Pressure

The corrected C-pressure p_2 is obtained by slowly deflating the dilatometer membrane (after the A and B pressure readings) until the buzzer is reactivated (contact is reestablished), and is usually measured about 1 minute after the testing depth is reached. The pressure p_2 has been compared with the pore pressure. The contention is that upon deflation of the DMT membrane, a gap opens between the DMT membrane and the soil, this gap fills with water and the DMT membrane feels the pore water pressure.

A piezoblade is a flat blade modified by replacing the membrane with a flush mounted porous stone/transducer system in the same position. This porous stone allows to measure the pore pressure. Lutenegger and Kabir (1988) compared p_2 values measured 1 minute after the testing depth was reached, with penetration pore pressures $u = u_o + u_e$ measured with a piezoblade immediately after the testing depth was reached, at the same locations (where u_o is the equilibrium pore pressure, and u_e is the excess pore pressure generated around the blade during penetration).

In cohesive soils, they found that the value of p_2 is a very close approximation of the penetration pore pressure u, especially in soft clay. After examining more than 100 data points (figure 6.1) they concluded that the value of p_2 is within about 5% of the penetration pore pressure value for cohesive soils.

In sand, Lutenegger (1988) and Robertson et al. (1988a) found that the p_2 pressure is equal to the equilibrium pore pressure u_o (figure 6.2). This is due to the fact that significant drainage occurs in sand 1 minute after penetration and that the equilibrium pore pressure u_o is reestablished by the time the p_2 pressure is measured.
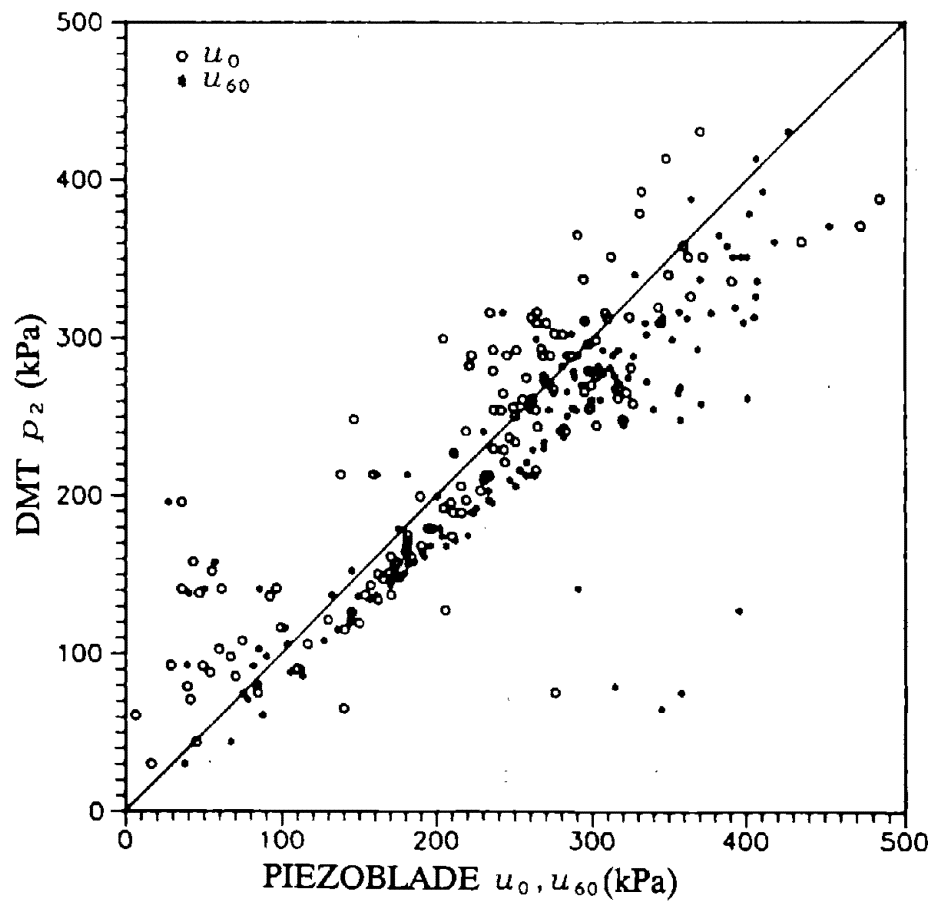
31

FIG. 6.1. Comparison Between Piezoblade u_{excess} and DMT p_2 (From Lutenegger and Kabir, 1988)
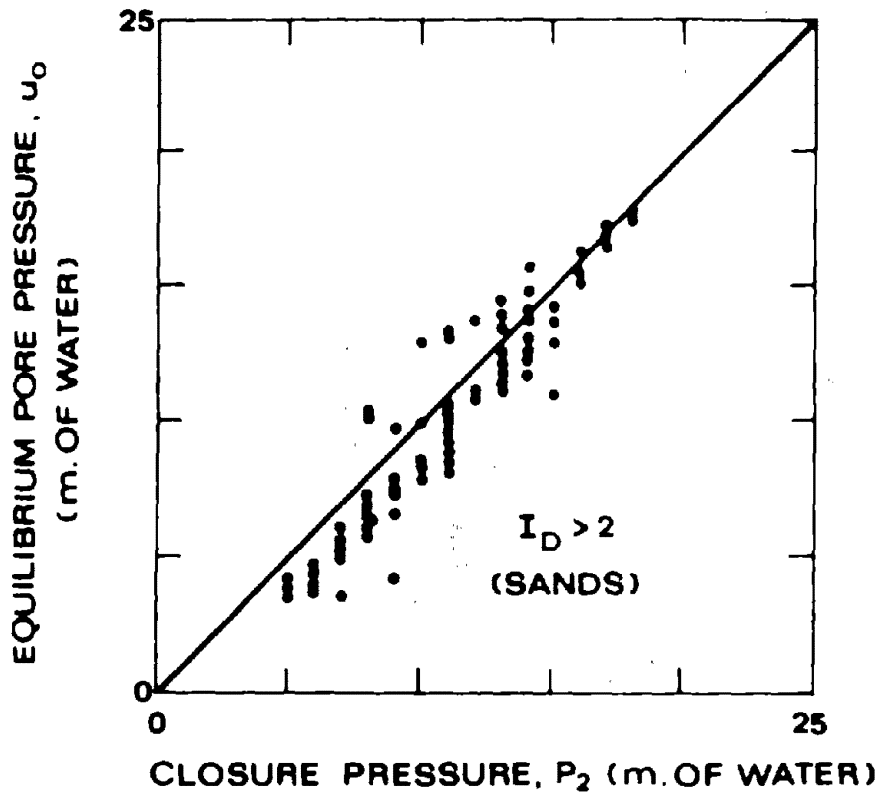
FIG. 6.2. Comparison of Closing Pressures and Equilibrium Static Pore Pressures in Sand (From Robertson et al. 1988)

Basnett (1991) suggests that a plot of p_2 versus depth can be used to obtain fairly accurate water table measurement as well as changes in soil type (e.g. OC clay, OC sand) by negative pore pressure differences.

Marchetti (1991) considers that obtaining pore pressure for DMT is still a controversial issue.

6.2 Coefficient of lateral earth pressure K_o

Clay

It is not possible to measure the pre-insertion in situ lateral stress directly with a dilatometer because the blade insertion disturbs the soil. However, empirical correlations have been proposed between the coefficient of lateral earth pressure K_o and the dilatometer horizontal stress index K_D.

Marchetti (1980) proposed the following relationship based on tests in Italian clays:

$$K_o = \left(\frac{K_D}{1.5}\right)^{0.47} - 0.6 \qquad (6.1)$$

This relationship is based on a comparison between 21 DMT and 21 laboratory tests on Italian clays, and is only recommended for soft and medium to stiff uncemented clays having $I_D \leq 1.2$ (Jamiolkowski et al. 1988).

However, several authors (Lacasse and Lunne 1988, Lunne et al. 1989) suggested that Marchetti's (1980) correlation needed some modification in order to fit the latest available data bases (figure 6.3). Also, Lunne et al. (1990) and Powell and Uglow (1988) showed that the correlation between K_D and K_o was different for young (< 60,000 years) and old (> 70 million years) clays.

In an attempt to implement the previous comments, Lunne et al. (1990) proposed:

$$\text{Young clays:} \quad K_o = 0.34 K_D^{0.54} (S_u/\sigma'_{vo} \leq 0.5) \qquad (6.2)$$

$$\text{Old clays:} \quad K_o = 0.68 K_D^{0.54} (S_u/\sigma'_{vo} > 0.8) \qquad (6.3)$$

Lunne's (1990) relationship for young clay compares well with the relationship proposed by Lacasse and Lunne (1988), which is based on results from ten test sites in Norway:

$$K_o = 0.34 K_D^m \quad for K_D < 4 \qquad (6.4)$$

where:

m = coefficient varying between 0.44 (highly plastic clay) and 0.64 (low plastic clay).
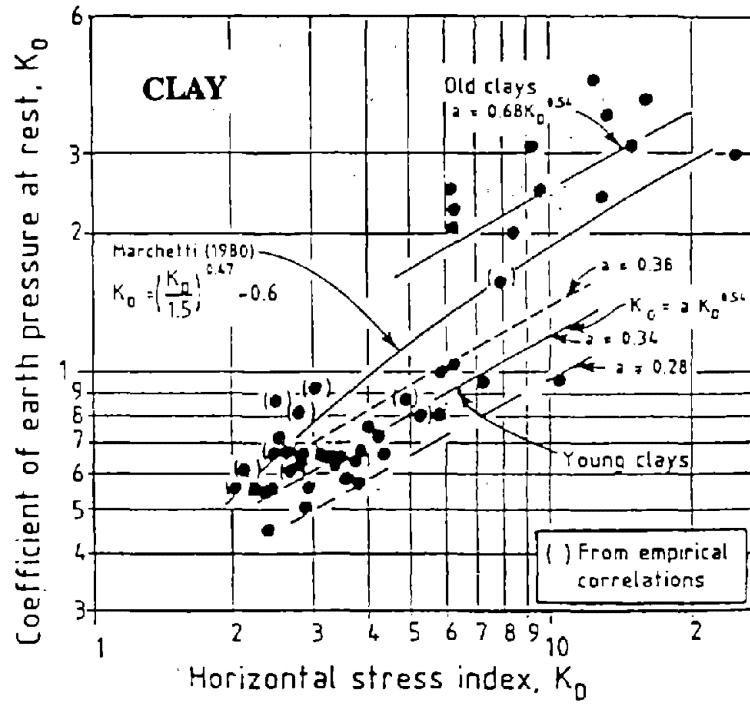
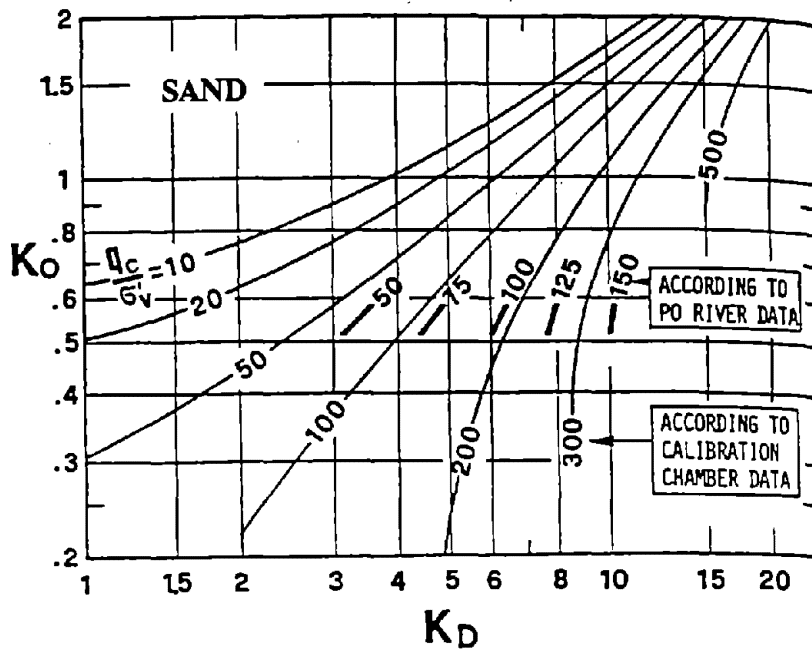**FIG. 6.3.** K_o from Dilatometer Horizontal Stress Index K_D (From Lunne et al. 1989)

FIG. 6.4. Chart for Interpreting K_0 from K_D (DMT) and q_c, With a Dual Scale:
1. According to Calibration Chamber Data, 2. According to Po River Data
(From Marchetti, 1985)

Therefore, it is recommended to use Lunne's (1990) method (equations 6.2 and 6.3) for soft and medium to stiff uncemented clays having $I_D \leq 1.2$ and $K_D < 4$.

Sand

Schmertmann (1983) proposed to estimate K_o of uncemented sands using the following equation:

$$K_o = \frac{40 + 23K_D - 86K_D(1 - \sin\phi'_{ax}) + 152(1 - \sin\phi'_{ax}) - 717(1 - \sin\phi'_{ax})^2}{192 - 717(1 - \sin\phi'_{ax})} \qquad (6.5)$$

where:

K_D = dilatometer horizontal stress index

ϕ'_{ax} = axisymmetric friction angle calculated from the plane-strain angle obtained in the dilatometer test (section 6.5)

Since Schmertmann method is complex, Lacasse and Lunne (1988) recommend to use Marchetti's (1985) chart (figure 6.4) to obtain a first estimate of the lateral stress. Marchetti's method requires to obtain q_c values from an adjacent cone penetrometer test. This method is based on calibration chamber tests as well as 25 tests in the Po river sand.

6.3 Soil Classification

Based on test results collected on different soil types it has been found that the material index I_D is a parameter which is dependent on the prevailing grain size of a soil (Marchetti, 1980), relatively independent of OCR (Marchetti, 1980) and independent of the degree of saturation of a soil (Lutenegger 1988, Schmertmann 1982, Lacasse and Lunne 1986). Therefore, the correlation of I_D versus soil type presented by Marchetti (1980) (table 6.1) can be expected to provide a good estimate of the soil type.

Marchetti and Crapps (1981) proposed an extended version of table 6.1 which can also be used for the determination of soil type (figure 6.5). Lutenegger (1991) points out that the profiles of p_o and p_1 versus depth can be very helpful with soil classification and stratigraphy.

Figure 6.6 presented by Davidson and Boghrat (1983) shows that the degree of dissipation of excess pore water pressure generated during penetration of the blade depends on the soil type: very little drainage occurs in clay while significant drainage occurs in sand after 1 minute penetration. Since the value of the closing pressure p_2 (usually measured 1 minute after penetration) is very similar to the initial pressure u_o plus the excess pore water pressure generated on the DMT membrane (1 minute after penetration),

36

TABLE 6.1. Soil Classification Based on I_D (From Marchetti 1980)

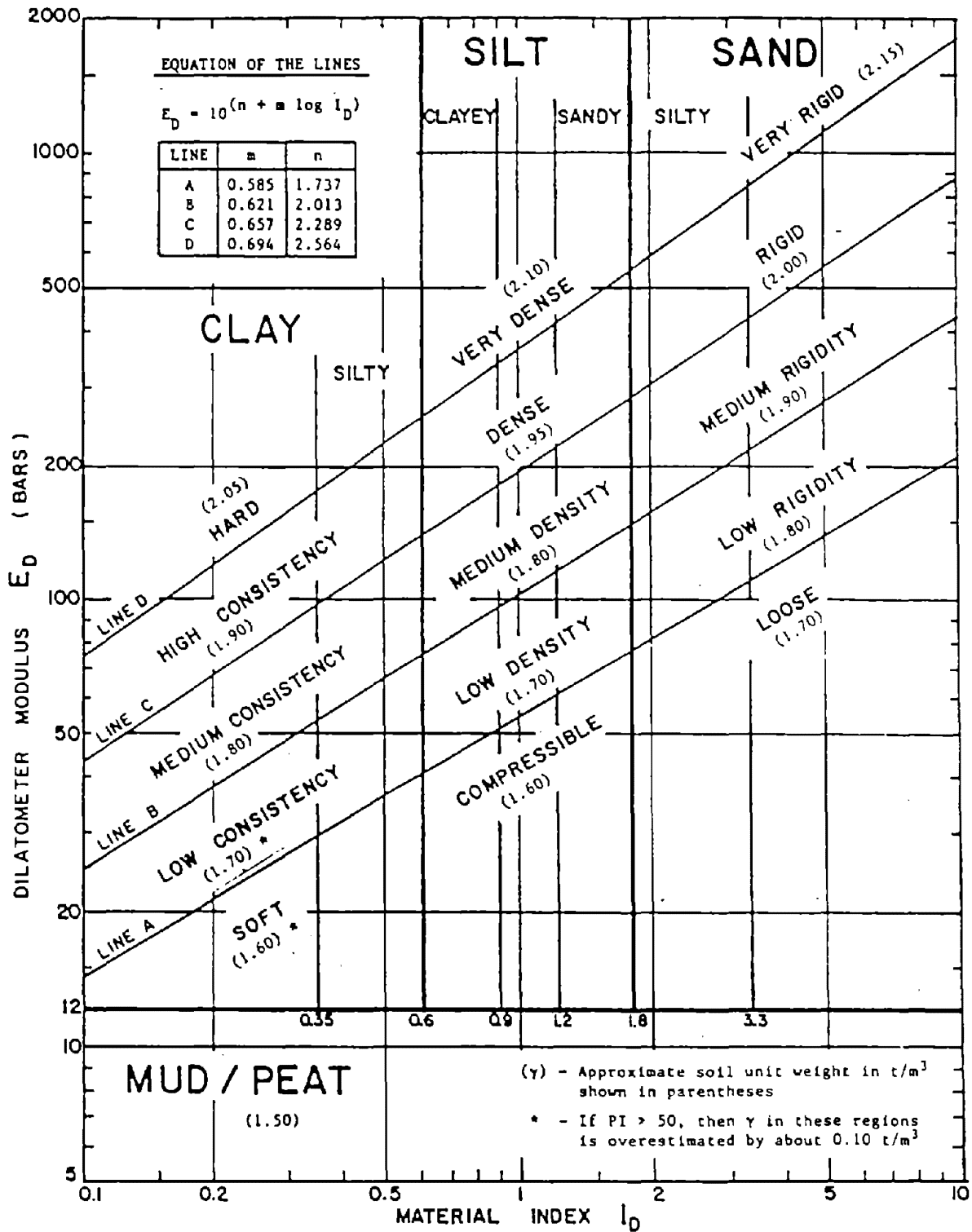| Soil Type	Material Index
Peat / Sensitive Clays	< 0.10
Clay	0.10 - 0.35
Silty Clay	0.35 - 0.60
Clayey Silt	0.60 - 0.90
Silt	0.90 - 1.20
Sandy Silt	1.20 - 1.80
Silty Sand	1.80 - 3.30
Sand	> 3.30

FIG. 6.5. Chart for Determination of Soil Description and Unit Weight (From Marchetti and Crapps 1981)
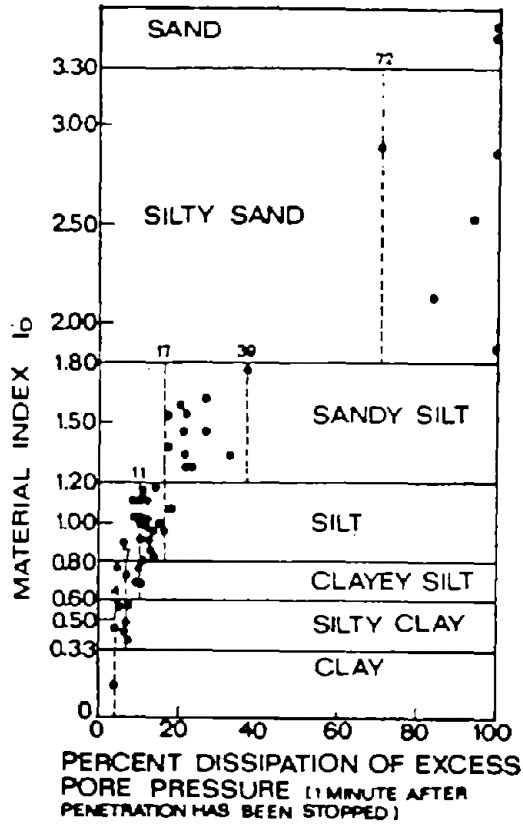
38

FIG. 6.6. Degree of Dissipation of Excess Pore Water Pressure 1 Minute After Penetration as a Function of I_D (From Davidson and Boghrat 1983)
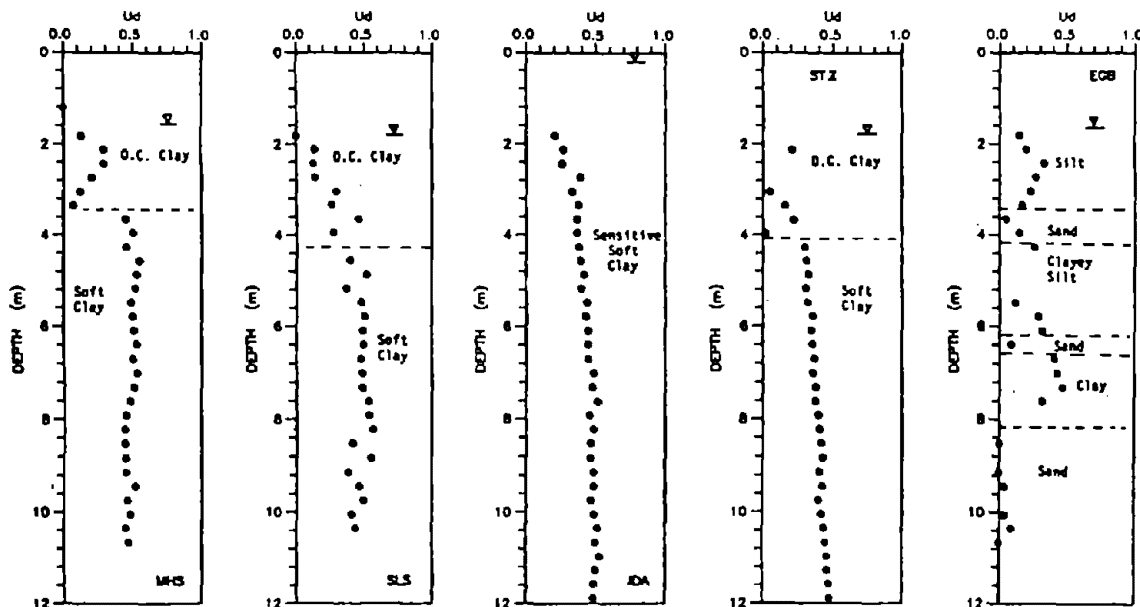

FIG. 6.7. Profile of U_D to Help Determine Site Stratigraphy (From Lutenegger and Kabir 1988)

39

Lutenegger and Kabir (1988) proposed to compare p_2 to the DMT p_o reading (measured immediately after penetration) in order to obtain an initial indication of stratigraphy. They defined the DMT pore pressure index U_D as follows:

$$U_D = \frac{p_2 - u_o}{p_o - u_o} \qquad (6.6)$$

where u_o = hydrostatic pressure.

In sands where the excess pore pressure dissipates quickly, U_D should be very low $(0 < U_D < 0.2)$ because p_2 is very similar to u_o. On the other hand in clays U_D should be higher.

Lutenegger and Kabir (1988) stated that " the U_D ratio can be useful for identifying changes in stratigraphy " as illustrated in figure 6.7. However, no relationship between U_D and soil type has been proposed yet.
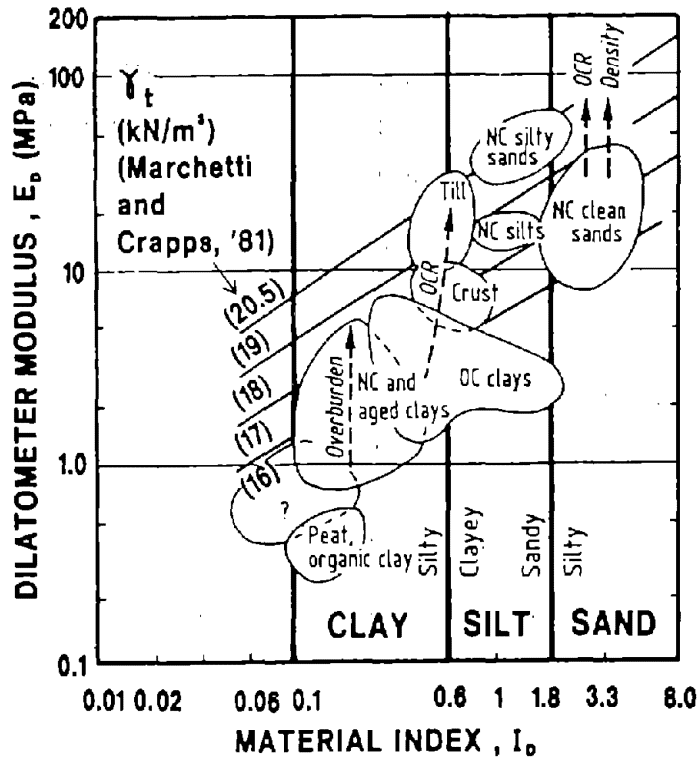
6.4 Unit Weight

Marchetti and Crapps (1981) presented a chart for predicting the unit weight of a soil, which makes use of the material index I_D and E_D (figure 6.5). This chart was later adapted by Lacasse and Lunne (1988) to account for the effect of OCR on I_D and E_D (figure 6.8). The same chart was evaluated by comparing the unit weight predicted by Marchetti's (1981) chart and reference unit weights measured in the laboratory (figure 6.9). Lacasse and Lunne (1988) concluded that figures 6.5 and 6.8 tend to underpredict the unit weight in soft clays.

6.5 Drained Friction Angle in Cohesionless Soils

The penetration of the DMT blade in sands represents a drained bearing capacity failure approximating a plane-strain condition. Therefore any drained friction angle determined from DMT results is a plane strain parameter: ϕ'_{ps}.

Schmertmann (1982) presented a method to estimate ϕ'_{ps} based on the vertical equilibrium of the DMT and the rods during penetration and on the wedge penetration theory developed by Durgunoglu and Mitchell (1975). In this equation the coefficient of friction between the blade and the soil is assumed to be equal to $\tan(\phi'_{ps}/2)$. Schmertmann's procedure requires the measurement of the thrust necessary to advance the dilatometer blade and rods.

For drained soils with $I_D \geq 1.2$ Schmertmann proposed:

NC = Normally consolidated

OC = Overconsolidated

FIG. 6.8 Classification Chart for Soils Tested. Effect of Overburden, Overconsolidation Ratio and Density (From Lacasse and Lunne 1988)
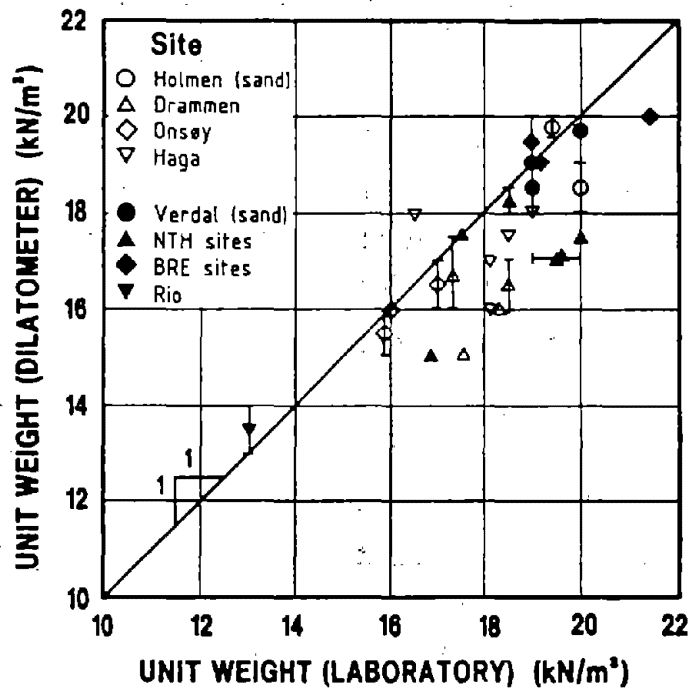

FIG. 6.9. Prediction of In Situ Unit Weight From Dilatometer Parameters (From Lacasse and Lunne 1988)

$$\tan(\phi'_{ps}/2) = [\text{THRUST} - (\pi/4) \cdot \text{DIAM}^2 \cdot u_o \cdot 1.019$$

$$- (A + (\pi/4) \cdot d^2 - B \cdot d) \cdot q_f + W \cdot (Z + 2)]/F_H \qquad (6.7)$$

where:

ϕ'_{ps} = drained friction angle of the soil - plane strain

THRUST = insertion thrust (kg)

DIAM = drill rod diameter (cm)

u_o = pore water pressure prior to insertion of the dilatometer (bars)

A = bearing area of the dilatometer (12.9 or 14.4 cm^2)

d = diameter of the friction reducer (cm)

B = thickness of the dilatometer (1.37 or 1.5 cm)

q_f = Durgunoglu and Mitchell bearing capacity (kg/cm^2) found as explained in the following paragraph

W = drill rod weight per unit length (kg/m)

Z = test depth (m)

F_H = horizontal force normal to the dilatometer blade

$= (p_o - u_o) \times a \times 1.019$ where a is the blade friction area (355 cm^2)

p_o = corrected dilatometer "A" reading (bars)

Durgunoglu and Mitchell (1975) proposed to estimate q_f as follows:

$$q_f = \gamma'_{AVG} \cdot B \cdot N_{\gamma q}/10 \qquad (6.8)$$

$$N_{\gamma q} = \frac{\cos(\psi - \delta)}{\cos \delta} \frac{(1 + \sin \phi'_{ps} \sin(2\gamma - \phi'_{ps}))}{\cos \phi'_{ps} \cos(\gamma - \phi'_{ps})} \left\{ \frac{\cos^2(\gamma - \phi'_{ps})}{4 \cos^2 \psi \cos^2 \theta} I_\theta \right.$$

$$+ \frac{3 \cos(\gamma - \phi'_{ps}) \cos^2 \beta}{4 \cos \psi \cos \phi'_{ps}} e^{2\theta_o \tan \phi'_{ps}} \left(m - \frac{2}{3}m' \right) - K \frac{\cos \psi \cos \phi'_{ps}}{\cos(\gamma - \phi'_{ps})}$$

$$\left. \cdot (m - m')^2 \cdot (m + 2m') + K \frac{\cos \psi \cos \phi'_{ps}}{\cos(\gamma - \phi'_{ps})} m^3 \right\} - \frac{\tan \psi}{4} \qquad (6.9)$$

$$m = D/B \qquad (6.10)$$

$$m' = \frac{\sin \beta \cos(\gamma - \phi'_{ps})}{2 \cos \psi \cos \phi'_{ps}} e^{\theta_o \tan \phi'_{ps}} \qquad (6.11)$$

$$\tan \gamma = (\sin \phi'_{ps} + \sqrt{1 + 2\cos \phi'_{ps}})/(2 + \cos \phi'_{ps}) \qquad (6.12)$$

$$\psi = 90° - \alpha \qquad (6.13)$$

42

$$\theta_o = 180° - (\psi + \gamma) + \beta \qquad (6.14)$$

$$I_\theta = \frac{1}{1 + 9\tan^2\phi'_{ps}} \left\{ 3\tan\phi'_{ps} \left(e^{3\theta_o \tan\phi'_{ps}} \cos\beta - \cos(\theta_o - \beta) \right) \right.$$

$$\left. + \left(e^{3\theta_o \tan\phi'_{ps}} \sin\beta + \sin(\theta_o - \beta) \right) \right\} \qquad (6.15)$$

where:

γ'_{AVG} = average effective unit weight for the soil above the dilatometer blade (t/m³)

$N_{\gamma q}$ = bearing capacity factor

ψ = penetrometer angle (figure 6.10)

α = half of dilatometer base angle; approx. 8 deg (figure 6.10)

β = angle to vertical tangency of failure surface (figure 6.10), assumed = ϕ'_{ps} (deg)

γ = angle of plane shear zone, originally an iterative solution but simplified by assumption for δ (figure 6.10)

δ = dilatometer to soil friction angle, = $\phi'_{ps}/2$ (deg) (figure 6.10)

m = ratio of dilatometer depth D to blade thickness

m' = ratio of distance between blade tip and vertical tangency of failure surface ("critical depth") to blade thickness

θ_o = defines logarithmic failure surface angle (deg) (figure 6.10)

K = coefficient of lateral earth pressure, assumed = K_o

The solution of equation 6.7 requires the following iterative procedure proposed by Schmertmann (1988):

1. Make an initial estimate for ϕ'_{ps}

2. Solve equations 6.10 - 6.15 for their respective parameters

3. Calculate K_o as shown in section 6.2

4. Substitute the parameters obtained in steps 2 and 3 into equation 6.9 to find $N_{\gamma q}$ bearing capacity factor

5. Find an average unit weight for the soil profile above the dilatometer and solve equation 6.8 for the bearing capacity

6. Calculate ϕ'_{ps} from equation 6.7

7. If the difference (calc. angle - assumed angle) is less than zero, then the assumed value was too low. If it is greater than zero, the assumed value was too high.
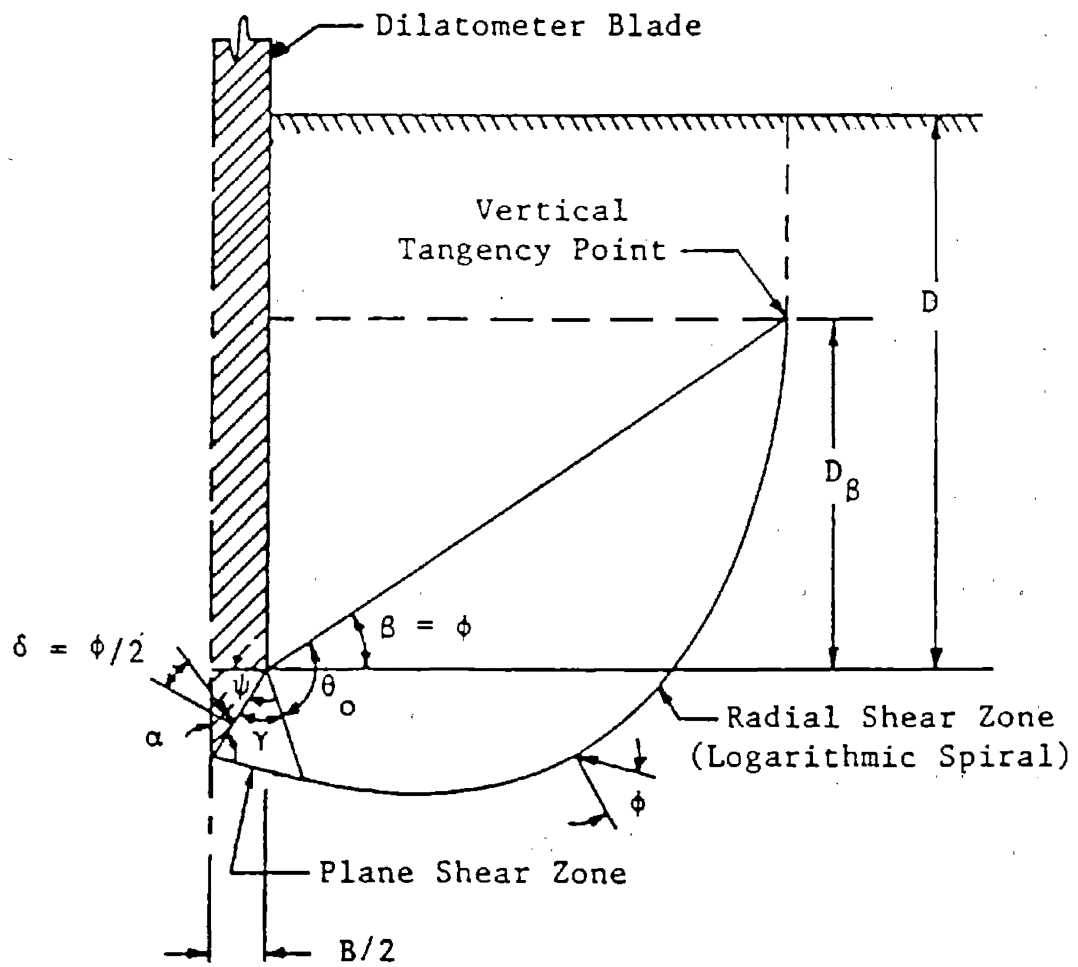
FIG. 6.10. Relationship of Bearing Capacity Parameters, Symbols Used and Assumed
Failure Planes (After Durgunoglu and Mitchell 1975)

8. Revise the angle estimated and repeat steps 1 - 7 until the difference between the assumed and calculated angle is < 1 degree. The final value may then be found by interpolation based on the error found in step 7.

The above method has been evaluated by several people. Using Schmertmann (1982) technique, Clough and Goeke (1986) obtained friction angle values for gravelly sand which were within 15% of the values obtained with laboratory triaxial compression tests. Jamiolkowski et al. (1988) stated that the Durgunoglu and Mitchell theory used in conjunction with the dilatometer wedge resistance, slightly underpredicts the value of ϕ'_{ps} (1 to 2 degrees lower than peak friction angle resulting from triaxial compression test) for silica sands. They found that the difference [$\phi'_{ps}(LAB) - \phi'_{ps}(DMT)$] increases with increasing sand density.

Schmertmann (1988) added that his method used for cemented and strongly dilatant sands usually yields friction angles in excess of the actual value.

Because of the non-linearity of the failure envelope, the angle ϕ'_{ps} is not uniquely defined, but depends on the magnitude of the effective normal stress σ'_{ff} on the failure plane at failure. Therefore any value of ϕ'_{ps} inferred on the basis of the DMT results corresponds to a secant angle of friction, whose magnitude is controlled by the average value of the effective normal stress σ'_{ff} acting on the failure plane around the penetration device. A knowledge of σ'_{ff} existing during the DMT test is necessary to link the ϕ'_{ps1} value inferred from a DMT with ϕ'_{ps2} of a specific design problem where a stress σ'_{ff2} exist on the failure plane. Schmertmann (1982) proposed:

$$\sigma'_{ff1} = (1 + \sin\phi'_{ps1}) \cdot \sigma'_{vo} \qquad (6.16)$$

where σ'_{vo} = vertical effective stress at the depth of the test.

Then the value of σ'_{ff2} is estimated for the problem considered and the friction angle ϕ'_{ps2} is obtained by using Baligh's (1976) work with a simplifying assumption:

$$\tan\phi'_{ps2} - \tan\phi'_{ps1} = 0.105\log\frac{(\sigma'_{ff1})}{(\sigma'_{ff2})} \qquad (6.17)$$

Schmertmann's method provides a drained plane strain friction angle which can be converted to an axisymmetric drained angle ϕ'_{ax} (Schmertmann, 1988):

$$for\,\phi'_{ps} \leq 32° \qquad \phi'_{ax} = \phi'_{ps} \qquad (6.18)$$
$$for\,\phi'_{ps} > 32° \qquad \phi'_{ax} = \phi'_{ps} - [(\phi'_{ps} - 32)/3] \qquad (6.19)$$

Marchetti (1985) presented a procedure to obtain ϕ'_{ps} which makes use of the cone resistance q_c measured during a neighboring cone penetration test, and K_o determined as explained in section 6.2 (figure 6.11). Lacasse and Lunne (1988) evaluated Marchetti's method and obtained friction angles comparing well with the results of drained triaxial compression tests. They recommended to use figure 6.11 to obtain the friction angle of sands.

6.6 Drained Constrained Modulus M

The drained constrained modulus M refers to the tangent modulus, as found from the vertical effective stress versus vertical strain curve obtained in a 1-dimensional oedometer laboratory test on high-quality samples. The modulus M is described in figure 6.12.

Sand

Marchetti (1980) presented a correlation between M and the dilatometer modulus E_D of the form:

$$M = R_M . E_D \tag{6.20}$$

where:

R_M = coefficient, function of the horizontal stress index K_D

If $I_D \leq 0.6$	$R_M = 0.14 + 2.36 \, \mathrm{Log} \, K_D$
If $I_D \geq 3.0$	$R_M = 0.5 + 2 \, \mathrm{Log} \, K_D$
If $0.6 < I_D < 3.0$	$R_M = R_{M,o} + (2.5 - R_{M,o}) \, \mathrm{Log} \, K_D$
	with $R_{M,o} = 0.14 + 0.15(I_D - 0.6)$
If $K_D > 10$	$R_M = 0.32 + 2.18 \, \mathrm{Log} \, K_D$

$$R_M \text{ is always} \geq 0.85$$

Baldi et al. (1986 and 1989) found that Marchetti's (1980) correlation underpredicts M, especially for O.C. sands (figure 6.13). As a result Leonard and Frost (1988) recommend to use $M = 1.3 M_{Marchetti}$ for NC sands and $M = 2.4 M_{Marchetti}$ for OC sands.

Marchetti (1991) disagrees with the need to factor $M_{Marchetti}$ for two reasons: 1) Schmertmann's evaluation of the shallow foundation settlement calculation method using $M_{Marchetti}$ gives a ratio of predicted over measured settlement equal to 1.18 (section 8.1.3); the above factors would make the average prediction unsafe, 2) the above factors come from calibration chamber tests where the sand may not be representative of natural sands.

Clay

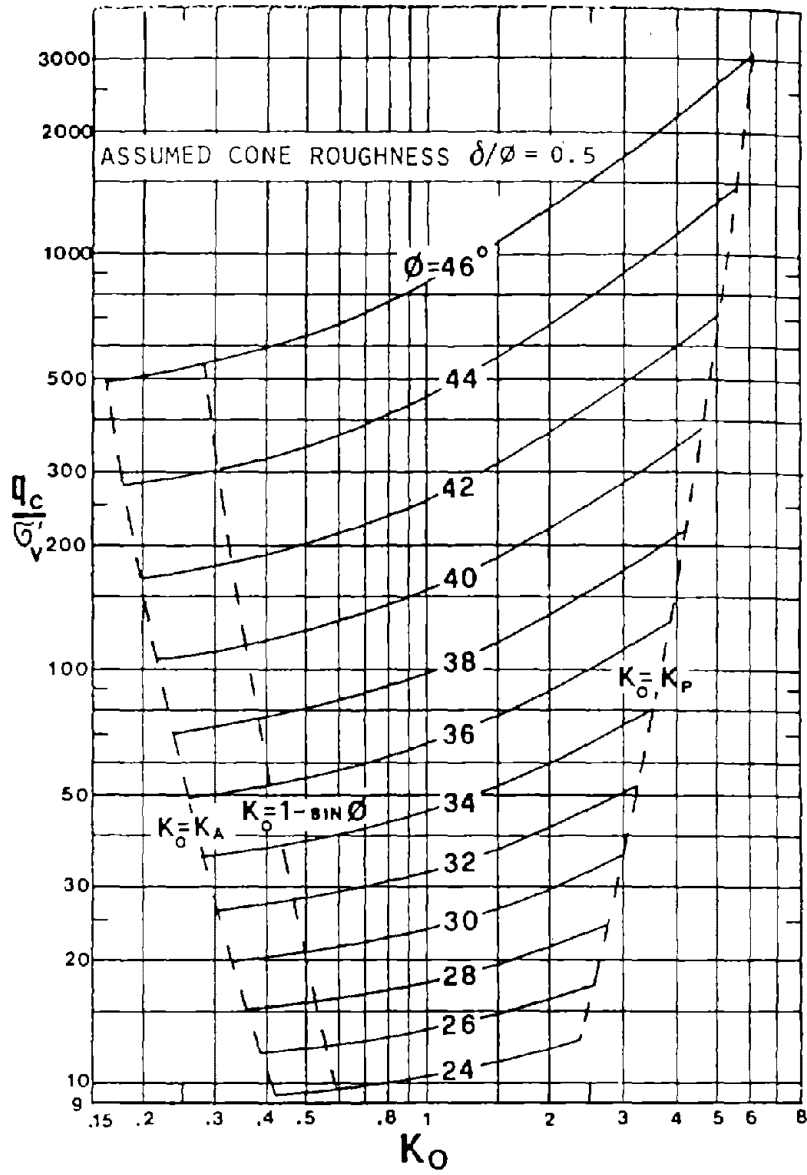Lunne et al. (1989) recommend to use Marchetti's (1980) correlation.

FIG. 6.11. Chart for Interpreting φ from CPT requiring an Evaluation of K_o (From Marchetti 1985)
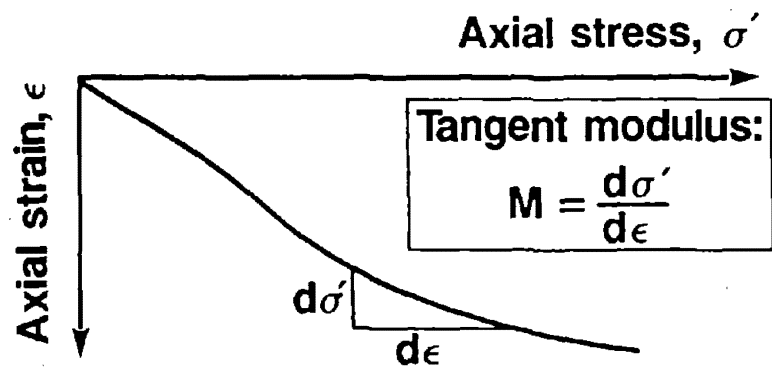
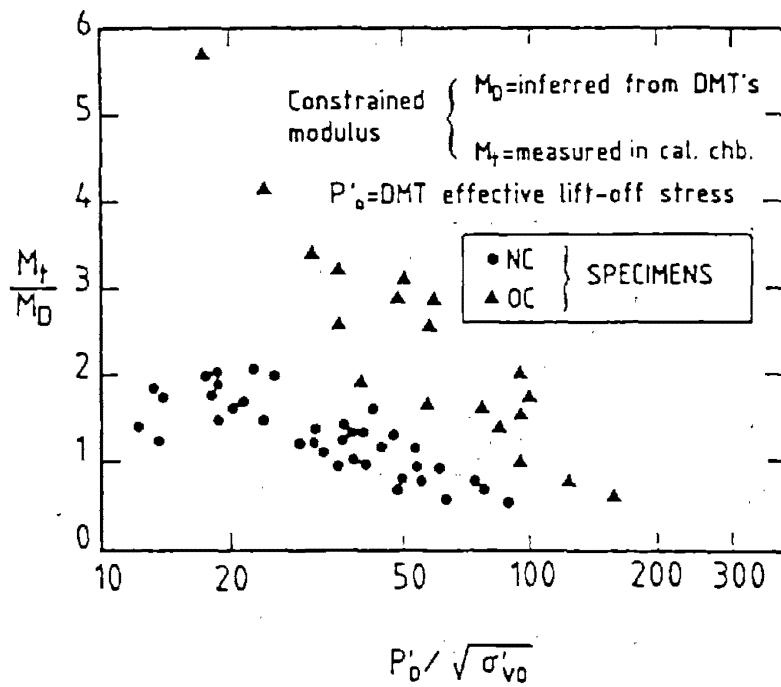FIG. 6.12. Definition of the Constrained Tangent Modulus M (From Sandven 1990)

FIG. 6.13. Constrained Tangent Modulus of Ticino Sand From Dilatometer Modulus
(From Baldi et al. 1989)

6.7 Elastic Modulus

To date, two values of the elastic modulus E have been investigated: 1. the secant Young's modulus at 25% of strength mobilization E_{25}, 2. the initial tangent modulus E_i. The reference E values were obtained from UU triaxial compression tests at confining pressures equal to the total horizontal stress estimated from the DMT. Evidence accumulated from several sources (Robertson et al. 1989a, Campanella et al. 1985, Baldi et al. 1986, Bellotti et al. 1989) suggests a simple relationship between E and the dilatometer modulus E_D:

$$E = F \cdot E_D \qquad (6.21)$$

Table 6.2 and figure 6.14 show the general trend for the F values. These values can be used to obtain a first estimate of E from equation 6.21.

6.8 Maximum Shear Modulus G_o

Sand

Lee and Stokoe (1986) argued that the maximum shear modulus G_o of cohesionless soils is mostly a function of the following variables:

$$G_o = f(D_R, \sigma'_a, \sigma'_b) \qquad (6.22)$$

where:

D_R = relative density

σ'_a = effective stress acting in direction of seismic wave propagation

σ'_b = effective stress acting in direction of soil particle displacement

Sully and Campanella (1989) acknowledged this fact and proposed to correlate G_o / E_D with the relative density D_R. They presented figure 6.15 which gathers most of the published data on sand. The data shown in figure 6.15 were obtained by comparing G_o measured during resonant column tests and cross hole tests, and the results of DMTs performed in a calibration chamber and in situ. This may explain the scatter in the data presented herein.

This method can be used to obtain a first estimate of G_o. However Sully and Campanella (1989) emphasized that "additional field data is required to verify the above points."

As an alternate to the previous method or maybe as a check, one can use figure 6.16 proposed by Baldi et al. (1989) which makes use of the effective lift-off pressure from the dilatometer $p'_o = (p_o - u_o)$ and the dilatometer modulus E_D.

TABLE 6.2. Suggested Correction Factor F (From Lutenegger 1988)

Soil Type	Modulus	F	Ref.
Cohesive soils	E_i	10	Robertson et al. (1989)
Sand	E_i	2	Robertson et al. (1989)
Sand	E_{25}	1	Campanella et al. (1985)
NC Sand	E_{25}	0.85	Baldi et al. (1986)
OC Sand	E_{25}	3.5	Baldi et al. (1986)

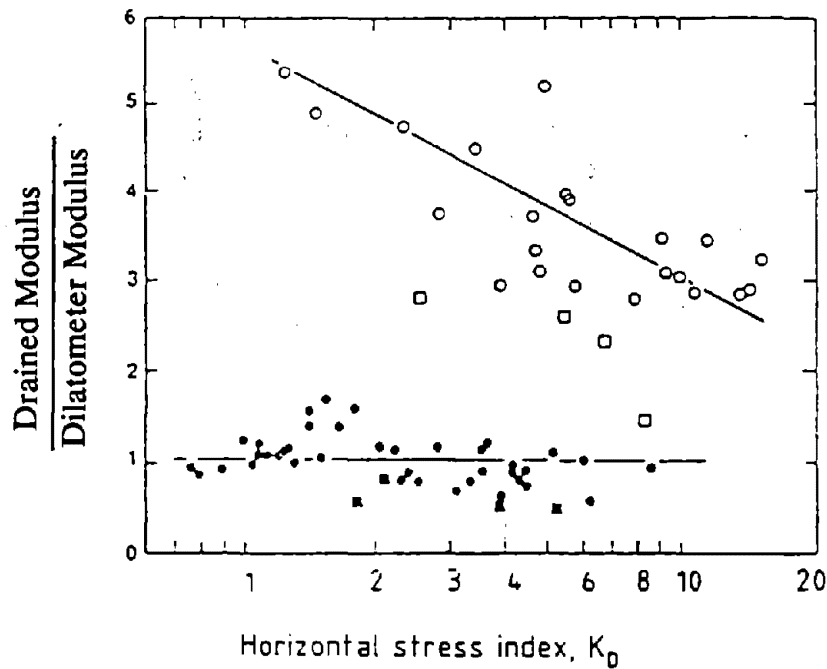| SAND	OCR	SYM
TICINO	1	●
	1.5 to 8.5	○
HOKKSUND	1	■
	3.0 to 8.3	□

FIG. 6.14. Evaluation of Drained Young's Modulus of Sand From Dilatometer test (From Belloti et al. 1989)
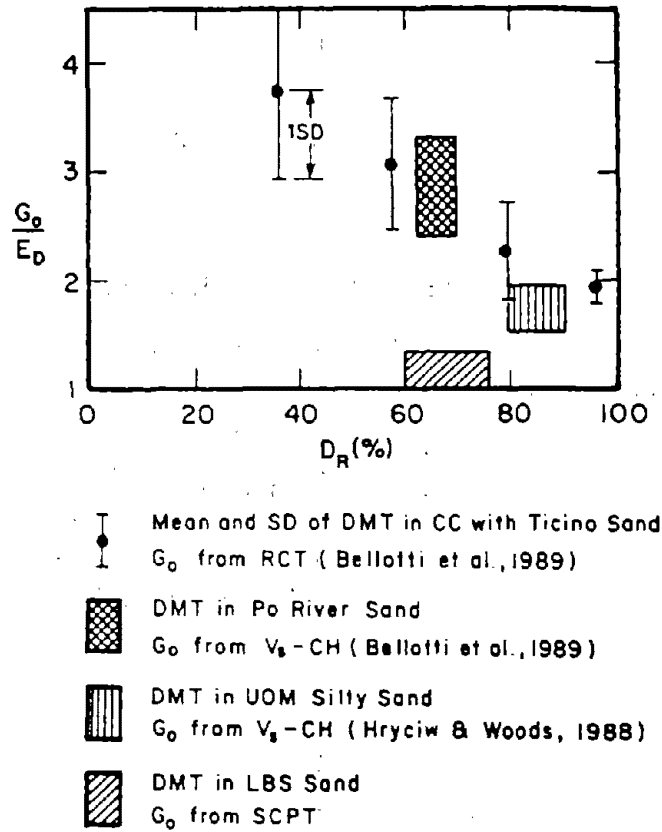
51

FIG. 6.15. $G_o - E_D$ Ratios for Published Data on Sand (From Sully and Campanella 1989)
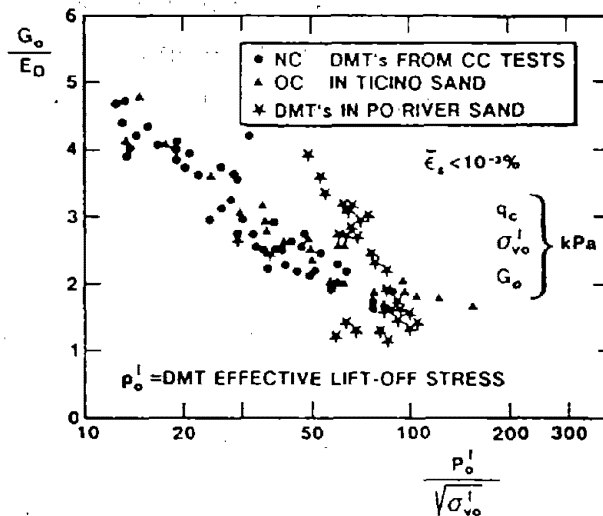

FIG. 6.16. Evaluation of Small Strain Shear Modulus From DMT's for Uncemented Silica Sands (From Baldi et al. 1989)

52

Clay

To date, no reliable correlation exists to obtain G_o of clays from dilatometer test data, although Lunne et al. (1989) tentatively proposed a correlation based on few dilatometer test results.

Sand and Clay

Recently, Hryciw (1990) proposed a new but well documented method to obtain G_o for both sand and clay. The method is based on a recent version of equation 6.22 proposed by Hardin and Blandford (1989):

$$G_o = \frac{OCR^k}{0.3 + 0.7e^2} \frac{S_{ij}P_a^{(1-n)}}{2(1+\upsilon)} (\sigma'_a \sigma'_b)^{n/2} \qquad 6.23$$

where OCR is the overconsolidation ratio, k is a constant which depends on the plasticity index (k = 0 for sands), e is the void ratio, S_{ij} is a dimensionless stiffness coefficient, P_a is the atmospheric pressure, and υ is Poisson's ratio. The equation proposed by Hryciw is:

$$G_o = \frac{530}{\left(\frac{\sigma'_v}{P_a}\right)^{0.25}} \times \frac{\frac{\gamma_D}{\gamma_w} - 1}{2.7 - \frac{\gamma_D}{\gamma_w}} \times K_o^{0.25} (\sigma'_v P_a)^{0.5} \qquad 6.24$$

where σ'_v is the vertical effective stress, γ_D is the total unit weight obtained from the DMT (figure 6.5), γ_w is the unit weight of water, and K_o is the coefficient of earth pressure at rest obtained by equation 6.1 for cohesive soils and by equation 6.5 for cohesionless soils. This method is based on studies at 9 sites in Italy, Norway, Canada and the USA. The data includes a variety of soils: gravel, sand, silt and clay. Figure 6.17 gives a comparison between observed and predicted G_{max} using the data base on which equation 6.24 is based.

6.9 Stress History

Clay

Marchetti (1980) proposed to correlate the overconsolidation ratio OCR from oedometer tests with the dilatometer horizontal stress index:

$$OCR = 0.5K_D^{1.56} \qquad (6.25)$$

Marchetti recommended to use the previous correlation with "materials free of cementation, attraction, etc. in simple unloading" and for $I_D \leq 1.2$.
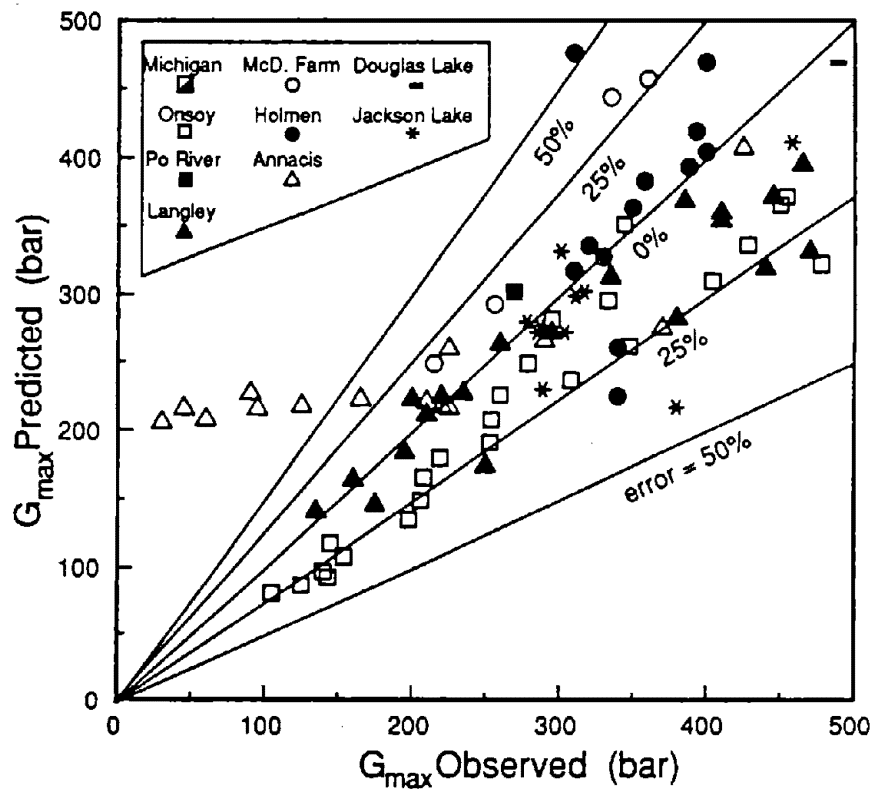
FIG. 6.17. G_{max} **Predicted versus** G_{max} **Observed (From Hryciw, 1990)**

Jamiolkowski et al. (1988) evaluated Marchetti's method based on results of dilatometer tests performed on two hard clays presented in tables 6.3 and 6.4 . They found the method to be promising for soft and medium to stiff uncemented clays, but suggested that more experimental work will be required for other clays.

Lacasse and Lunne (1988) found that the coefficient of Marchetti's correlation should be changed to fit their data accumulated at different test sites in Norway.

To date the most comprehensive work to evaluate Marchetti's correlation has been done by Lunne et al. (1989). Their data base is presented in figure 6.18. It is recommended to use the procedure proposed by Lunne et al. (1989) in order to estimate O.C.R. This procedure consists of:

- Use the ratio S_u/σ_{vo}' or geological evidence to check whether the clay is young or old. Lunne et al. (1990) proposed:

  Young clays: $S_u/\sigma_{vo}' \leq 0.8$

  Old clays : $S_u/\sigma_{vo}' > 0.8$

- For young clays, use $OCR = 0.3 K_D^{1.17}$.

  For old clays, use $OCR = 2.7 K_D^{1.17}$.

  The uncertainty in the O.C.R. determination in this manner is about $\pm$ 30%.

Sand

Schmertmann (1988) adapted a relationship by Mayne and Kulhawy (1982) for finding OCR from the lateral earth pressure coefficient K_o and the drained axisymmetric friction angle ϕ_{ax}'. Schmertmann proposed for sand, with $I_D \geq 1.2$:

$$OCR = \left(\frac{K_o}{1 - \sin \phi_{ax}'} \right)^{(1/(0.8 \sin \phi_{ax}'))} \tag{6.26}$$

where:

ϕ_{ax}' = drained axisymmetric friction angle calculated from the plane strain angle obtained in the dilatometer test (section 6.5)

K_o = coefficient of lateral earth pressure from dilatometer (section 6.2)

Schmertmann (1988) does not recommend his method for old and/or cemented sands. For other types of sands he indicates that the method appears to overpredict OCR by an average of 16%.

TABLE 6.3. Laboratory vs DMT Results in Taranto Silty-Clay (From Jamiolkowski et al. 1988)

BB/S	Depth		σ'_{vo}	γ	PI	C_u UU	σ'_p	OCR	M	$CaCO_3$	CF	P_o	P_1	K_D	I_D	$\dfrac{C_u^{DMT}}{C_u}$	$\dfrac{OCR^{DMT}}{OCR}$	$\dfrac{M^{DMT}}{M}$
No.	from m	to m	kPa	kN/m³	%	kPa	MPa	-	MPa	%	%	MPa	MPa	-	-	-	-	-
1/1	2.5	3.1	54.9	19.8	39.9	783	-	-	-	29.0	44	1.14	2.77	20.8	1.43	N.A.	-	-
1/2	5.5	6.1	113.8	19.9	29.7	823	-	-	-	26.5	33	1.21	2.93	10.6	1.42	N.A.	-	-
1/3	7.9	8.5	158.9	19.6	42.7	886	-	. -	-	26.0	38	2.49	3.91	15.7	0.57	0.52	-	-
1/4	10.9	11.5	188.4	18.7	29.7	747	-	-	-	25.5	34	2.49	4.26	13.1	0.72	0.58	-	-
3/2	5.5	6.1	106.9	20.1	30.7	305.1	1.77	16.5	35.3	29.5	34	1.01	1.63	9.4	0.62	0.53	0.68	1.48
3/3	7.0	7.6	121.6	19.4	28.7	252.1	1.49	12.3	29.5	26.5	34	1.21	1.91	9.8	0.59	0.77	0.97	2.04
3/4	8.5	9.1	136.4	20.0	30.8	302.1	2.28	16.7	39.2	27.0	32	1.45	2.24	10.3	0.56	0.77	0.77	1.77
3/5	10.0	10.6	151.1	21.0	27.1	483.0	≈3.13	20.7	59.8	27.5	37	1.75	2.79	11.2	0.61	0.59	0.71	1.49
3/6	11.5	12.1	165.8	20.8	22.3	485.0	≈3.27	19.7	88.3	27.0	39	2.21	3.44	12.9	0.57	0.77	0.93	1.33
3/11	22.0	22.6	268.8	20.4	25.2	676.4	3.12	11.6	54.0	24.0	30	2.92	4.17	10.2	0.45	0.67	1.10	2.03
3/11*	22.0	22.6	268.8	20.3	25.2	676.4	2.75	10.2	48.6	24.0	30	2.92	4.17	10.2	0.45	0.67	1.25	2.25
3/12*	26.5	27.1	312.9	20.5	-	-	≈4.44	15.8	108.9	-	-	3.25	4.67	9.7	0.47	-	0.72	1.13
3/14	35.5	36.1	401.2	20.6	26.4	845.6	4.91	12.3	81.4	49.5	35	4.09	5.62	9.4	0.41	0.72	0.91	1.60
5/4	9.0	9.6	113.8	19.9	27.0	200.0	1.62	14.2	27.7	25.0	35	0.37	1.51	3.2	3.78	N.A.	0.30	2.16
5/6	13.6	14.2	158.9	20.0	25.2	475.8	2.35	14.7	38.5	26.5	36	0.69	1.69	3.6	1.74	N.A.	0.28	1.38
5/8	17.5	18.1	197.2	20.3	26.6	-	2.97	15.0	59.8	28.5	32	1.60	2.54	7.3	0.65	-	0.50	1.21

NOTES: GWL ≈ 0.00 ABOVE M.S.L.; GL ≈ +8.0, +5.1, 2.3 RESPECTIVELY BB-1, BB-3 and BB-5;
M = TANGENT CONSTRAINED MODULUS AT ≈ 0.9 · σ'_p;
* = CRS-OEDOMETER TEST, ALL OTHER IL TESTS

TABLE 6.4. Laboratory vs DMT Results in Augusta Clay (From Jamiolkowski et al. 1988)

BB/S	Depth		σ'_{vo}	γ	PI	C_u UU	C_u CK_oU	σ'_p	OCR	M	$CaCO_3$	CF	P_o	P_1	K_D	I_D	$\dfrac{C_u^{DMT}}{C_u}$	$\dfrac{OCR^{DMT}}{OCR}$	$\dfrac{M^{DMT}}{M}$
No.	from m	to m	kPa	kN/m³	%	kPa	kPa	kPa	-	MPa	%	%	kPa	kPa	-	-	-	-	-
1/1	5.3	5.9	81.4	18.2	51.1	130.5	126.1	784.8	9.6	11.3	14.0	51	777.4	1191.9	8.3	0.55	0.95	1.15	2.55
1/1*	5.3	5.9	81.4	18.2	51.1	130.5	126.1	833.9	10.2	13.7	21.0	51	777.4	1191.9	8.3	0.55	-	1.08	2.10
1/2	7.0	7.6	97.1	18.0	51.9	142.2	-	932.0	9.6	19.6	21.0	54	1044.8	1554.9	10.4	0.51	1.18	1.36	2.29
1/4	12.0	12.6	141.3	18.5	48.3	234.5	-	1275.3	9.0	21.6	16.5	51	1648.1	2261.2	11.1	0.39	1.13	1.61	2.57
1/4**	12.0	12.6	141.3	18.5	48.3	234.5	-	1422.5	10.0	24.0	16.5	51	1648.1	2261.2	11.1	0.39	-	1.45	2.31
1/6	17.0	17.6	185.4	18.3	50.5	181.5	-	1471.5	7.9	20.6	21.0	58	1819.8	2469.7	9.1	0.39	1.49	1.35	2.63
1/6*	17.0	17.6	185.4	18.3	50.5	181.5	-·	1569.6	8.5	21.6	21.0	58	1819.8	2469.7	9.1	0.39	-	1.25	2.51
1/8·	25.0	25.6	256.0	18.1	49.7	-	197.7	1569.6	6.1	21.1	16.5	60	2138.6	2952.8	7.5	0.40	1.49	1.29	2.95

NOTES: GWL AT 3.6 M BELOW GL; M = TANGENT CONSTRAINED MODULUS AT ≈0.9 σ'_p; * CRS OEDOMETER TESTS;
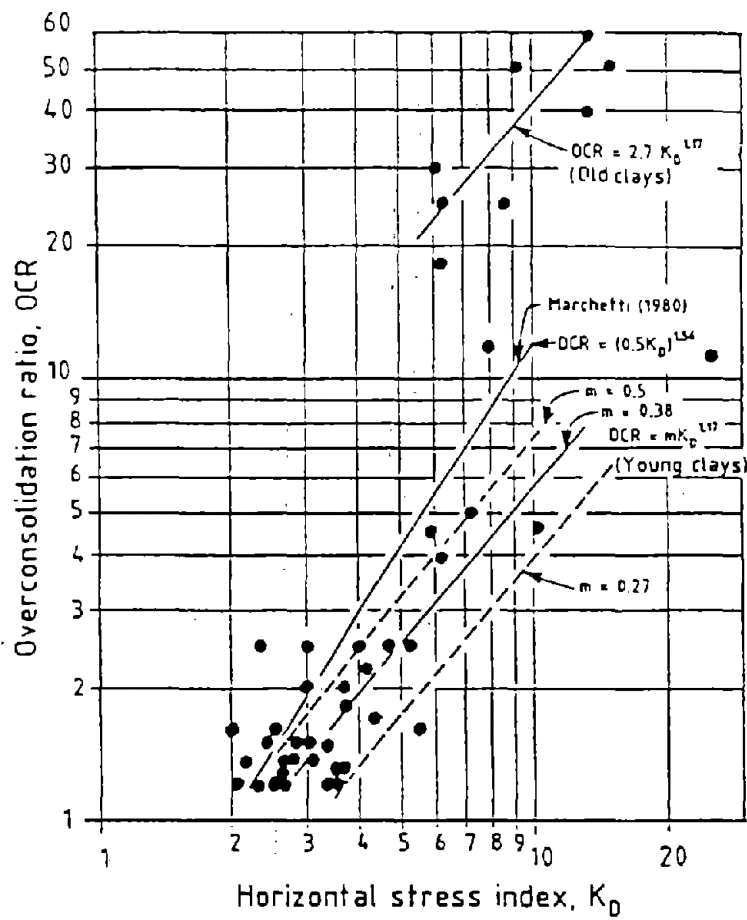** INSTRUMENTED OEDOMETER TESTS ALLOWING MEASUREMENT OF RADIAL STRESS, ALL OTHER IL TESTS

56

FIG. 6.18. Revised OCR Correlation for Dilatometer Test (From Lunne et al., 1989)

K ᴅ **Profile**

As pointed out by Marchetti (1991) the K_D profile is very useful in describing the stress history of the deposit. Indeed, inspecting the K_D profile (figure 6.19) and comparing it to the dashed lines for the K_D = 1.5 and 2 which correspond to OCR = 1 gives a good idea of the stress history of the deposit.

6.10 Undrained Shear Strength

Marchetti (1980) proposed to correlate the undrained shear strength S_u with the horizontal stress index K_D :

$$S_u = 0.22\sigma'_{ov}(0.5K_D)^{1.25} \tag{6.27}$$

The previous correlation was developed using field vane test results, UU triaxial tests and unconfined compression tests. The available pairs of values for S_u/σ'_{ov} and K_D are plotted in figure 6.20 on a log-log scale.

Several authors (Lacasse and Lunne, 1983; Fabius, 1985; Greig et al., 1986; Lutenegger and Timian, 1986; Ming-Fang, 1986) have shown that the DMT prediction of undrained shear strength using equation 6.27 in soft uncemented saturated clays compares fairly well with uncorrected field vane results.

Figure 6.21 proposed by Lutenegger (1988) compares the measured error in S_u between DMT and field vane for a number of clay sites; it shows that the accuracy of the prediction of S_u is strongly linked to the material index I_D and that the error can be significant. Lutenegger (1988) suggests that equation 6.27 would be best used in clays with $I_D \leq 0.33$.

The use of equation 6.27 is not recommended for OC cemented and/or fissured clays. Indeed, the experimental data (tables 6.3 and 6.4) presented by Jamiolkowski (1988) indicate that for these types of clays further calibration of the DMT correlation is required.

Powell et al. (1986), working at sites in the UK, found that Marchetti's 1980 correlation was significantly overestimating the undrained shear strength in one highly over consolidated clay and underestimating it in glacial tills.

The measured value of S_u varies depending on which test is used to establish S_u for a given soil. Lacasse and Lunne (1988) acknowledged this fact and presented three correlations (figures 6.22, 6.23, 6.24) between K_D and S_u for the uncorrected field vane strength, the simple shear strength and the triaxial compression strength, adapted from Marchetti's 1980 correlation.

HOW TO READ DMT RESULTS

Id : Gives indication on material type
(Sand , Silt , Clay)

M : One dimensional
modulus at   utilized
geostatic stress   in the
                    usual
Cu : Undrained shear   way
strength

Kd : Similar in shape to OCR profile.
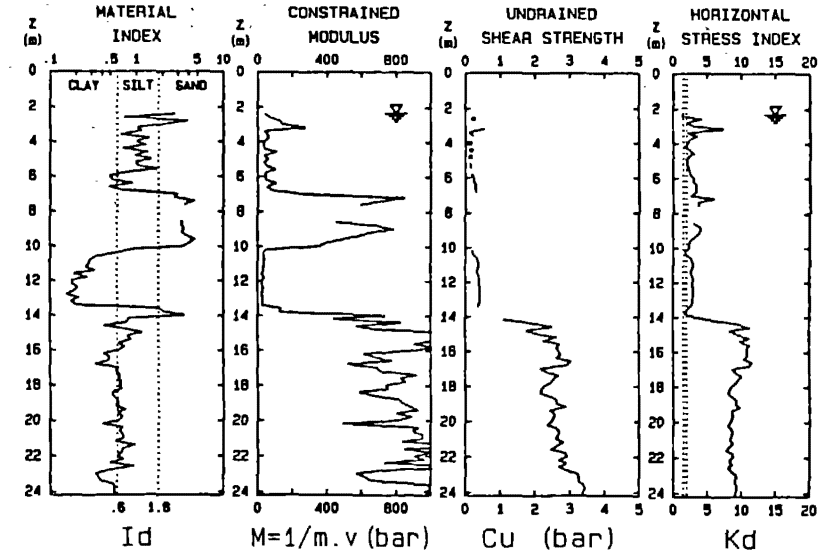Kd≈2 indicates OCR≈1
Detects top crusts & buried crusts

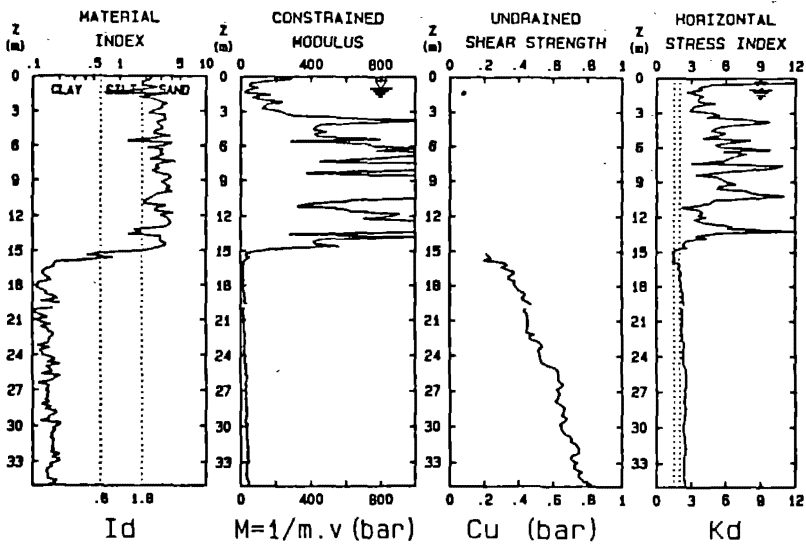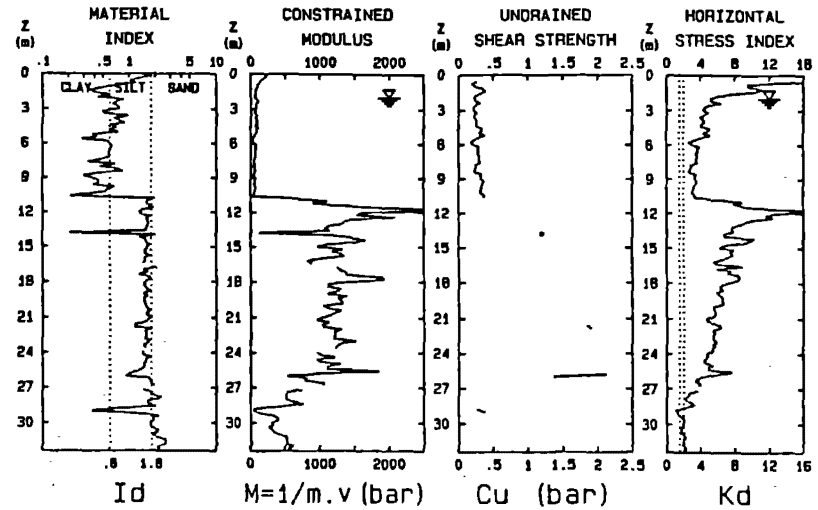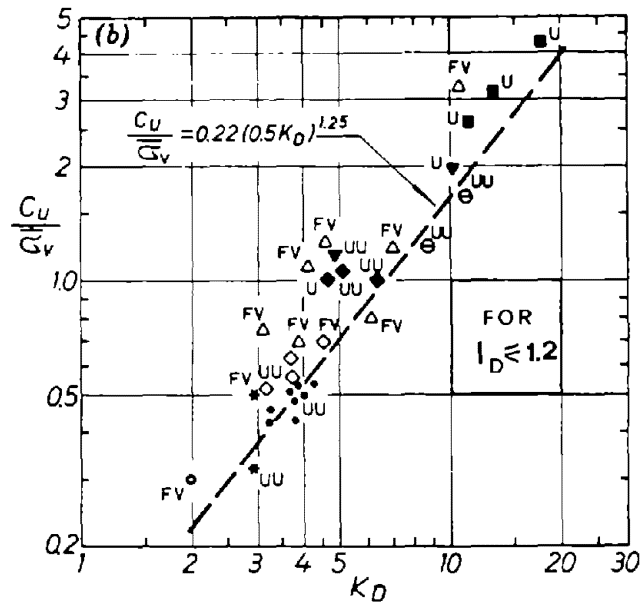**FIG. 6.19. Obtaining Stress History from K_D Profile**

FIG. 6.20. Correlation Between C_u/σ'_{vo} and K_D (From Marchetti, 1980)
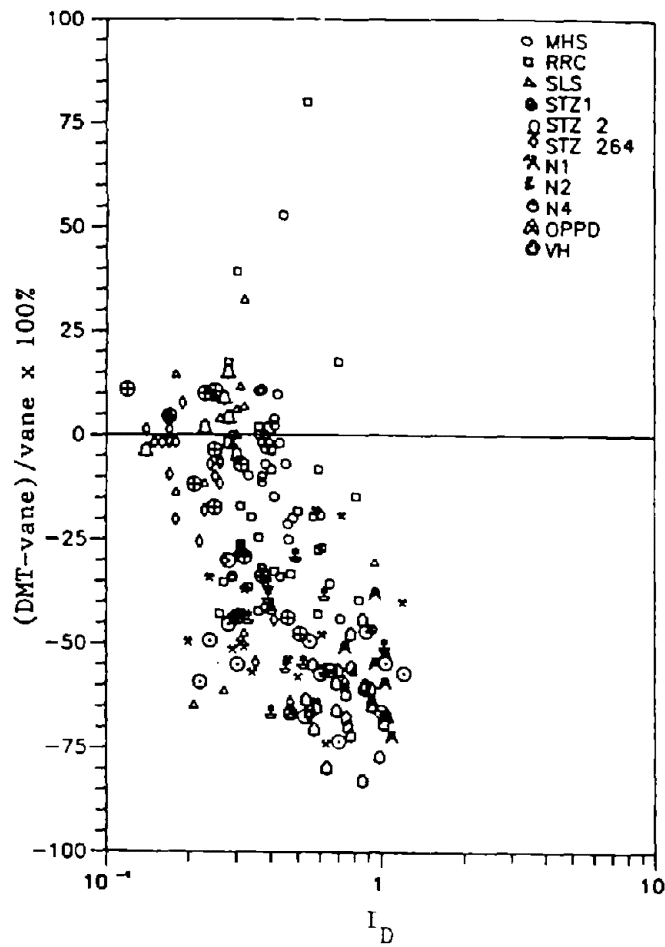
FIG. 6.21. Accuracy in Estimate of DMT S_u (as Proposed by Marchetti 1980) as a Function

of I_D (From Lutenegger 1988)

FIG. 6.22. S_u/σ'_{vo} vs K_D

FIG. 6.23. S_u/σ'_{vo} vs K_D

FIG. 6.24. S_u/σ'_{vo} vs K_D
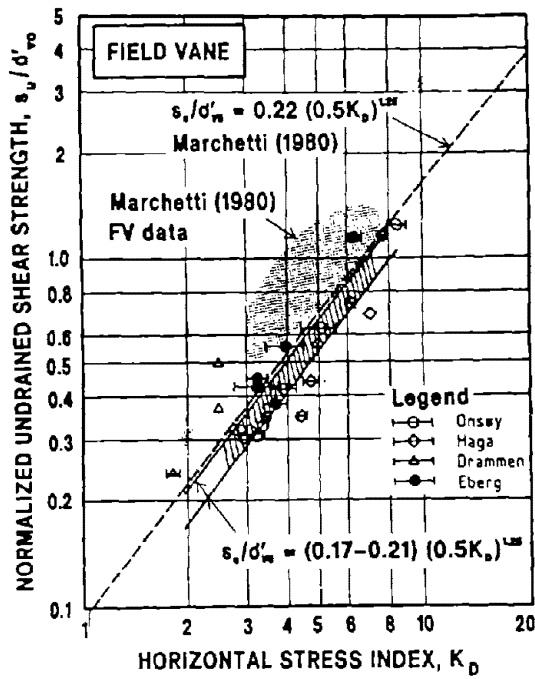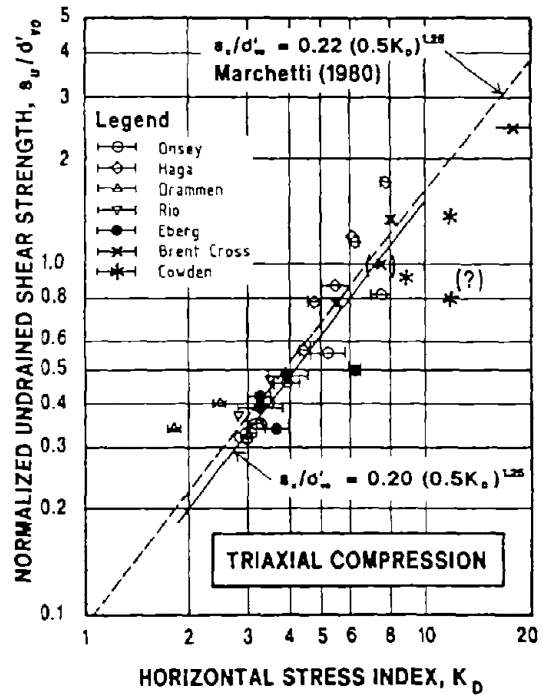
McDONALDS FARM SITE
22.0m DEPTH. CLAYEY SILT (OCR=1)

FIG. 6.25. Repeated A, B, and C Readings (Corrected for Membrane Stiffness p_o, p_1, p_2) Using Standard DMT Compared with DMT Pore Pressure Dissipation (McDonald Farm Site) (From Robertson et al., 1988)

61

Lacasse and Lunne (1988) recommended that the user should select the diagram corresponding to the strength needed for design. These three correlations are only recommended for soft uncemented clays.

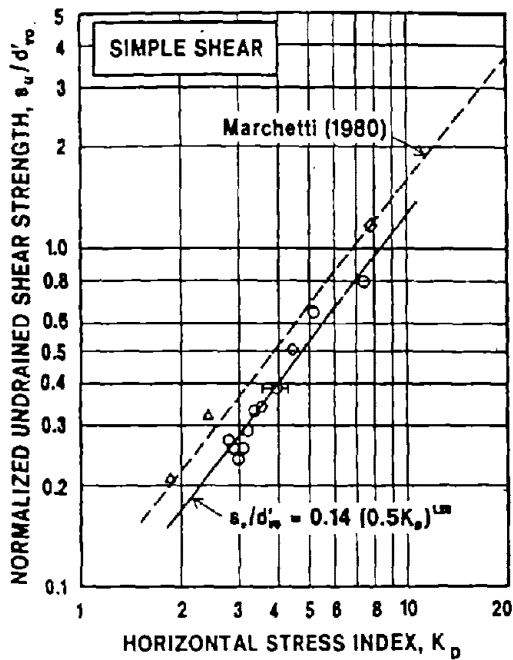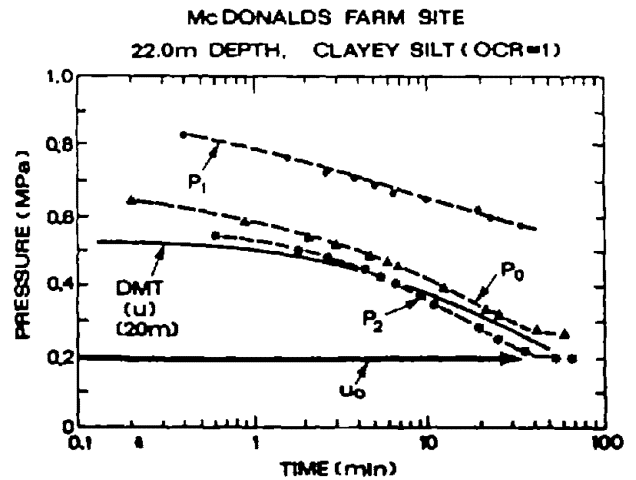Roque et al. (1988) argued that the dilatometer insertion can be considered as a footing loaded horizontally to failure. Therefore, they proposed to use the classical bearing capacity formulas to estimate the undrained shear strength of the soil:

$$S_u = \frac{p_1 - \sigma_{ho}}{N_c} \qquad (6.28)$$

where:

p_1 = initial (maximum) DMT expansion pressure

σ_{ho} = total horizontal in situ stress, estimated by the formula $\sigma_{ho} = K_o \cdot \sigma'_{vo} + u_o$

σ'_{vo} = in situ vertical effective overburden

u_o = in situ pore pressure

K_o = coefficient of lateral earth pressure at rest (see section 6.2)

Roque et al. (1988) proposed the following N_c values:

Soil type	N_c
Brittle clay and silt	5
Medium clay	7
Non sensitive plastic clay	9

Dilatometer tests performed in Glava clay in Norway and reported by Roque et al. (1988) shows that for this type of clay, undrained shear strengths determined using this last method were in good correspondence with strength values from triaxial compression tests.

Overall, it appears that if one method is to be favored, the method by Rogue et al. should be the one.

6.11 Coefficient of Horizontal Consolidation

Two testing procedures were presented in section 4.3 in order to obtain the coefficient of horizontal consolidation C_h : the DMTC procedure and the DMTA procedure. The two corresponding calculation procedures are described in this section.

Several workers have shown that the DMT closing pressure P_2 (or C-pressure) is very similar to the initial pore pressure plus the excess pore water pressure generated on the DMT membrane (dilatometers equipped with pore pressure devices). Furthermore, Robertson et al (1988) found that the P_2 readings follow a very similar dissipation curve to that of the actual DMT pore pressure (figure 6.25). They presented a method to obtain c_h from the P_2 dissipation curve, which is comparable to the CPTU method.

Schmertmann (1988) combined the work of Robertson et al. (1988), Baligh and Levadoux (1986), Gupta (1988), Lutenegger (1988) and presented the following step-by-step procedure to obtain the horizontal coefficient of consolidation C_h from a DMTC dissipation test:

1. Run a DMTC dissipation test (section 4.3).

2. Plot the C-pressures against a square root of time scale (figure 6.26), making at least enough measurements to find C_{50}, the C-pressure at 50% of the dissipation to the equilibrium C-pressure, C_{100}.

   Determine t_{50}, the time required to reach C_{50} on the dissipation curve. Use the following method to get C_{50}: (the 30% distribution time may also be used to save time if u_o is known accurately)

   i) extrapolate the beginning of the dissipation curve back to the C-pressure intercept at time t=0, C_o, mathematically or graphically; use a straight line through the early data points.

   ii) extrapolate the end of the dissipation curve forward to estimate the asymptotic C-pressure, C_{100}, or alternatively the operator may estimate C_{100} by calculating the expected in situ pore water pressure at the test depth and subtracting the value of A.

   iii) average C_o and C_{100} to find C_{50} at 50% dissipation.

3. After estimating the E/S_u ratio, calculate the DMT C_h using the following equation:

$$C_h = 600 \left(\frac{T_{50}}{t_{50}} \right), \quad \left(\frac{mm^2}{min} \right) \qquad (6.29)$$

where:

t_{50} = time required to reach C_{50} on the dissipation curve

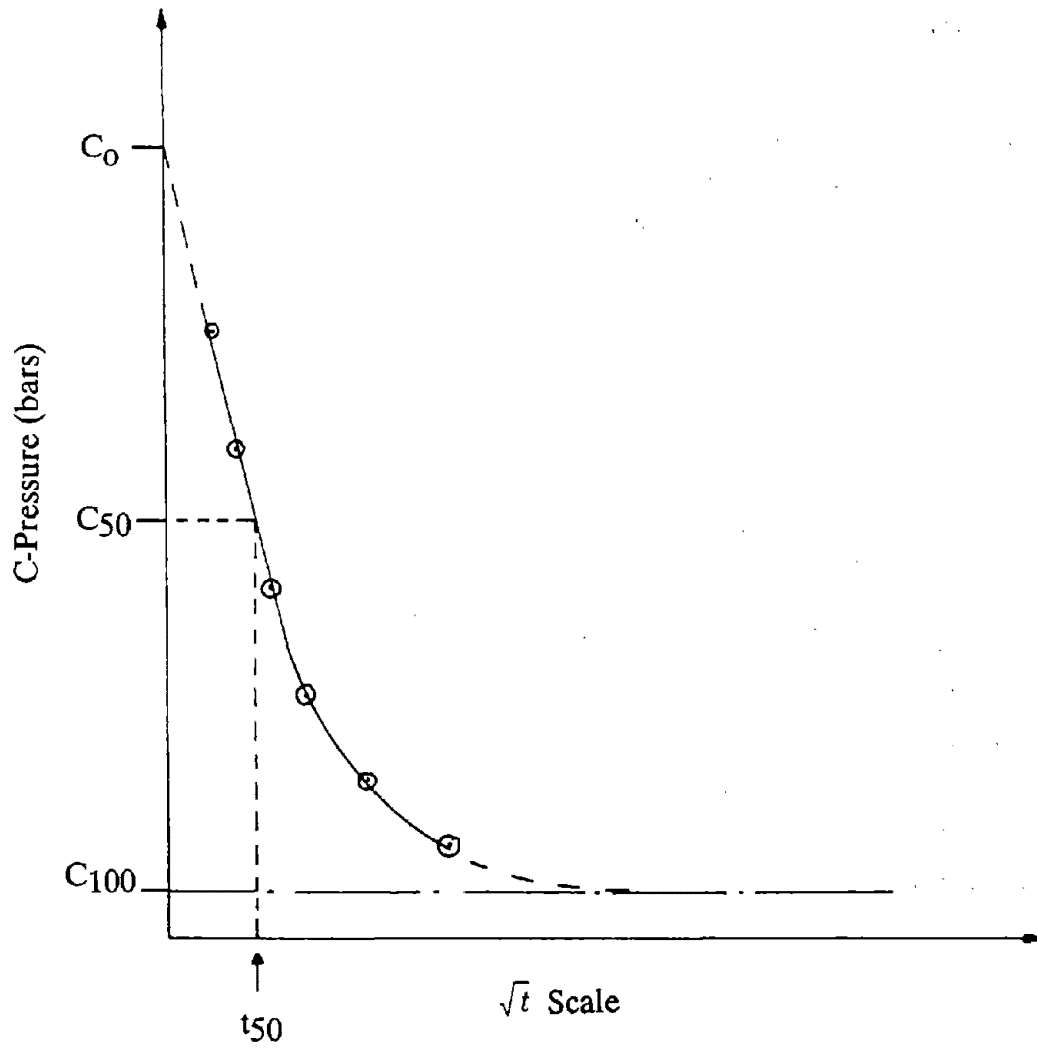T_{50} = time factor estimated using the following table adapted from the work by Gupta (1983):

FIG. 6.26. Graph to Get t_{50}

E/S_u	100	200	300	400
T_{50} (min)	1.1	1.5	2.0	2.7
T_{30} (min)	0.47	0.59	0.72	0.89

Estimating the field C_h requires another correction to account for the recompression behavior in the DMT vs. possible virgin behavior in the field. Schmertmann (1988) suggested the following correction factors. They depend on whether the expected field behavior will be entirely virgin compression (NC), a combination recompression-virgin (NC-OC), recompression near the preconsolidation stress (LOC), or recompression in a highly overconsolidated soil (HOC).

Field Behavior	NC	NC-OC	LOC	HOC
C_{hDMT}/C_{hField}	7	5	3	1

Marchetti and Totani (1989) describe the procedure to calculate C_h based on the DMTA dissipation test procedure. In this procedure a characteristic time T_{flex} is defined: T_{flex} is the time which corresponds to the point of reverse curvature on the A pressure versus log time curve discussed in section 4.3. An example curve is shown in figure 6.27. The reasons for choosing T_{flex} for this procedure and the advantages thereof can be found in Marchetti and Totani (1989). The authors then give a rating on consolidation speed depending on the value of T_{flex} (table 6.5). They also propose a simple equation:

$$C_{h,oc} \times T_{flex} = 5 \ to \ 10 cm^2$$

As pointed out by the authors this equation should be used cautiously and is likely to evolve as more data becomes available. $C_{h,oc}$ is the coefficient of horizontal consolidation for an overconsolidated soil and is the one measured with this procedure since the DMT is a horizontal loading test which prestresses the soil before obtaining its properties. Marchetti and Totani point out that the coefficient of vertical consolidation for a normally consolidated soil may be many times smaller than $C_{h,oc}$. A ratio of 35 is mentioned as an order of magnitude.

65
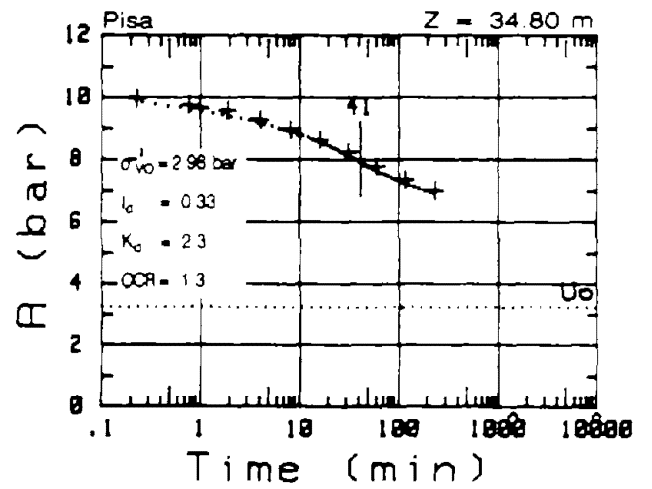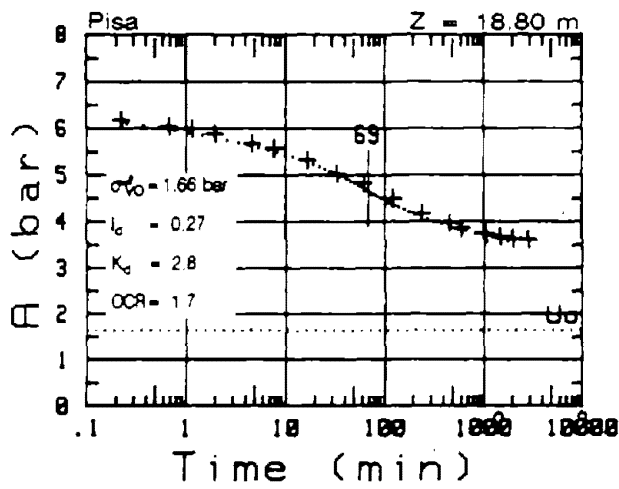
FIG. 6.27. Obtaining T_{flax} from DMTA A-Pressure versus Log(time) Curves (From Marchetti and Totani, 1989)

Kabir and Lutenegger (1990) present some useful data on the comparison between a piezocone and a peizoblade as well as three approaches to obtain the in situ C_h from a dilatometer.

6.12 Automatic Data Reduction

A computer program exists to reduce and interpret the data automatically (GPE, Inc. 1991). Another program called DILLY which also includes settlement calculations for spread footings is available from McTrans (Dumas, 1990; McTrans 1991).

TABLE 6.5. RATING ON CONSOLIDATION SPEED BASED ON T_{flex}

T_{flex} (minutes)			Consolidation Rate
	<	10	very fast
10	to	30	fast
30	to	80	medium
80	to	200	slow
	>	200	very slow

67

7. DESIGN OF LATERALLY LOADED PILES

7.1 Introduction

The purpose of this section is to describe a method to estimate the response of laterally loaded piles. The theoretical approach used herein is the non-linear subgrade reaction method. In this method, the pile is considered to be an elastic beam-column with a bending stiffness EI, and shear induced deformations are ignored. The soil is modeled by uncoupled springs distributed along the length of the pile. Because the response of real soils is non-linear, the springs idealizing the load-deformation response of the soil-pile mechanism are also taken to be non-linear. The load-deflection curves are usually referred to as P - y curves, where P is the soil reaction in load per unit length of pile, and y is the horizontal deflection. These curves are defined by the coefficient of subgrade reaction k.

The behavior of the laterally loaded pile (no axial load) is governed by the equation:

$$E_p I_p \frac{d^4 y}{dZ^4} + kBy = 0 \qquad (7.1)$$

where:

E_p = modulus of elasticity of the pile

I_p = moment of inertia of pile section around the bending axis

y = pile deflection

B = width of the pile

Z = depth below the ground surface

k = coefficient of subgrade reaction, in units of $force/length^3$ (pressure / displacement).

The solution to the above equation may be obtained either analytically or numerically. Analytical solutions are only available in convenient form for the case of a constant k value along the pile. In the general case, the P - y curves are non-linear and vary with depth. A standard way to treat this non-linear problem is to solve the above differential equation by using a numerical finite difference method. To do so, the embedded part of the pile is divided into discrete segments with the soil resistance along each segment modelled by a horizontal spring with non-linear behavior. Thus, the first step is to determine the P - y curves associated with each spring from the DMT results.

7.2 P - y Curves: Robertson et al. (1989a) Method for Driven Piles

Robertson et al. (1989a) presented a preliminary semi-empirical method for the evaluation of P - y curves using Matlock's original method and data obtained from the DMT.

Matlock (1970) proposed:

$$\frac{P}{P_u} = 0.5(y/y_c)^{0.33}$$

(7.2)

where:

P = soil lateral resistance in force per unit length of pile.

P_u = ultimate soil lateral resistance in forde per unit length of pile.

y_c = ultimate horizontal deflection of the pile element corresponding to $P = 0.5P_u$.

y = horizontal deflection of the pile element.

P_u and y_c can be calculated as follows:

Cohesive soils (undrained conditions)

Robertson et al. (1989a) proposed:

$$y_c = \frac{23.67 S_u D^{0.5}}{F_c . E_D}$$

(7.3)

where:

y_c = ultimate horizontal deflection of the pile element corresponding to $P = 0.5P_u$ in cm.

S_u = undrained shear strength from DMT.

D = pile diameter in cm.

E_D = dilatometer modulus.

$F_c = \frac{E_i}{E_D}$ taken equal to 10 as a first approximation.

E_i = initial tangent modulus.

$$P_u = N_p S_u D$$

(7.4)

where:

N_p = non dimensional ultimate resistance coefficient

S_u = undrained shear strength from DMT

D = pile diameter

Matlock (1970) proposed to compute N_p from:

$$N_p = 3 + \frac{\sigma'_{vo}}{S_u} + \left(J \frac{x}{D} \right)$$

and

$$N_p \leq 9$$

where:

x = depth

σ'_{vo} = vertical effective stress at depth x

J = empirical coefficient found from the following table:

Value of J	Soil Type	Soil Tested
0.5	Soft Clay	Sabine Clay
0.25	Stiff Clay	Lake Austin Clay

Lutenegger and Blanchard (1990) discuss the problem of DMT and laterally loaded piles and point out that for the predictions the DMT test should be performed after allowing for pore pressure dissipation around the DMT since this is likely to be the case around the pile.

Cohesionless soils

Robertson et al. (1989a) proposed:

$$y_c = \frac{4.17 \sin \phi' . \sigma'_{vo}}{E_D . F_s . (1 - \sin \phi')} \times D \qquad (7.5)$$

where:

ϕ' = angle of internal friction (section 6.5)

σ'_{vo} = vertical effective stress at depth x

D = pile diameter

E_D = dilatometer modulus

$F_s = \frac{E_i}{E_D}$ taken equal to 2 as a first approximation

E_i = initial tangent modulus

Robertson et al. (1989a) used the work of Reese et al. (1974) and of Murchison and O'Neill (1984) to determine P_u from the lesser value given by the two following equations:

$$P_u = \sigma'_{vo}[D(K_p - K_a) + xK_p \tan\phi' \tan\beta] \qquad (7.6)$$

$$P_u = \sigma'_{vo}D[K_p^3 + 2K_oK_p^2 \tan\phi' + \tan\phi' - K_a] \qquad (7.7)$$

where:

σ'_{vo} = vertical effective stress at depth x

D = pile diameter

ϕ' = angle of internal friction (section 6.5)

K_a = Rankine active coefficient = $(1 - \sin\phi')/(1 + \sin\phi')$

K_p = Rankine passive coefficient = $1/K_a$

K_o = coefficient of earth pressure at rest

β = $45° + \phi/2$

7.3 Response of Laterally Loaded Pile using LATPILE.UBC: Robertson et al. (1989) Procedure

In order to predict the lateral behavior of a pile subjected to a horizontal loading and/or a moment loading at the ground surface, one can use the following procedure (Robertson et al. 1989a):

1. Obtain the DMT field data.

2. Interpret the data using the computer program DMT.UBC (based on Marchetti 1980), or using the methods presented in chapter 6.

3. Calculate P_u and y_c at each test depth, as explained in section 7.2, or using the computer program PU-YC.UBC.

4. Average the previous sets of values into a maximum of 20 (P_u, y_c) sets of values.

5. Run the PY.UBC computer program in order to generate the P - y curves, or use equation 7.2.

6. Run the computer program LATPILE.UBC (P.C. version of LATPILE adapted from Reese, 1980) or any other suitable computer program (LTBASE, BMCOL76) to obtain the pile response.

71

7.4 Precision of Robertson et al. (1989) Procedure

This method is only suited for laterally loaded piles under static, one-way loads. Robertson et al. (1989b) evaluated their method using the results from three lateral load tests on three driven pipe piles. The soil profile at the test site was constituted of a surface layer of fill overlying an organic silty clay layer to a depth of about 15 m. Below this upper layer was a medium dense sand deposit, locally silty down to about 30 m. Underlying the sand, to a depth of about 150 m was a normally consolidated clayey silt deposit containing thin sand layer.

The calculated and measured load deflection curves as well as the piles' geometries are presented in figures 7.1, 7.2, 7.3. This method provided a good prediction of pile response.

Robertson et al. (1989) method requires further field validation, and is only recommended to obtain a first estimate of the response of laterally loaded piles.

7.5 P - y Curves: Gabr and Borden (1988) Method in Cohesionless Soils

Murchison and O'Neill (1984) proposed to determine the P-y curves for cohesionless soils from:

$$P = n \cdot A \cdot P_u \cdot \tanh\left[\left(\frac{k_o \cdot Z}{A \cdot n \cdot P_u}\right) \cdot y\right]$$ (7.8)

where:

n = 1.5 for uniformly tapered piles, such as timber piles, and H piles

n = 1.0 for circular, prismatic piles

A = 0.9 for cyclic loading

A = $3 - 0.8\left(\frac{Z}{D}\right) \geq 0.9$ for static loading

D = width of the pile

k_o = initial coefficient of subgrade reaction in units of force/length^3

Z = depth

P_u = ultimate soil resistance = lesser value given by equations 7.6 and 7.7

Evaluuation of k_o

Gabr and Borden (1988) proposed:

$$k_o = \frac{P_o - \sigma_h}{h}$$ (7.9)

LATERAL LOAD (kN)

200

150 MEASURED

100 DMT

PILE TEST No.3
PILE DIMENSIONS

50 LENGTH 16.8m
DIAMETER 324 mm
WALL 9.5mm

0

0   10   20   30   40   50
LATERAL DEFLECTION AT GROUND SURFACE (mm)
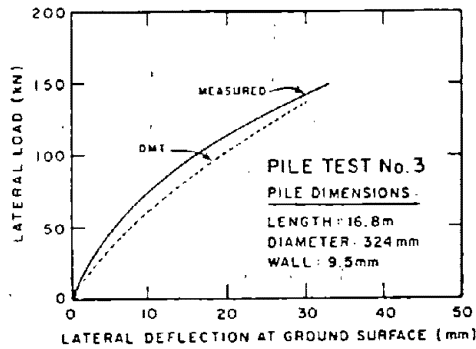
FIG. 7.1. Measured vs Calculated Pile Top Deflection: Test 3 (From Robertson et al. 1989b)

LATERAL LOAD (kN)

200

DMT

150 MEASURED

100

PILE TEST No.5
PILE DIMENSIONS

50 LENGTH 31.1m
DIAMETER 324 mm
WALL 11.5mm

0

0   10   20   30   40   50
LATERAL DEFLECTION AT GROUND SURFACE (mm)
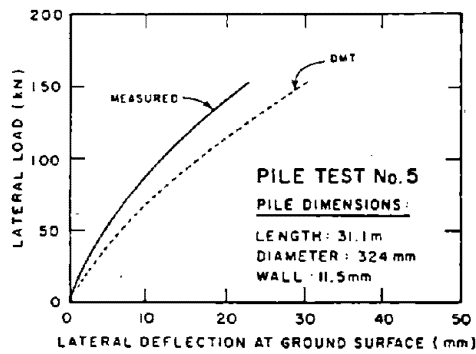
FIG. 7.2. Measured vs Calculated Pile Top Deflection: Test 5 (From Robertson et al. 1989b)

LATERAL LOAD (kN)

1200

MEASURED

1000

DMT

800

PILE TEST No.C

600 PILE DIMENSIONS

LENGTH 94m
400 DIAMETER 914 mm
WALL 19mm

200

0

0   50   100   150   200   250
LATERAL DEFLECTION AT GROUND SURFACE (mm)

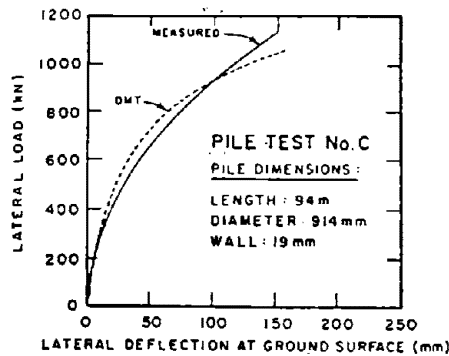**FIG. 7.3.** Measured vs Calculated Pile Top Deflection: Test C (From Robertson et al. 1989b)

73

where:

P_o = dilatometer reading, A, corrected

σ_h = in-situ total horizontal stress at rest

h = half the blade thickness = 0.27 in. if P_o and σ_h are in psi

The estimation of σ_h can be achieved providing that the coefficient of at rest earth pressure, K_o is known. The method presented in section 6.2 can be used to obtain K_o although Gabr and Borden have suggested that an educated guess should be sufficient to estimate σ_h.

7.6 Response of Laterally Loaded Piles in Cohesionless Soils Using Gabr and Borden P-y Curves

The lateral behavior of a pile subjected to a horizontal loading and/or a moment loading at the ground surface can be estimated as follows:

1. Divide the soil profile around the pile into layers of approximately constant behavior.

2. Obtain the P - y curves for each layer using the method described in section 7.5.

3. Run a suitable finite difference computer program such as LATPILE.UBC (University of British Columbia), LTBASE (Borden and Gabr, 1987) or BMCOL76 to obtain the pile response.

7.7 Precision of Gabr and Borden (1988) Method

This method is only adapted to laterally loaded piles under static, one way loads. The Murchison and O'Neill method was proposed for driven piles, however, Gabr and Borden (1988) evaluated their method using the results from three lateral load tests on three bored piles, 30 in. (.762 m) in diameter and 7 ft (2.13 m) long, constructed on a highway embankment with side slopes of 3.5:1. The test piers #1 and #2, were loaded along the direction of the highway (horizontal ground surface). Pier #3 was loaded down the side slope of the embankment. The piers were subjected to a lateral load and an overturning moment. A lateral load was applied at the top of a 30 ft-column supported by the pier being tested. The load-deflection response for the 3 piers is shown in figure 7.4. The predicted load-deflection behaviors of the piers were obtained using the computer program LTBASE and are shown in figure 7.4. This method provided good predictions of the bored piles responses. Gabr and Borden (1988) stated that their method can be expected to produce good results for bored piles. However an enlarged data base is
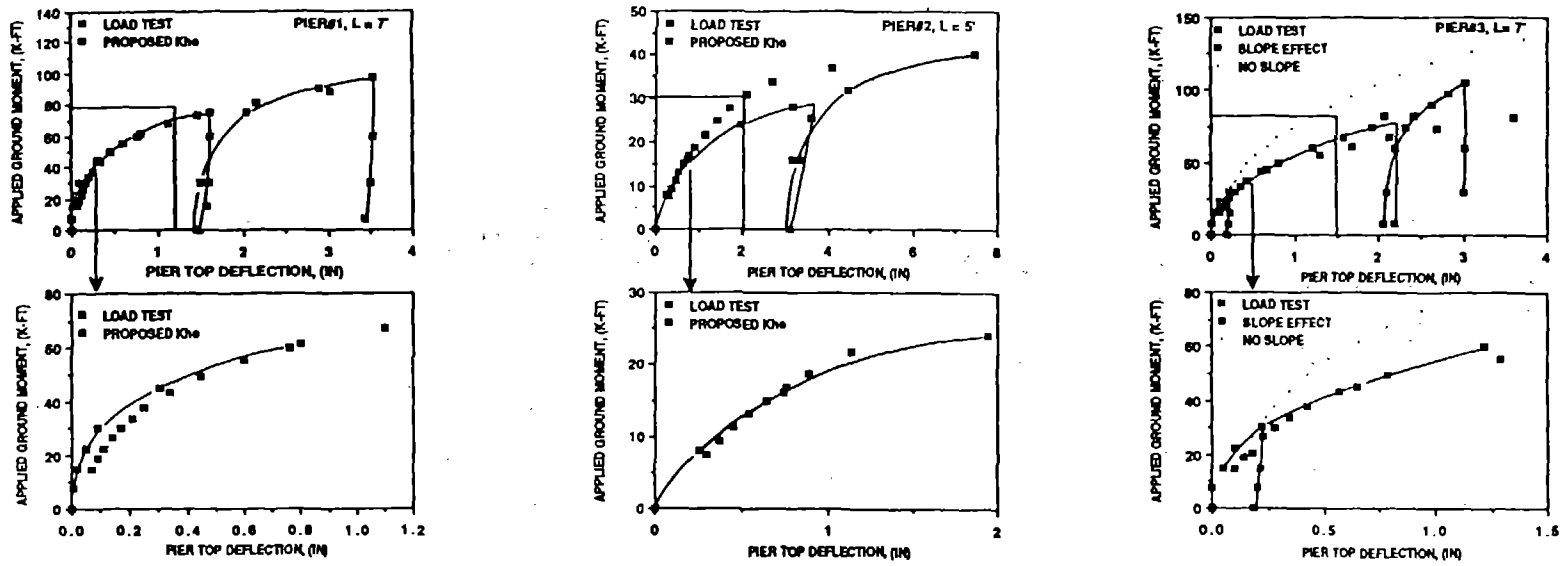
74

FIG. 7.4. Measured vs Calculated Pile Top Deflection (From Gabr et al.1988)

required to further assess the model applicability. More recently Borden and Lawter (1989) further evaluated the method on 2 jetted then driven 24 in. square prestressed concrete piles. The results continue to be encouraging especially at small deflections.

8. DESIGN OF SHALLOW FOUNDATIONS

8.1 Settlement of Shallow Foundations

8.1.1 Settlement: Introduction

The settlement of a shallow foundation due to soil consolidation may be computed from:

$$S = \sum \frac{\Delta \sigma_i}{M_i} \cdot h_i \qquad (8.1)$$

where:

S = total settlement

h_i = thickness of the ith layer

$\Delta \sigma_i$ = expected change in stress at the middle of the ith soil layer

M_i = average constrained modulus of the ith layer

The value of the constrained modulus M_i is not unique for a given soil. Indeed, M_i varies with the effective stress in a different manner for various soil types. The DMT determines the property of the soil in situ at the time of the test and at one point on the $M_i - \sigma_v'$ curve. The vertical effective stress during the loading of the foundation is often different from the σ_v' at the time of the DMT. Therefore it may be necessary to adjust M_i from the DMT to the average vertical effective stress during the shallow foundation loading.

Schmertmann (1986b) acknowledged this fact and presented two methods to estimate the settlement of shallow foundations:

- The ordinary method which makes use of the M_i values obtained directly from the DMT data.

- The special method which includes steps for adjusting the M_i values to the effective stress which exists for the problem under investigation. An expanded version of this method has been automated in a computer program called DILLYSET (Dumas, 1991).

Only the ordinary method is outlined in this manual. Indeed, Schmertmann (1986b) stated that the ordinary method usually suffices to predict the settlement with good accuracy (section 8.1.3), and that the special method produces calculated settlements which

are at most 20% less than the settlement calculated with the ordinary method. One should keep in mind that the scatter on the plot of M predicted from DMT versus measured values exceeds ± 20% (figure 6.13).

Leonards and Frost (1988) presented a detailed method for granular soils with particular emphasis on the influence of the overconsolidation ratio.

8.1.2 Settlement: Schmertmann's (1986b) Ordinary Method

Schmertmann recommended the following procedure:

1. Prepare a table with the following headings

Layer #	h_i	M_i	$\Delta\sigma_i$	$\dfrac{\Delta\sigma_i}{M_i} \cdot h_i$

$$S = \sum \frac{\Delta\sigma_i}{M_i} \cdot h_i$$

2. Perform a DMT sounding at each settlement analysis location and determine the profiles of M through the soil layers of interest using Marchetti's (1980) method described in section 6.6.

3. Divide the soil into layers of approximately constant $\Delta\sigma$. Since $\Delta\sigma$ does not vary linearly with depth, the layer thickness h_i should be small right below the footing, and increase with depth.

4. Determine the average M_i value from the DMT results for each layer in step 3.

5. Estimate the expected change in stress $\Delta\sigma_i$ at the center of each layer using the following methods; these methods give the increase in stress under the center of the footing.

<u>**Circular footing:**</u>

$$\Delta\sigma = \Delta p \left[1 - \left(1 + \left(\frac{R}{Z} \right)^2 \right)^{-3/2} \right] \tag{8.2}$$

where:

Δp = net footing pressure = $q - \sigma'_1$

q = footing bearing pressure

σ'_1 = effective stress at the footing depth

R = radius of the footing

Z = distance from the bottom of the footing to the center of the soil layer

Rectangular footing:

$$\Delta\sigma = 4\Delta p \cdot I_{(m,n)} \qquad (8.3)$$

where:

Δp = net footing pressure defined as before

$I_{(m,n)}$ = stress influence factor calculated using figure 8.1 where $n \times Z$ is half the width of the footing, $m \times Z$ is half the length of the footing, and Z is defined as above.

For the increase in stress $\Delta\sigma$ under the corner of the footing, the equation is:

$$\Delta\sigma = \Delta p \cdot I_{(m,n)} \qquad (8.4)$$

where $I_{(m,n)}$ is obtained as shown on figure 8.1.

6. Calculate the 1-D settlement s_i of each layer using the following equation:

$$s_i = \frac{\Delta\sigma_i}{M_i} \cdot h_i \qquad (8.5)$$

7. Calculate the total 1-D settlement S using equation 8.1.

8.1.3 Settlement: Precision of Schmertmann Method

The settlement calculation method presented in section 8.1.2 should only apply to consolidation or volume change settlement under a perfectly flexible loaded area, in 1-D compression. The previous situation is seldom encountered in reality. However it seems that Schmertmann's method still gives relatively good results when applied to real situations. Schmertmann (1986b) evaluated the accuracy of his method by comparing the DMT calculated settlement with the measured settlement for 16 structures at 11 locations. The ratios of estimated to measured settlements, the soil types and the structures' dimensions are presented in table 8.1. Overall, the ratio of predicted to measured settlement (ordinary method only) had a mean of 1.22 and a standard deviation of 0.39. Thus, this method overpredicts the settlement on the average and for this data base. From the work of Leonards and Frost (1988) one can infer that the ordinary method is likely to be more conservative for overconsolidated granular soils than for normally consolidated granular soils.
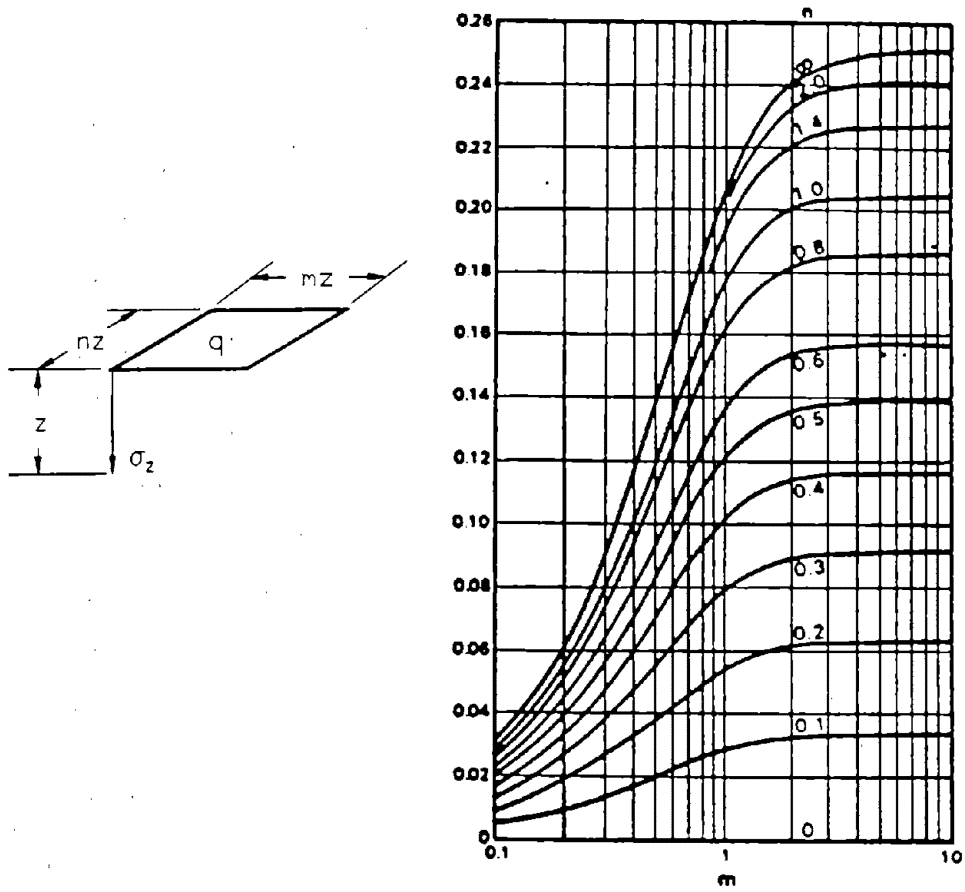
FIG. 8.1 Vertical Stress Under Corner of Uniformly Loaded Rectangular Area (From Fadum 1948)

TABLE 8.1. Comparisons Between DMT-Calculated and Measured Settlements (From Schmertmann 1986b)

| No. | Location | Structure | Compress. soil | Settlement (mm) | | | ratio |
				DMT	**	Meas.	DMT/Meas.
1	Tampa	bridge pier	HOC Clay	* 25	b,d	15	1.67
2	Jacksonvll.	Power Plant	compacted sand	* 15	b,o	14	1.07 (ave. 3)
3	Lynn Haven	factory	peaty sd.	188	a	185	1.02
4	British Columbia	test embankment	peat org. sd.	2030	a	2850	0.71
5a	Fredricton	surcharge	sand	* 11	a	15	0.73
b	"	3' plate	sand	* 22	a	28	0.79
c	"	building	quick cl. silt	* 78	a	35	2.23
6a	Ontario	road embankment	peat	*300	a,o	275	1.09
b	"	building	peat	*262	a,o	270	0.97
7	Miami	4' plate	peat	93	b	71	1.31
8a	Peter-borough	Apt. bldg	sd.& si.	* 58	a,o	48	1.21
b	"	Factory	"	* 20	a,o	17	1.18
9	"	water tank	si. clay	* 30	b,o	31	0.97
10a	Linkoping	2x3 m plate	si. sand	* 9	a,o	6.7	1.34
b	"	1.1x1.3m plate	si. sand	* 4	a,o	3	1.33
11	Sunne	house	silt & sand	* 10	b,o	8	1.25

* Denotes Ordinary M method used

** b denotes settlements calculated before the event
   a denotes settlements calculated after the event
   o denotes settlement calculations by other than the writer
   d denotes dilatometer advanced by driving with SPT hammer.

81

8.1.4 Settlement: Design Example

The data for use in this example, as well as the footing shape are presented below.
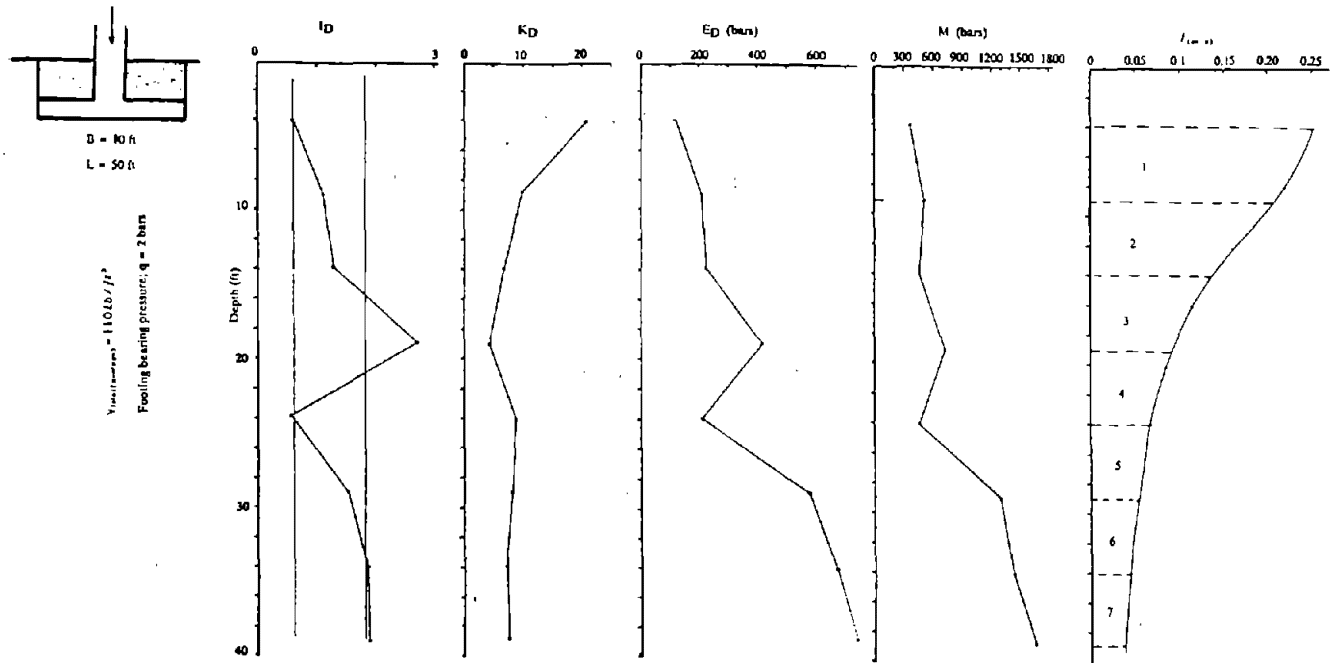
The method used to estimate the settlement of this rectangular footing is described in sections 8.1.1 and 8.1.2.

Layer #	h_i(ft)	M_i(bars)	$\Delta\sigma_i$(bars)	$\dfrac{\Delta\sigma_i}{M_i}h_i$
1	5	446	1.68	0.019
2	5	494	1.20	0.012
3	5	602	0.80	0.007
4	5	609	0.55	0.005
5	5	908	0.41	0.002
6	5	1384	0.34	0.001
7	5	1545	0.29	0.001

* The profile of M is obtained using Marchetti's (1980) method presented in section 6.6 and the given profile of E_D. Then for each layer the average value M_i is calculated.

* The profile of the stress influence factor $I_{(m,n)}$ is obtained using figure 8.1.

The net footing pressure Δp is calculated as follows:

$$\Delta p = q - \sigma'_1$$

where:

q = footing bearing pressure = 2 bars

σ'_1 = effective stress at the footing depth = 110 * 4 = 440 lb/ft^2 = 0.21 bars

σ'_1 = 0.21 bars

So

Δp = 2 - 0.21 = 1.79 bars

The expected change in stress $\Delta \sigma_i$ at the center of each layer is computed from:

$$\Delta \sigma_i = 4 \Delta p I_{(m,n)}$$
$$\Delta \sigma_i = 4 \times 1.79 \times I_{(m,n)}$$
$$\Delta \sigma_i = 7.16 I_{(m,n)}$$

* The settlement of the footing is:

$$S = 0.047 ft \quad (1.4 cm)$$

8.2 Bearing Capacity of Shallow Foundations

8.2.1 Cohesionless Soils (Drained Behavior; $I_D > 2$)

The Terzaghi bearing capacity equation for cohesionless soils is:

$$q_u = K_q \cdot \gamma' \cdot D \cdot N_q + \frac{1}{2} \cdot K_\gamma \cdot \gamma' \cdot B \cdot N_\gamma \qquad (8.6)$$

where:

q_u = ultimate bearing capacity.

γ' = effective unit weight of the soil obtained from DMT data (see section 6.4).

D = depth of embedment of the footing.

B = width of the footing.

$N_q = (\text{Exp}[\pi \tan \phi'])(\tan^2(45° + \phi'/2))$

$N_\gamma = 2(N_q + 1) \tan \phi'$

ϕ' = effective friction angle. This effective stress friction angle should be the plane strain friction angle obtained from the DMT data and corrected for the stress level $\sigma_{f/2}$ developed under the footing (section 6.3). The average stress $\sigma_{f/2}$ can be estimated as 1/3 to 1/2 of the bearing capacity value, q_u.

K_q, K_γ = two correction factors which account for load inclination, footing shape, depth of embedment, inclination of base and inclination of ground surface. These factors are described in detail by Vesic (1975).

An appropriate factor of safety should be used to obtain the safe bearing pressure, usually 3.

8.2.2 Cohesive Soils (Undrained Behavior; $I_D < 0.6$)

The ultimate bearing capacity of a footing on cohesive soils under undrained conditions is:

$$q_u = S_u \cdot N_c \cdot K_c + \gamma \cdot D \tag{8.7}$$

where:

q_u = ultimate bearing capacity.

γ = total unit weight of the soil obtained from DMT data (see section 6.4).

D = depth of embedment of the footing.

N_c = Skempton's bearing capacity factor which accounts for footing shape and depth of embedment (figure 8.2)

L = length of the footing.

S_u = undrained shear strength obtained from DMT data (see section 6.10).

K_c = a correction factor which accounts for load inclination, base inclination and ground inclination. This factor is described in detail by Vesic (1975).

An appropriate factor of safety should be used to obtain the safe bearing pressure, usually 3.
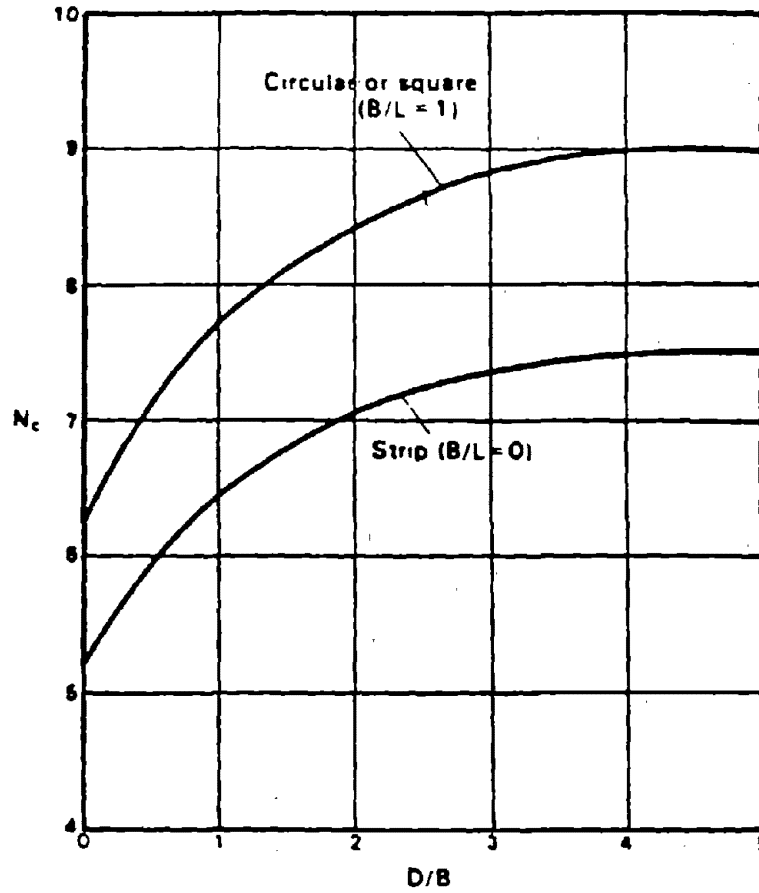
FIG. 8.2. Skempton's Bearing Factor N_c for Undrained Clay Conditions (From Peck,

Hanson, and Thornburn, 1974)

9. DESIGN OF VERTICALLY LOADED DRIVEN PILES

There is no well recognized DMT method to calculate pile capacity. The approach consists of calculating the capacity by another method and using the DMT data to help in estimating the necessary parameters.

9.1 Ultimate Bearing Capacity of Driven Piles: Introduction

The ultimate bearing capacity in compression for a pile is:

$$Q_L = Q_p + Q_s \tag{9.1}$$

or

$$Q_L = q_p \cdot A_p + \sum f \cdot A_s \tag{9.2}$$

where:

Q_p = total end bearing resitance, lb (kN)

Q_s = skin friction resistance, lb (kN)

f = average unit skin friction within a chosen layer, lb/ft^2 (kPa)

A_s = pile shaft area within a chosen layer, ft^2 (m^2)

q_p = ultimate end bearing, lb/ft^2 (kPa)

A_p = pile gross end bearing area, ft^2 (m^2)

In the special case of an open-ended pipe pile, the ultimate bearing capacity in compression requires the calculation of $Q_{L(unplugged)}$ and $Q_{L(plugged)}$. The value of $Q_{L(plugged)}$ is obtained by equation 9.2. The value of $Q_{L(unplugged)}$ is obtained as follows:

$$Q_{L(unplugged)} = Q_p + Q_s \tag{9.3}$$

or

$$Q_{L(unplugged)} = q_p \cdot A'_p + \left(\sum f \cdot A_s + \sum f \cdot A'_s\right) \tag{9.4}$$

where:

Q_p = total end bearing resistance, lb (kN)

Q_s = skin friction resistance, lb (kN)

f = average unit skin friction within a chosen layer, lb/ft^2 (kN/m^2)

A_s = outer pile shaft area within a chosen layer, ft^2 (m^2)

A_s' = inner pile shaft area within a chosen layer, ft^2 (m^2)

q_p = ultimate end bearing, lb/ft^2 (kpa)

A_p' = cross sectional area of pile point = $\pi t(d_o - t)$, ft^2 (m^2)

t = pile wall thickness, ft (m)

d_o = outer pile diameter, ft (m)

The pile capacity is the lower of the two values: $Q_{L(unplugged)}$ and $Q_{L(plugged)}$.

For H piles, the ultimate bearing capacity in compression should be calculated by considering that the pile is half plugged (Tucker and Briaud, 1988). In tension, the enclosing outside perimeter should be used.

9.2 Ultimate Bearing Capacity: Procedure for Driven Piles

The following procedure is the pile design method described and recommended in API RP2A 18th edition (1989), where the soil parameters are obtained from the DMT.

<u>Cohesive soils</u>

1. Obtain the S_u vs depth profile from DMT data using one of the methods described in section 6.10.

2. Divide the S_u profile in layers. Then, average S_u for each layer.

3. For each layer, calculate the unit skin friction f:

$$f = \alpha \cdot S_u \qquad (9.5)$$

where:

S_u = undrained shear strength from DMT data.

$\alpha = 0.5(S_u/\sigma_{vo}')^{-0.5}$ if $(S_u/\sigma_{vo}') \le 1.0$

$\alpha = 0.5(S_u/\sigma_{vo}')^{-0.25}$ if $(S_u/\sigma_{vo}') > 1.0$

with $\alpha \le 1.0$

σ_{vo}' = vertical effective stress at the point in question

4. Calculate the unit end bearing q_p:

$$q_p = 9 \cdot S_u \qquad (9.6)$$

where:

S_u = undrained shear strength from DMT data at the pile end (see section 6.10).

5. Compute the ultimate bearing capacity as described in section 9.1.

Cohesionless soils

1. Obtain the dilatometer modulus E_D and the material index I_D profiles from the ground surface to the pile tip.

2. Divide the soil profile into layers of approximately constant I_D and E_D. Then, average the values of I_D and E_D for each layer.

3. Assign a soil type as in table 9.1 to each average set of values using figure 6.5.

4. For each layer calculate the unit skin friction f:

$$f = K \cdot \sigma'_{vo} \cdot \tan \delta \qquad (9.7)$$

where:

K = 0.8 for low displacement piles.

K = 1.0 for high displacement piles.

σ'_{vo} = vertical effective stress at the point in question.

δ = friction angle between the soil and pile wall estimated using table 9.1

f should not exceed the limit friction values given in table 9.1.

5. Calculate the unit end bearing q_p:

$$q_p = \sigma'_{vo} \cdot N_q \qquad (9.8)$$

where:

σ'_{vo} = vertical effective stress at the pile tip

N_q = dimensionless bearing capacity factor from table 9.1.

q_p should not exceed the limiting end bearing values given in table 9.1.

6. Compute the ultimate bearing capacity using equation 9.2 or 9.4.

9.3 The DMT - σ_{h_c} Method for Estimating the Friction on Driven Piles

This method is based on the DMT data alone (Marchetti et al., 1986). Equation 9.7 above can be rewritten:

TABLE 9.1. Design Parameters for Cohesionless Siliceous Soil (From RP2A 18th Edition 1989)

Density	Soil Description	Soil-Pile Friction Angle. δ Degrees	Limiting Skin Friction Values kips/ft² (kPa)	N_q	Limiting Unit End Bearing Values kips/ft² (MPa)
Very Loose Loose Medium	Sand Sand-Silt** Silt	15	1.0 (47.8)	8	40 (1.9)
Loose Medium Dense	Sand Sand-Silt** Silt	20	1.4 (67.0)	12	60 (2.9)
Medium Dense	Sand Sand-Silt**	25	1.7 (81.3)	20	100 (4.8)
Dense Very Dense	Sand Sand-Silt**	30	2.0 (95.7)	40	200 (9.6)
Dense Very Dense	Gravel Sand	35	2.4 (114.8)	50	250 (12.0)

*The parameters listed in this table are intended as guidelines only. Where detailed information such as in situ cone tests, strength tests on high quality samples, model tests, or pile driving performance is available, other values may be justified.

**Sand-Silt includes those soils with significant fractions of both sand and silt. Strength values generally increase with increasing sand fractions and decrease with increasing silt fractions.

$$f = \sigma_h' \tan \delta \qquad (9.8)$$

The DMT allows to obtain σ_h' by taking A readings as a function of time until it stabilizes.

The coefficient $\tan \delta$ varies from 0.2 to 0.4. The DMT in this case should be driven in place in order to duplicate the pile insertion. Lutenegger (1991) goes on to measure the thrust after the A reading dissipation is complete in order to back calculate $\tan \delta$. This method is based on testing analogy and common sense; it shows promise and must be verified by further comparison to load tests.

10. SPECIAL PROBLEMS

10.1 Liquefaction

10.1.1 Liquefaction Potential: Robertson and Campanella (1986) Method

Soils which may liquefy when subjected to large dynamic shocks are typically saturated loose uncemented sands and silts, having little stress history, in a low horizontal stress environment.

Marchetti (1982) argued that the horizontal stress index K_D obtained from a DMT is influenced by the following factors:

. Relative density, D_r

. In-situ stresses, K_o

. Stress history and pre-stressing

. Aging

Consequently, he suggested to correlate the cyclic stress ratio to cause liquefaction (τ_l / σ'_{vo}) with the horizontal stress index K_D in order to estimate the liquefaction potential of a soil (figure 10.1).

Robertson and Campanella (1986) proposed such a correlation (figure 10.1) for normally consolidated uncemented sands under level ground conditions, based on results from 4 calibration chamber tests and 2 site tests. The following procedure should be used:

1. Calculate the average cyclic stress ratio τ / σ'_{vo} induced by the design earthquake:

$$\frac{\tau}{\sigma'_{vo}} = 0.65 \frac{a_{max}}{g} \frac{\sigma_o}{\sigma'_{vo}} r_d \qquad (10.1)$$

where:

a_{max} = acceleration in the sand layer being considered

g = acceleration due to gravity

σ'_{vo} = initial vertical effective stress on the sand layer being considered

σ_o = total vertical stress on the sand layer being considered

r_d = a stress reduction factor varying from a value of 1 at the ground surface to a value of 0.9 at a depth of about 30 ft (10 m).

2. Using figure 10.1, estimate the cyclic stress ratio τ_l / σ'_{vo} to cause liquefaction of the soil.
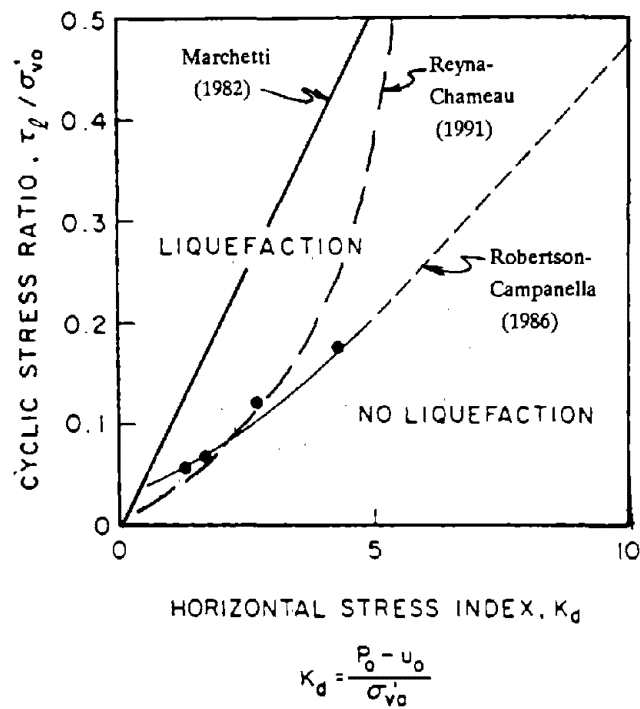
FIG. 10.1. Chart for Estimating Liquefaction Potential (After Reyna and Chameau, 1991)

3. If $\tau_l / \sigma'_{vo} > \tau / \sigma'_{vo}$ the soil is not likely to liquefy.

If $\tau_l / \sigma'_{vo} < \tau / \sigma'_{vo}$ the soil may liquefy.

Reyna and Chameau (1991) corrected the two previous recommendations on the basis of results at 3 sites in California (figure 10.1). They show that the Robertson-Campanella recommendation is appropriate at low cyclic stress ratios while the Marchetti recommendation is appropriate at higher cyclic stress ratios.

10.1.2 Liquefaction: Precision of the Method

The correlations proposed are based on limited data and require considerable field verification. However, they should give at least a preliminary indication of a sand's susceptibility to liquefaction.

10.2 Compaction Control

Dynamic compaction, compaction grouting, vibratory rolling, etc, are commonly used for modifying the bearing capacity and settlement characteristics of loose granular soils and weak cohesive soils.

The dilatometer appears to be a very useful tool to control the compaction effect on settlement potential because it gives a modulus E_D from which the tangent constrained modulus can be obtained.

Results of about 50 DMTs (reported by Lacasse and Lunne 1986, Lutenegger 1986, and Schmertmann et al. 1986) performed before and after soil compactions show the following general tendency:

.   The material index I_D does not change before and after compaction.

.   The horizontal stress index K_D and the dilatometer modulus E_D increase due to compaction.

.   The constrained tangent modulus M obtained from DMT data (section 6.6) increases due to compaction.

If the compaction requirement is to obtain a minimum M value over a depth interval, then the dilatometer is a very useful tool to check compaction effectiveness.

However, if the engineer wants to obtain a minimum value of the relative density D_r, the DMT is useless because no method is available to assess D_r from DMT data alone.

11. ADVANTAGES, DISADVANTAGES, AND COSTS

The following non-exhaustive list of advantages and disadvantages provides a guide to the strengths and weaknesses of the DMT.

11.1 Disadvantages

From the testing point of view, one of the primary disadvantages is that the blade penetration disturbs the soil.

The DMT cannot be used in cobbles, boulders and rocks. The penetration depth is limited in the strongest soils where the blade and membrane can be damaged.

Any hydraulic jacking system (CPT rigs, drill rigs etc) can be used to insert the blade in the soil. The SPT hammer can also be used to force the dilatometer blade into the soil, but it is recognized that dynamic penetration affects DMT results.

From the design point of view, the dilatometer test is a fairly recent testing technique which is still not widely used, and the available design rules are not well documented and require further field validation. Also, the methods used to obtain the soil parameters (chapter 6) are mainly based on correlations instead of theory. Therefore it is recommended that the first time the DMT is used in a new geologic setting, local correlations be established and compared with those outlined in this manual.

11.2 Advantages

From the testing point of view, the DMT has the advantage of being fast, economical, and easy to perform by a technician. The data obtained during the test are highly reproducible and the test results are much less operator-dependent than with other in situ tests.

The parameters are measured in situ, which avoids the delay and costs of laboratory testing and allows to "understand" the deposit (figure 11.1).

The DMT equipment is mechanically very simple (no sophisticated electronics), easy to repair, and is fully portable.

An ASTM suggested method for performing the test exists.

The data from a DMT can be easily reduced using a personal computer.

The equipment is relatively inexpensive ($15,000 in 1989) and can be used readily with any drilling rig or CPT rig provided the suitable rod adaptators are available.

HOW TO READ DMT RESULTS

Id: : Gives indication on material type
(Sand , Silt , Clay)

M : One dimensional
modulus at
geostatic stress   utilized
in the
usual
Cu : Undrained shear   way
strength

Kd : Similar in shape to OCR profile.
Kd≈2 indicates OCR≈1
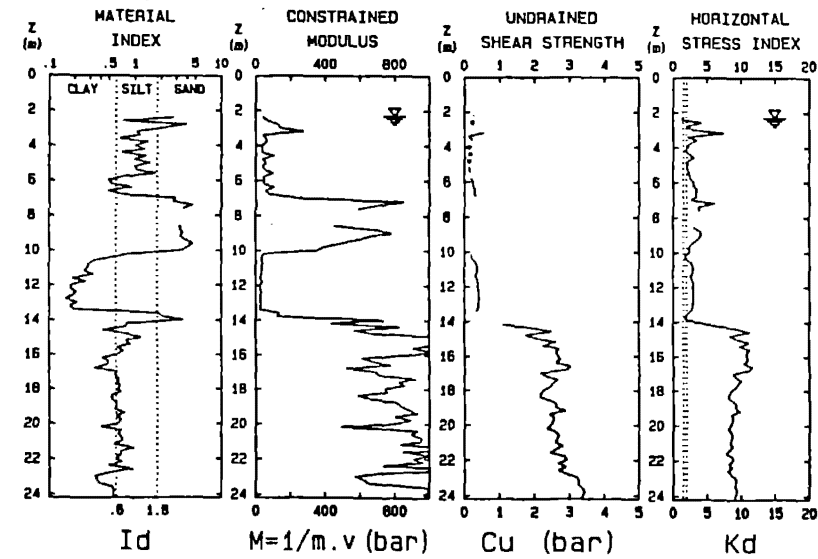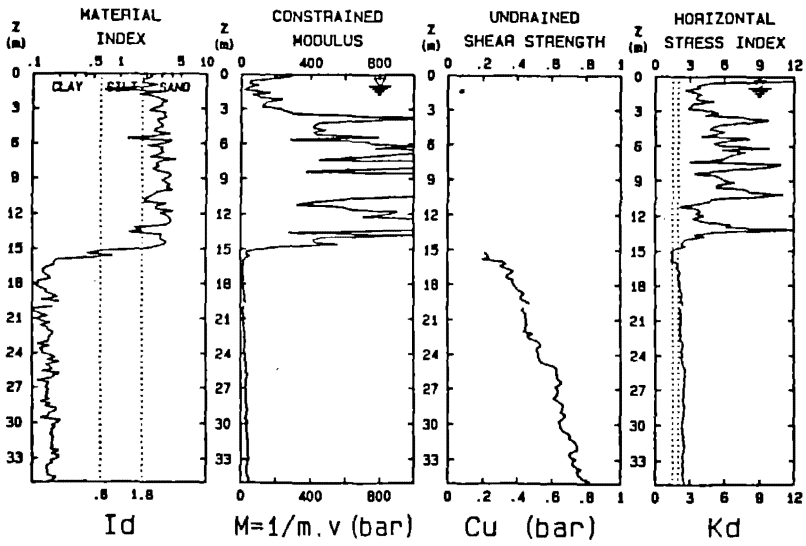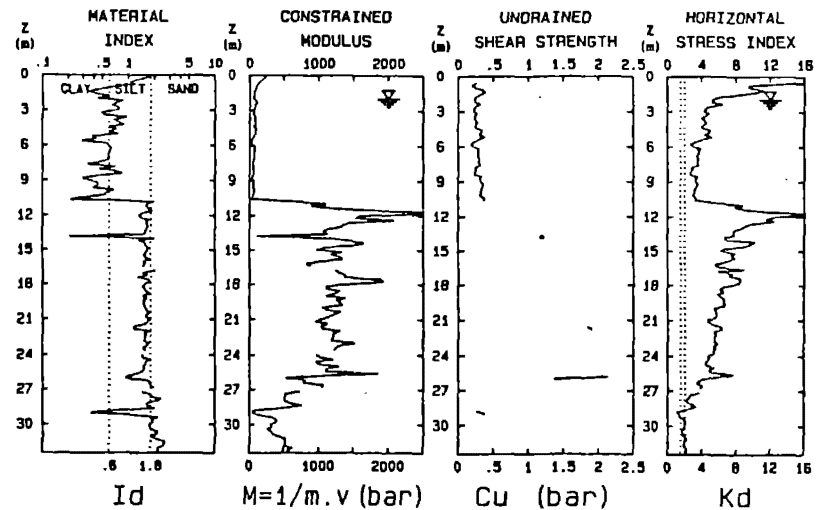Detects top crusts & buried crusts

95

FIG. 11.1. DMT Profiles (Marchetti, 1991)

From the design point of view, the best applications are the design of horizontally loaded piles, and settlement of shallow foundations. Indeed, there is a close analogy of loading of the soil in the case of horizontally loaded piles; settlement calculations can also be readily made since the DMT provides the engineer with a modulus.

11.3 Cost and Time Required

The cost of the equipment is about $15,000. This includes 2 flat blades, several pneumatic electrical cables, one cable exit adaptor, two types of rod adaptor, a tool kit with twenty spare membranes (H and S types), 1 ground cable, the control unit with a built-in calibration unit (the push rods are not included, but this equipment can be used with ordinary drill rods).

Commercial costs vary from approximately $15-30 per test, including insertion and data reduction.

In favorable soil conditions (no drilling required), the time required to perform a 10 m deep DMT sounding, with readings taken every 20 cm is about 1.5 to 2 hours.

12. REFERENCES

API Recommended Practice 2A (RP2A) 18th Edition (1989). "Recommended Practice for Planning, Designing and Constructing Fixed Offshore Platforms." American Petroleum Institute, 1220L Street, Northwest Washington, DC 20005.

Baldi, G., Bellotti, R., Rhienna, V., Jamielkowski, M., Marchetti, S., and Pasqualini, E. (1986). "Flat Dilatometer Test in Calibration Chambers." Proceedings of In Situ' 86 ASCE Specialty Conference on Use of In Situ Tests and Geotechnical Engineering, Virginia Tech, Blacksburg, Virginia, 431-446.

Baldi, G., Bellotti, R., Ghionna, V.N., Jamiolkowski, M., and Lo Presti, D.C. (1989). "Modulus of Sands from CPT's and DMT's." Paper to the 12th International Conference on Soil Mechanics and Foundation Engineering, Session 2, Rio de Janeiro, Brazil, 165-170.

Baligh, M.M., (1976). "Cavity Expansion in Sands with Curved Envelopes." ASCE, Journal of Geotechnical Engineering, Nov.

Baligh, M.M., and Levadoux, J.N. (1986). "Consolidation After Undrained Piezocone Penetration: II. Interpretation." ASCE Journal of Geotechnical Engineering, Vol. 112, No. 7, 727-745.

Basnett, Curt (1991). Written communication, February 15.

Bellotti, R., Ghionna, V., Jamiolkowski, M., and Robertson, P.K. (1989). "Design Parameters of Cohesioless Soils From In Situ Tests." Paper Submitted to In situ Testing of Soil Properties for Transportation Facilities. National Research Council, Transportation Research Board, Washington, D.C., USA.

Boghrat, A. (1982). "The Design and Construction of a Piezoblade and an Evaluation of the Marchetti Dilatometer in some Florida Soils." Ph.D. dissertation, University of Florida, 312 pp.

Borden, R.H, and Lawter, R.S. (1989). "Load-Deflection Response of Piles in Sand: Performance Prediction Using the DMT." Transportation Research Record 1235, 79-88.

Briaud, J.L. (1991). "The Pressuremeter." A. A. Balkema, Rotterdam.

Campanella, R., Robertson, P.K., Gillepsie, D., and Grieg, J. (1985). "Recent Developments in In Situ Testing of Soils." Proceedings of the 11th International Conference on Soil Mechanic and Foundation Engineering, Vol. 2, 849-854.

Clough, G.W., and Goeke, P.M. (1986). "In Situ Testing for Lock and Dam 26 Cellular Cofferdam." Use of In Situ Tests in Geotechnical Engineering, ASCE, 131-145.

Davidson, J.L., Bloomquist, D.G., and Basnett, C.R. (1988). "Dilatometer Guidelines and the Effect of Dynamic Insertion." Report to the Florida Department of Transportation, Civil Engineering Department, University of Florida.

Davidson, J.L., and Boghrat, A. (1983). "Flat Dilatometer Testing in Florida." Proceedings of the International Symposium on In Situ Testing of Soil and Rock, Paris, Vol. 2, 251-255.

Davidson, J.L., and Boghrat, A. (1983). "Displacements and Strains Around Probes in Sand." ASCE Specialty Conference on Geotechnical Practice in Offshore Engineering, Austin, Texas, 181-203.

Dumas, C.E. (1990). "DILLY-Version II, Data Input, Data Reduction, and Settlement Predictions from Dilatometer Field Data." Master of Engineering report, University of Florida.

Dumas, C.E. (1991). Written communication, March 27.

Durgunoglu, H.T., and Mitchell, J.K. (1975). "Static Penetration Resistance of Soils: I. analysis, II. Evaluation of Theory and Implications for Practice." Proceedings of the ASCE Symposium of In Situ Measurements of Soils Properties, Raleigh, Vol. 1, 151-171.

Fabius, M. (1985). "Experience With the Dilatometer in Routine Geotechnical Design." Proceedings of the 38th Canadian Geoteghnical Conference.

Fadum, R.E. (1948). "Influence Values for Estimating Stresses in Elastic Foundations." Proc. 2nd Int. Conf. on Soil Mechanics and Foundation Engineering, Vol. 2.

Gabr, M.A., and Borden, R.H. (1988). "Analysis of Load Deflection Response of Laterally Loaded Piers Using DMT." Proceedings of the 1st International Conference on Penetration Testing, ISOPT-1, Orlando, Florida, Vol. 1, 513-520.

G.P.E. Inc., (1991). 4509 N.W. 23rd. Avenue, Suite 19, Gainesville, Florida, 32606, Tel: 904-378-2792.

Gravesen, S. (1960). "Elastic Semi-Infinite Medium Bounded by a Rigid Wall With a Circular Hole." Laboratoriet for Bygninsteknik, Danmarks Techniske Hojskole, Meddelelse No. 10, Copenhagen, Denmark.

Greig, J.W., Campanella, R.G., and Robertson, P.K. (1986). "Comparison of Field Vane Results With Other In Situ Test Results." Soil Mechanics Series No. 106, Department of Civil Engineering, University of British Columbia.

Gupta, R.C. (1988). "Determination of the In Situ Coefficients of Consolidation and Permeability of Submerged Soils Using Electrical Piezoprobe Soundings." PhD. Dissertation to the University of Florida, 1983, 282pp.

Hardin, B.O. and Blandford, G.E. (1989). "Elasticity of Particulate Materials." ASCE Journal of Geotechnical Engineering, Vol. 115, No. 6, 788-805.

Hryciw, R.D. (1990). "Small-Strain Shear Modulus of Soil by Dilatometer." ASCE Journal of Geotechnical Engineering, Vol. 116, No. 11, 1700-1716.

Jamiolkowski, M., Ghionna, V.N., Lancellota, R., and Pasqualini, E. (1988). "New Correlations of Penetration Tests For Design Practice." Proceedings of the 1st International Symposium on Penetration Testing, ISOPT-1, Orlando, Florida, Vol. 1, 263-296.

Kabir, M.G. and Lutenegger, A.J. (1990) "In Situ Estimation of the Coefficient of Consolidation in Clays." Canadian Geotechnical Journal, Vol. 27, 58-67.

Lacasse, S., and Lunne, T. (1983). "Dilatometer Tests in Two Soft Marine Clays." Norwegian Geotechnical Institute Publication No. 146, 1-8.

Lacasse, S., and Lunne, T. (1986). "Dilatometer Tests in Sands." Use of In Situ Tests in Geotechnical Engineering, ASCE, 686-699.

Lacasse, S., and Lunne, T. (1988). "Calibration of Dilatometer Correlations." Proceedings of the 1st International Symposium on Penetration Testing, ISOPT-1, Orlando, Florida, Vol. 1, 539-548.

Lee, S.H.H., and Stokoe, K.H. (1986). "Investigation of Low Amplitude Shear Wave Velocity in Anisotropic Materials." Geotechnical Engineering, Report No. GR86-6, Civil Engineering Department, The University of Texas at Austin.

Leonard, G.A., and Frost, J.D. (1988). "Settlement of Shallow Foundations on Granular Soils." ASCE Journal of Geotechnical Engineering, Vol. 114, No.GT7, 791-809.

Lunne, T., Lacasse, S., Rad, N.S., and Decourt, L. (1989). "SPT, CPT, Pressuremeter Testing and Recent Developments on In Situ Testing." Norwegian Geotechnical Institute, Report No. 591390-1.

Lunne, T., Powell, J.J.M., Hauge, E.A., Uglow, I.M., and Mokkelbost, K.H. (1990). "Correlation of Dilatometer Readings to Lateral Stress." Paper Submitted to Specialty Session on Measurement of Lateral Stress. 69th Annual Meeting of the Transportation Research Board. Washington, D.C., USA.

Lutenegger, A.J. (1986). "Application of Dynamic Compaction in Friable Loess." ASCE Journal of Geotechnical Engineering, Vol. 112, 663-667.

Lutenegger, A.J. (1988). "Current Status of the Marchetti Dilatometer Test." Proceedings of the 1st International Symposium on Penetration testing, ISOPT-1, Orlando, Florida, Vol. 1, 137-155.

Lutenegger, A.J. (1991). Written communication, May 19.

Lutenegger, A.J. and Blanchard, J.D. (1990). "A Comparison between Full Displacement Pressuremeter Tests and Dilatometer Tests in Clay." Third Int. Symp. on Pressuremeters, Thomas Telford, London.

Lutenegger, A.J., and Kabir, M. (1988). "Dilatometer C-Reading to Help Determine Stratigraphy." Proceedings of the 1st International Symposium on Penetration testing, ISOPT-1, Orlando, Florida, Vol. 1, 549-554.

Lutenegger, A.J., and Timian, D.A. (1986). "Flat-Plate Penetrometer Tests in Marine Clays." Proceedings of the 39th Canadian Geotechnical Conference, 301-309.

Marchetti, S. (1980). "In Situ Tests by Flat Dilatometer." ASCE Journal of Geotechnical Engineering, Vol. 106, 299-321.

Marchetti, S. (1982). "Detection of Liquefiable Sand Layers by Means of Quasi Static Penetration Tests." Proceedings of the 2nd European Symposium on Penetration Testing, ESOPT II, Amsterdam, Vol. 2, 689-695.

Marchetti, S. (1985). "On the Field Determination of K_o in Sand." Panel Presentation Session: In Situ Testing Techniques, Proceedings of the 11th International Conference on Soil Mechanics and Foundation Engineering, San Francisco.

Marchetti, S. (1991). Written communication, March 12.

Marchetti, S. and Crapps, D.K. (1981). "Flat Dilatometer Manual." Internal report of GPE Inc., Distributed to Purchasers of the DMT Equipment.

Marchetti, S. and Totani, G. (1989). C_h Evaluations from DMTA Dissipation Curves." Int. Conf. on Soil Mechanics and Foundation Engineering, Rio de Janeiro.

Marchetti, S., Totani, G., Campanella, R.G., Robertson, P.K., and Taddei, B. (1986). "The DMT-σ_{hc} Method for Piles Driven in Clay." ASCE Specialty Conference In Situ 86, June.

Matlock, H. (1970). "Correlations for Design of Laterally Loaded Piles in Soft Clay." Proceedings of the 2nd Offshore Technical Conference. Houston, Texas, Vol.1, 577-594.

Mayne, P.W., and Kulhaway, F.H. (1982). "K_o- OCR Relationship in Soil." ASCE Journal of Geotechnical Engineering, Vol. 108, No. GT6, 851-872.

McTrans (1991). University of Florida, 512 Weil Hall, Gainesville, Florida, 32611-2083, Tel: 904-392-0378.

Ming-Fang, C. (1986). "The Flat Dilatometer Test and Its Application to Two Singapore Clays." Proceedings of the 4th International Geotechnical Seminar on Field Instrumentation and In Situ Measurements, Singapore, 85-101.

Murchison, J.M. and O'Neill, M.W. (1984). "Evaluation of P-y Relationships in Cohesionless Soils." Proceedings of ASCE Symposium on Analysis and Design of Pile Foundations.

Peck, R.B., Hanson, W.E., and Thornburn, T.H. (1974). "Foundation Engineering, 2nd Edition." John Wiley and Sons, New York, N.Y.

Powell, J.J.M., and Uglow, I.M. (1988). "Marchetti Dilatometer Testing in UK Soils." Proceedings of the 1st International Symposium on Penetration Testing, ISOPT-1, Orlando, Florida, Vol. 1, 555-562.

Reese, L.C., Cox, W.R., and Koop, F.D. (1974). "Analysis of Laterally Loaded Piles in Sand." Paper OTC 2080, Presented at the 6th Annual Offshore Technology Conference, Houston, Texas.

Reyna, F. and Chameau, J.L. (1991). "Dilatometer Based Liquefaction Potential of Sites in the Imperial Valley." 2nd Int. Conf. on Recent Advances in Geot. Earthquake Engrg. and Soil Dyn., St. Louis, May.

Robertson, P.K. and Campanella, R.G. (1986). "Estimating Liquefaction Potential of Sands Using the Flat Dilatometer." Geotechnical Testing Journal, GTJODJ, Vol. 9, 38-40.

Robertson, P.K., Campanella, R.G., Davies, M.P., and Sy, A. (1989b). "An Evaluation of Pile Design in Fraser River Delta Using In Situ Tests." Foundation Engineering Current Principles and Practices, ASCE, Evanston, IL, 92-105.

Robertson, P.K., Campanella, R.G., and Gillespie, D. (1988). "Excess Pore Pressure and the Flat Dilatometer Test." Proceedings of the 1st International Symposium on Penetration Testing, ISOPT-1, Orlando, Florida, Vol. 1, 567-576.

Robertson, P.K., Davies, M.P., and Campanella, R.G. (1989a). "Design of Laterally Loaded Driven Piles Using the Flat Dilatometer." Geotechnical Testing Journal, GTJODJ, Vol. 12, No. 1, 30-38.

Roque, R., Janbu, N., and Senneset, K. (1988). "Basic Interpretation Procedures of Flat Dilatometer Tests." Proceedings of the 1st International Symposium on Penetration Testing, ISOPT-1, Orlando, Florida, Vol.1, 577-587.

Schmertmann, J.H. (1982). "A Method for Determining the Fricton Angle in Sands from the Marchetti Dilatometer Tests." Proceedings of the 2nd European Symposium on Penetration testing, ESOPT-II, Amsterdam, Vol.2, 853-861.

Schmertmann, J.H. (1983). "Revised Procedure for Calculating K_o and OCR from DMT's With $I_D > 1.2$ and Which Incorporates the Penetration Measurement to Permit Calculating the Plane Strain Friction Angle." DMT Digest No. 1, GPE INC., Gainsville, Florida, USA.

Schmertmann, J.H. (1986a). "Suggested Method For Performing the Flat Dilatometer Test." Geotechnical Testing Journal, GTJODJ, Vol. 9, No. 2, 93-101.

Schmertmann, J.H. (1986b). "Dilatometer to Compute Foundation Settlement." Proceedings of In Situ' 86 ASCE Specialty Conference on Use of In Situ Tests and Geotechnical Engineering, Virginia Tech, Blacksburg, Virginia, 303-321.

Schmertmann, J.H. (1988). "Guidelines for Using the CPT, CPTU and Marchetti DMT for Geotechnical Design." U.S. Department of Transportation, Federal Highway Administration, Office of Research and Special Studies, Report No. FHWA-PA-87-023+24, Vol. 3-4.

Schmertmann, J.H., Baker, W., Gupta, R., and Kessler, K. (1986). "CPT/DMT QC of Ground Modification at a Power Plant." Use of In Situ Tests in Geotechnical Engineering, ASCE, 985-1001.

Sully, J.P., and Campanella, R.G. (1989). "Correlation of Maximum Shear Modulus With DMT Test Results in Sands." Paper to 12th International Conference on Soil Testing and Foundation Engineering, Session 2, Rio de Janeiro, 339-343.

Tucker, L.M. and Briaud, J.L. (1988). "Analysis of the Pile Load Test Program at the Lock and Dam 26 Replacement Project." U.S. Army Engineer Waterways Experiment Station, Misc. Paper GL-88-11.

Vesic, A.S. (1975). "Bearing Capacity of Shallow Foundations, Foundation Engineering Handbook." Edited by H.F. Winterkorn and H.Y. Fang, Van Nostrand Publishing Company.